

***In Vitro* Analysis of FGF-23 Induced Gene Expression**

A Thesis
Submitted to the Faculty
Of the
WORCESTER POLYTECHNIC INSTITUTE

In partial fulfillment of the requirements for the
Degree of Master of Science
In Biotechnology

By

Csaba C. Pazmany
January 8, 2003

APPROVED:

Susan C. Schiavi, Ph.D.
Genzyme Corporation
Primary Investigator

David S. Adams, Ph.D.
WPI
Major Advisor

Elizabeth F. Ryder, Ph.D.
WPI
Committee Member

ABSTRACT

Fibroblast growth factor 23 (FGF-23) has recently been shown to be involved in phosphate regulation and bone mineralization. This study evaluated the effect of FGF-23 on three human cell lines (Caco-2, HK-2, SaOS-2) representing three different sites of phosphate regulation (small intestine, kidney proximal tubules, and bone, respectively). FGF-23 induced gene expression was studied using Clontech human Atlas glass microarrays containing various assortments of genes and by a custom designed oligo microarray containing specific genes selected for their biological relevance to FGF-23's potential function. FGF-23 induced differential gene expression in all three cell types, suggesting that FGF-23 may be capable of acting on these three primary sites of phosphate regulation. Human small intestine-like endothelial cell line, Caco-2, showed upregulation of several genes including parathyroid hormone receptors 1 and 2. FGF-23 inhibited the expression of water channel transporters aquaporin 5 and 6 in human osteoblast-like SaOS-2 cells while upregulating aquaporin expression in HK-2 cells. Somatostatin receptors 1-4 were identified to be upregulated in the human kidney, HK-2 cell line. Mucin 2, a gene that is linked to abnormal cellular growth, was consistently induced by FGF-23 in all three cell lines. Families of aquaporins, somatostatins, parathyroid hormones, and other identified differentially expressed genes are involved in different signaling pathways that are associated with phosphate and calcium regulation. Selected candidates were analyzed further by real-time RT-PCR. These data support FGF-

23 induced regulation of aquaporin 5 mRNA in HK-2 cells and 1 α OHase mRNA in Caco cells. FGF-23 induced changes in mRNA analysis of four additional genes was less than two-fold in triplicate analysis of selected samples. Taken together, these results suggest that each cell type may have responded to FGF-23, but additional validation of the array data set will be required to identify those genes specifically regulated by FGF-23. Further refinement of this data set will undoubtedly uncover additional functions of FGF-23 and may provide valuable insight into designing therapeutic approaches for phosphate specific disorders.

TABLE OF CONTENTS

Signature Page	1
Abstract	2
Table of Contents	4
Acknowledgements	5
List of Figures	6
List of Tables	8
Background	9
Project Purpose	34
Abbreviations	35
Materials and Methods	36
Results	51
Discussion	107
Appendix	123
Bibliography	127

ACKNOWLEDGEMENTS

I would like to thank Dr. Susan Schiavi for giving me the opportunity to conduct my thesis research at Genzyme Corporation, Framingham Massachusetts and for all her hard work. I would also like to thank Ann Bowe, Rich Finnegan, Dr. Marlon Pragnell, Stephen O'Brien, and John Vassiliadis for their daily technical assistance. Additionally I would like to thank many member of the Applied Genomics group at Genzyme Corp. for support throughout this project. Furthermore, I would like to thank Dr. David Adams, my primary academic advisor and Dr. Elizabeth Ryder for their guidance and support. Last, but most definitely not the least, I would like to thank my parents for having me and for their relentless support.

LIST OF FIGURES

Figure 1- Pro-convertase processing of full length FGF-23.....	12
Figure 2- Sequence comparison between FGF-19, FGF-21 and FGF-23...	13
Figure 3- X-linked hypophosphatemia bone deformation	18
Figure 4- PHEX mediated regulation of FGF-23	19
Figure 5- Summary of OOM, XLH, ADHR	20
Figure 6- Illustration of phosphate regulation in the kidney	23
Figure 7- X-ray image of FGF-23 over expressing mouse.....	24
Figure 8- Calcium and phosphate homeostasis model.....	26
Figure 9- FGF receptor 1-4 expression in HK-2, Caco-2 and Saos-2 cells..	54
Figure 10- FGF-23 purification.....	56
Figure 11- HK-2 total RNA Ethidium bromide stained agarose gel	59
Figure 12- Commercial microarray variability	65
Figure 13- Custom microarray variability	66
Figure 14- Venn diagram of up regulated genes	74
Figure 15- Venn diagram of down regulated genes	78
Figure 16- RT-PCR expression of APC in Caco-2 and HK-2	88
Figure 17- RT-PCR of vitamin D related genes in Caco-2 and HK-2	91
Figure 18- RT-PCR expression of mucin-2 in HK-2.....	92
Figure 19- RT-PCR expression of FRP-4 in Caco-2	93
Figure 20- RT-PCR expression of AQP-5 in HK-2.....	94
Figure 21- FRP-4 RT-PCR standard curve.....	97
Figure 22- 1 α OHase RT-PCR standard curve	98

Figure 23- APC RT-PCR standard curve	99
Figure 24- 24OHase RT-PCR standard curve	100
Figure 25- Mucin-2 RT-PCR standard curve	101
Figure 26- PTHR-2 RT-PCR standard curve	102
Figure 27- HK-2 24 hour GAPDH analysis.....	103
Figure 28- Caco-2 24 hour GAPDH analysis	104
Figure 29- AQP-5 ethidium bromide agarose gel	105
Figure 30- Generalized Wnt/ β -Catenin signaling pathway	113
Figure 31- PTH response to low serum calcium.....	116
Figure 32- FGF-23 biological activity via opossum kidney assay.....	123
Figure 33- RT-PCR expression of SSTR-2 in Caco-2	124
Figure 34- AQP-6 ethidium bromide agarose gel	124

LIST OF TABLES

Table 1- Functions of human FGFs	11
Table 2- Clinical evidence of hypophosphatemia	14
Table 3- PCR primers for FGF receptor 1-4 and GAPDH	41
Table 4- Real-time RT-PCR validation primers	48
Table 5- Microarray replicate summary	61
Table 6- Selected genes of interest up and down	71
Table 7- Triplicate commercial microarray analysis of HK-2 expression.....	73
Table 8- 24 hour up regulated commercial microarray gene list.....	76
Table 9- 72 hour up regulated commercial microarray gene list	77
Table 10- 24 hour down regulated commercial microarray gene list	80
Table 11- 72 hour down regulated commercial microarray gene list	81
Table 12- Custom microarray upregulated genes.....	82
Table 13- Custom microarray downregulated genes	84
Table 14- Real-time RT-PCR and microarray summary expression.....	95
Table 15- custom microarray house keeping gene expression.....	105
Table 16- custom microarray low signal intensity gene list.....	124

BACKGROUND

Introduction

The maintenance of serum phosphate homeostasis is among the factors important for basic cellular survival and is involved in vital biological processes such as calcification of skeletal tissues, generation and transformation of cellular energy, and modulation of protein activity (Broadus 99). Phosphate dysregulation is associated with several medical conditions that detrimentally affect patient morbidity and mortality such as autosomal dominant hypophosphatemic rickets (ADHR), X-linked hypophosphatemic rickets (XLH), oncogenic osteomalacia (OOM) and end stage renal disease (ESRD). Until recently, it was well accepted that phosphate homeostasis is maintained by the calcitrophic hormones 1,25 dihydroxyvitamin D₃ (1,25(OH)₂D₃) and parathyroid hormone (PTH), the same hormones involved in calcium homeostasis. This view was inconsistent with the observation that under certain disease states (XLH, OOM, ADHR) serum phosphate levels were abnormally low despite normal serum calcium concentrations. These symptoms cannot be explained by the known actions of vitamin D and PTH. Subsequently, increased serum levels of fibroblast growth factor (FGF)-23 were found in individuals with ADHR (White *et al.* 2002), OOM (Jonsson *et al.* 2002, Yamazaki *et al.* 2002) and XLH (Jonsson *et al.* 2002, Yamazaki *et al.* 2002). Recently, FGF-23 has been shown to specifically modulate phosphate uptake without affecting net calcium homeostasis. This finding supports the hypothesis that a novel control mechanism exists whose

primary function is to control phosphate. Understanding FGF-23's mechanism of action may provide insight into this pathway as well as enable the development of more effective phosphate regulating therapeutics, that eliminate the detrimental calcium side effects associated with current therapies.

Fibroblast growth factor family

FGF-23 is a member of a large family of peptide factors (ADHR consortium 2000). The FGF family consists of 23 distinct genes and five known receptors. Knowledge of other FGF binding and signaling characteristics can be leveraged to develop an understanding of FGF-23's specific mechanism of action. FGF family members are associated with diverse vital functions throughout embryonic development, cell proliferation, cell-survival activities, tissue repair, and tumor growth. Most FGFs contain a secretion signal sequence to allow for extracellular localization and contain strong heparin binding domains that generally affect signaling by modifying FGF binding specificity (Powers *et al.* 2000). A core of 140 amino acids remains highly homologous throughout the FGF family. These conserved amino acids form 12 anti-parallel beta-strands that create a cylindrical barrel, a defining feature of the FGF family (Zhang *et al.* 1991). It is this topological similarity that unites the FGFs, not their biological function. The receptor binding interactions and the diverse functions of FGFs can be appreciated by viewing table 1.

Table 1. Functions of human FGFs. Fibroblast growth factors are involved in various functions and pathways.

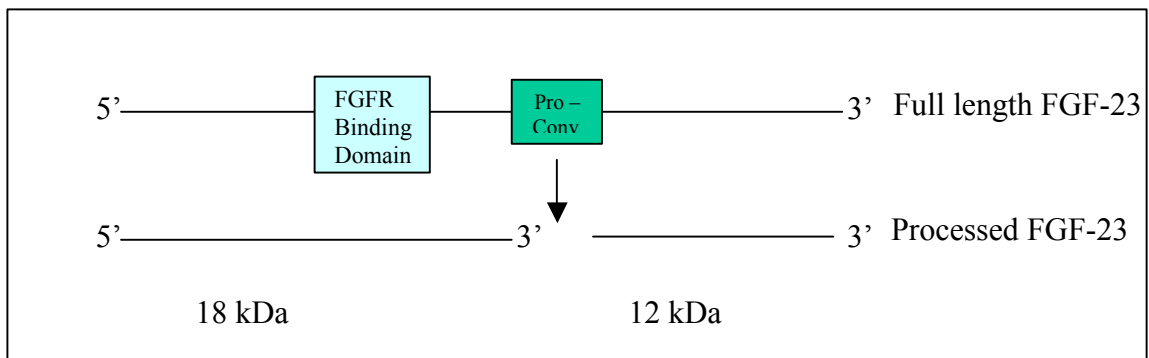
Name	Synonym(s)	Signaling through high-affinity receptors	Comments*
FGF-1	Acidic FGF, aFGF	FGFR-1,IIIb &IIIc;FGFR-2,IIIb & IIIc;FGFR-3,IIIb & IIIc; FGFR-4	Broad mitogenic and cell survival activities. Involved in similar functions as FGF-2
FGF-2	FGF-2 Basic FGF, bFGF	FGFR-1,IIIb &IIIc;FGFR-2,IIIc; FGFR-3,IIIc;FGFR-4	embryonic development, cell growth, morphogenesis, tissue repair, tumor growth and invasion
FGF-3	Int-2	FGFR-1,IIIb;FGFR-2,IIIb	Over expression results in abnormal prostate and Wolffian duct development
FGF-4	kFGF, kaposi FGF hst-1	FGFR-1,IIIc;FGFR-2,IIIc;FGFR-3, IIIc;FGFR-4	Regulate cell number in the nascent limb bud and are required for survival of cells located far from the apical ectodermal ridge. Similar functions as FGF-8.
FGF-5		FGFR-1,IIIc;FGFR-2,IIIc	Signal sequence
FGF-6	hst-2	FGFR-1,IIIc;FGFR-2,IIIc,FGFR-4	Signal sequence
FGF-7	KGF	FGFR-2,IIIb	Homologous rodent genes are implicated with morphogenesis of epithelium, hair development and early lung organogenesis
FGF-8	AIGF	FGFR-1,FGFR-2,IIIc;FGFR-3, IIIc,FGFR-4	7 isoforms, all with signal sequences. Transgenic expression in mice induces differentiation of pancreatic islet cells into hepatocytes and exocrine cells
FGF-9	GAF	FGFR-2,IIIc;FGFR-3,IIIb & IIIc, FGFR-4	Expression of the mouse homologue was found to be dependent on Sonic hedgehog signaling. Potential role in testicular embryogenesis.
FGF-10	KGF-2	FGFR-1,IIIb;FGFR-2,IIIb	Lunatic fringe, FGF, and BMP regulate the Notch pathway during epithelial morphogenesis of teeth.
FGFs 11 – 14	FGFs	Unknown	Associated with nervous system development Multiple isoforms exist
FGF-15		Unknown	Gene is activated byE2A-Pbx1
FGFs 16 – 18		FGF-17;FGFR-1,IIIc;FGFR-2,IIIc	may play a role in development of brown adipose tissue, brain development and stimulates hepatic and intestinal proliferation
FGF-19		FGFR-4	high affinity, heparin dependent ligand for FGFR4
FGF-20 XFGF-20	XFGF-20	Unknown	Sequence homology to FGF-9. Expressed in the brain and able to enhance the survival of midbrain dopaminergic neurons <i>in vitro</i> .
FGF-21		Unknown	Sequence homology to novel mouse FGF-21, FGF-9
FGF-22		Unknown	Sequence homology to FGF-10 and FGF-7
FGF-23		FGFR-2, FGFR-3, FGFR-4	associated with phosphate regulation

*Modified from Powers *et al.* (2000).

Identification of human FGF-23

As shown in figure 1, FGF-23 is a 30 kDa secreted protein that is processed by a pro-convertase type enzyme into two smaller fragments of approximately 18 kDa (amino fragment) and 12 kDa (carboxy fragment). The biological activities of the intact, amino, and carboxyl fragments of FGF-23 have not yet been delineated. The wild type FGF-23 contains the pro-convertase site and can be processed into two fragments in the presence of the enzyme.

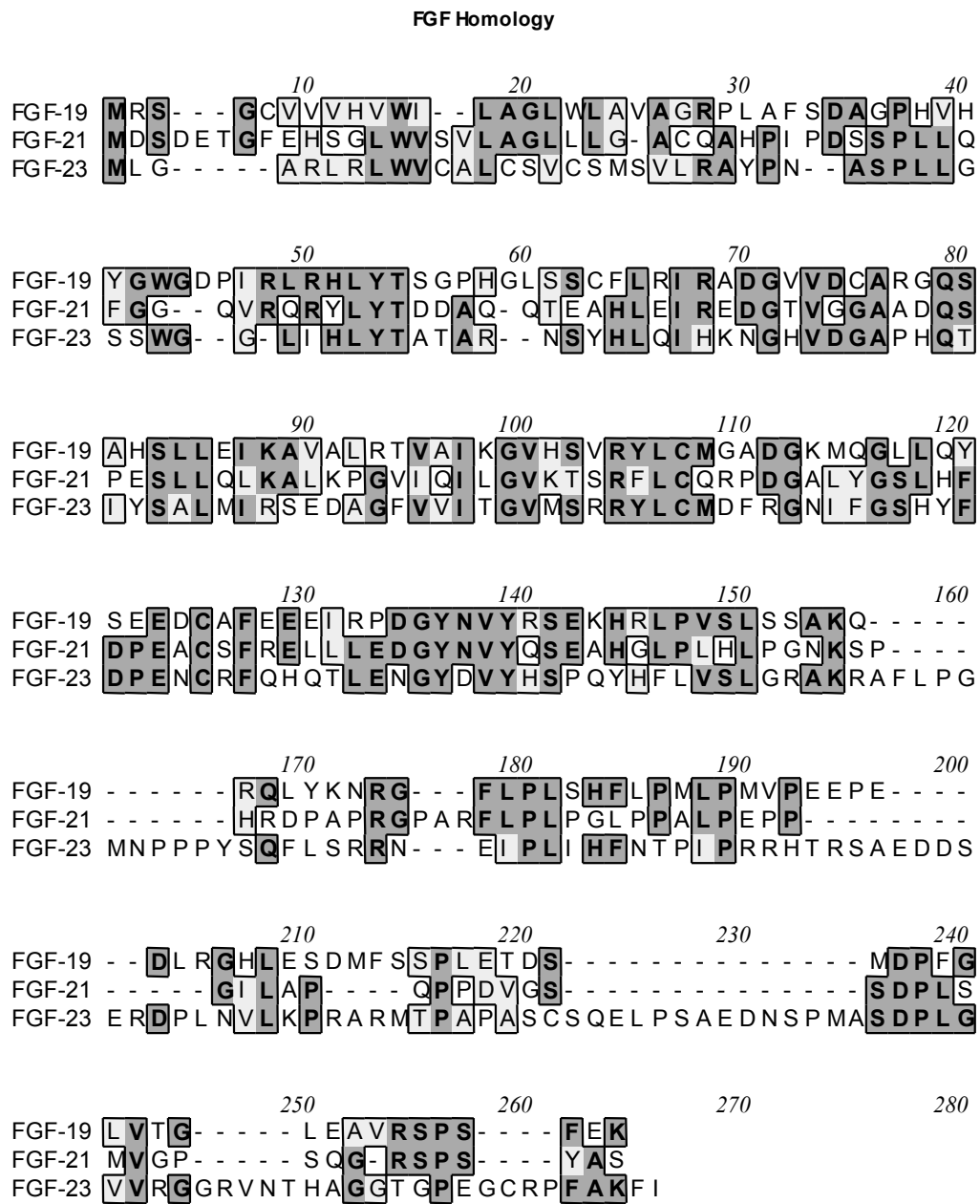
Figure 1. Pro-convertase processing of full length FGF-23. A cleavage site at amino acid 176-179 (RXXR motif) cuts the full length FGF-23 into two fragments.



Several independent groups identified FGF-23 utilizing distinct strategies. Mouse FGF-23 was identified and cloned from a murine brain tissue cDNA library and using a computer homology search, human FGF-23 was identified (Yamashita *et al.* 2000). At the time of discovery, these investigators had no insight into FGF-23's physiological function. More recently, FGF-23 has been shown to be expressed in OOM tumors, human heart, liver and thyroid/parathyroid tissue by northern analysis (ADHR Consortium 2000, figure 2). Sequence comparisons show that FGF-23 is most similar to FGF-19 and FGF-21 (ADHR

Consortium 2000). The specific functions of FGF-19 and FGF-21 are not known but they have not been associated with phosphate regulation. FGF-23 is significantly distinct from other FGFs in that it is the only family member to contain a pro-convertase processing site.

Figure 2. Sequence comparison between FGF-19, FGF-21 and FGF-23. Both FGF-19 and FGF-21 have a 26% identity homology to FGF-23.



FGF-23 association to genetically inheritable diseases

Identification of FGF's function arose from studies centered on a class of hypophosphaturic and hyperphosphatemic disorders which included autosomal dominant hypophosphatemic rickets (ADHR), X-linked hypophosphatemic rickets (XLH) and oncogenic osteomalacia (OOM) (Table 2). The kidneys of individuals with these disorders have a reduced capacity to reabsorb phosphate that results in phosphate wasting through urine excretion (i.e. phosphaturia). Subsequently, these individuals have low serum phosphate levels, (i.e. hypophosphatemia) due to a reduced capability of the kidneys to reabsorb phosphate back into the blood stream (Econs *et al.* 1997). In order to maintain the proper phosphate serum concentrations, the phosphate reservoir in bone is tapped. As the phosphaturia continues, the reservoir in the bone is depleted and the bone matrix strength is compromised. The bone is no longer capable of proper growth and mineralization, and the result is poor skeletal integrity (Shore 1999). Strikingly, each of these individuals have normal levels of calcium and the two known regulators of phosphate and calcium homeostasis; $1,25(\text{OH})_2\text{D}_3$ (the active form of vitamin D) and parathyroid hormone (PTH). As discussed below, recent evidence has established a link between increased circulating levels of FGF-23 and each of these disorders.

Table 2. Clinical evidence that calcium homeostasis is maintained in patients with hypophosphatemia. Serum phosphate levels are low while calcium is maintained through PTH and vitamin D activity.

Clinical Features	XLH	ADHR	OOM
Serum phosphate	Low	Low	Low
Serum calcium	Normal	Normal	Normal
$1,25(\text{OH})_2\text{D}_3$	Low/normal	Low	Low/Normal
$25(\text{OH})\text{D}_3$	Normal	Normal	Normal
PTH	Normal	Normal	Normal

The correlation between FGF-23 and ADHR was established by statistical genetic analysis. A large lod score to the ADHR pedigree, a value of 7.68 (ADHR consortium 2000) helped to identify a region on chromosome 12 that was most likely to contain specific mutations responsible for ADHR. A lod score analysis is a statistical determination of events occurring at random chance. A small lod score suggests that there is little or no linkage between the events in question while a high lod score represents a statistical association and suggests that there may be a biological association. Using a positional cloning approach on the region identified by the lod score analysis, the ADHR Consortium identified a specific site within a novel gene they named FGF-23 to be associated with the genetic disorder. Sequence analysis revealed that all ADHR individuals contain a mutation within a 12 base pair region of the 251 FGF-23 amino acid coding sequence that were not found in unaffected individuals. Interestingly, the mutated region (positions 176-180) encodes a motif site (RXXR) that is sensitive to endopeptidase cleavage by a pro-convertase. This raised the possibility that failure to process FGF-23 during its synthesis alters FGF-23 activity. As described below, it is now believed that this activating mutation is responsible for elevated levels of biologically active circulating FGF-23 by somehow stabilizing FGF-23, by preventing cleavage and, in turn, inhibits reabsorption of phosphate from the kidney into the blood resulting in phosphate wasting (White *et al.* 2001). The association of the identified FGF-23 mutations to phosphate dysregulation and their association to ADHR are among the contributing factors that lead to the

desire and need to elucidate the properties of FGF-23. ADHR belongs to a class of hypophosphatemic disorder that includes OOM and XLH.

Evidence of FGF-23 association with a tumor induced hypophosphatemia

In addition to ADHR, FGF-23 has also been associated with a tumor-induced phosphate wasting disorder, oncogenic osteomalacia (OOM). Like ADHR patients, these individuals have low serum phosphate levels, low/normal 1,25(OH)₂D₃ (active form of vitamin D) and osteomalacia. Upon excision of the tumors, patient's serum phosphate levels return to near normal and bone mineralization resumes (Kumar *et al.*, 2000) suggesting that the tumor was responsible for the phosphate wasting disorder. Three groups independently linked the overexpression of human FGF-23 to OOM (White *et al.* 2001, Shimada *et al.* 2001, Jan de Beur *et al.* 2002). White *et al.* (2001) verified that FGF-23 was a secreted protein by Western blot analysis of sera. Shimada *et al.* (2001) used a differential expression cloning strategy to identify cDNA clones representing abundantly expressed OOM tumor genes that were not expressed in normal tissue adjacent to the tumor. Wild type FGF-23 was among the identified candidates. Independent of Shimada's work, SAGETM (Serial Analysis of Gene Expression) was used to identify genes of high expression levels in OOM tumors compared to histologically matched control tumors that did not induce phosphate wasting. FGF-23 was identified as one of several candidates over expressed within OOM tumors (Jan de Beur *et al.* 2002). SAGETM is unique to other gene quantification technologies because it does not require knowledge of the gene

sequence prior to quantification and hence allows for identification and quantification of novel genes. In SAGE analysis, a concatamer of 10-14 oligonucleotide tag representing each gene transcript is constructed, sequenced and quantified. The identified 10-14 oligonucleotide fragment is compared to databases to identify the corresponding gene. The association of FGF-23 to two phosphaturic conditions, OOM and ADHR provided strong evidence linking the function of this gene to phosphate regulation.

FGF-23 association to X-linked hypophosphatemia

Similar to ADHR, X-linked hypophosphatemia (XLH) is another genetically inheritable medical condition that induces phosphate wasting (Meyer *et al.* 1989). XLH patients have biochemical and clinical features similar to ADHR. Figure 3 shows the classic leg deformities often found in XLH and ADHR patients. Low serum phosphate levels result in poor bone mineralization and classic bowing of the legs. OOM patients who acquire tumors later in life suffer from osteomalacia but do not have bowing of the legs.



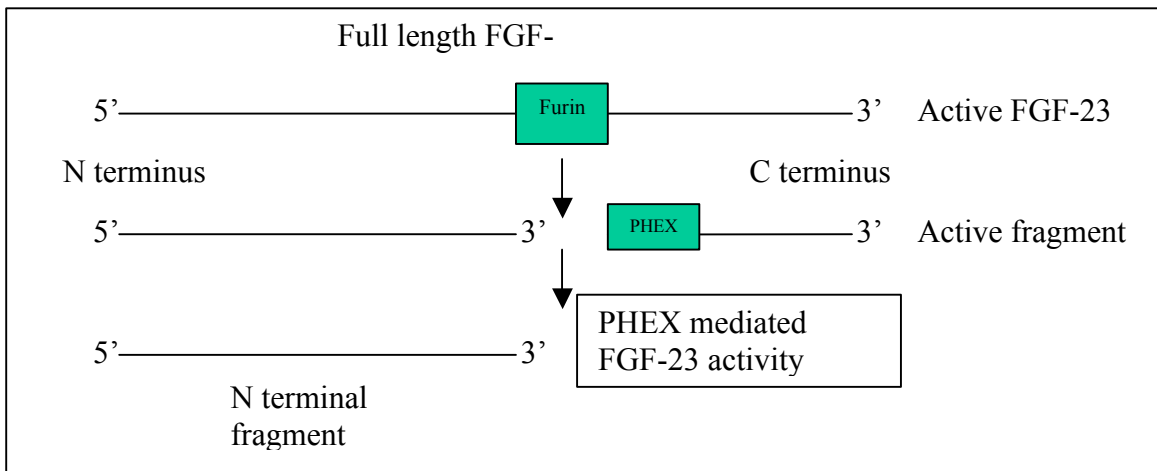
Figure 3. An illustration of bone deformation in children suffering from x-linked hypophosphatemia. Due to poor bone mineralization, structural integrity is weakened resulting on poor growth and bowing.

In XLH, ADHR, and OOM, elevated serum levels of biologically active FGF-23 are observed in most patients but the dysregulation of FGF-23 in XLH occurs in a different manner (HYP Consortium 1995). XLH patients have a mutated membrane bound endopeptidase, *PHEX* (Phosphate regulating gene with homology to Human Endopeptidase on the X chromosome). *PHEX* is a member of a family of homologous endopeptidases, many of which have been shown to control the activity of peptide factors by cleavage. *Bowe et al.* (2001) demonstrated that FGF-23 may be degraded by *PHEX* with a crude *in vitro* assay. Using recombinant human secreted *PHEX*, an *in vitro* assay was used to identify a consensus *PHEX* cleavage site (Boileau 2001). Coincidentally, this motif is present within the carboxyl fragment of FGF-23 (figure 4). These results are consistent with the hypothesis that the inactivating *PHEX* mutation protects FGF-

23 from degradation, which results in elevated levels of FGF-23 that, in turn, causes phosphate wasting.

The results of the Bowe *et al.* (2001) study was challenged by Guo *et al.* (2001). These investigators were unable to demonstrate that mouse recombinant PHEX cleaves a 14 amino acid peptide representing a fragment of human FGF-23 that contains the putative PHEX cleavage site. They suggest that FGF-23 is not a substrate for PHEX but that FGF-23 may be involved in a more complex model where FGF-23 may alter the production of the true PHEX substrate or alter the activity of PHEX. However, their results may also be explained if a PHEX-mediated cleavage of their FGF-23 peptide was not observed due to the absence of additional required recognition sites located outside the small 14 amino acid fragment used in their experiment. Furthermore, it is unlikely that the detection method used in this study would have distinguished the predicted cleavage product from the intact peptide.

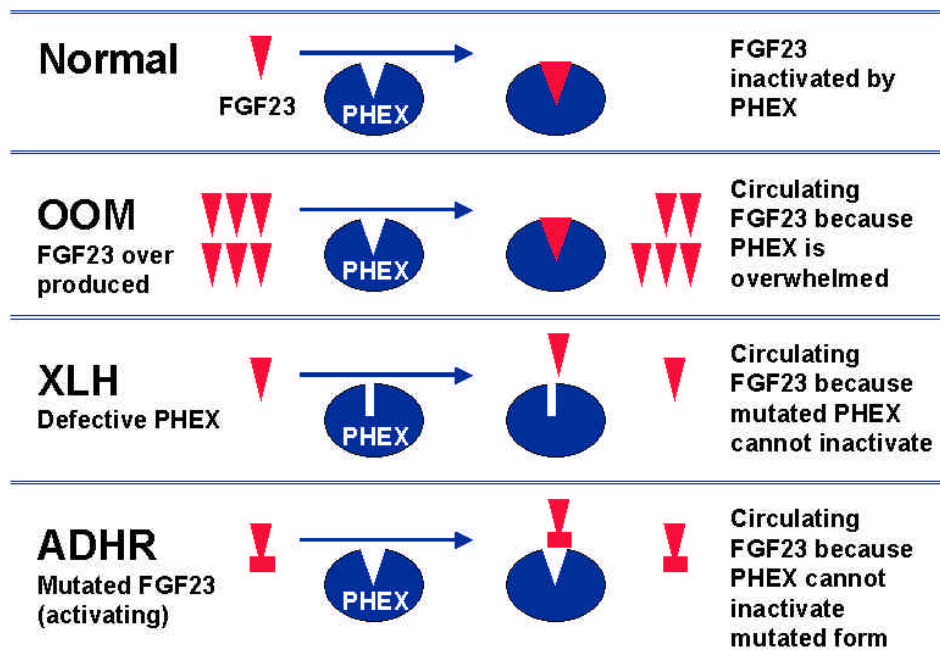
Figure 4. Illustration of PHEX mediated regulation of FGF-23 activity via an initial pro-convertase cleavage at the furin processing site. A pro-convertase cleaves FGF-23 into two fragments at the furin cleavage site and subsequently PHEX is capable of modulating FGF-23 activity.



Summary of phosphate dysregulation

XLH, OOM and ADHR cause a dysregulation of phosphate homeostasis resulting in hypophosphatemia that can lead to bone defects even though calcium homeostasis is maintained. Figure 5 illustrates a proposed model explaining the link of FGF-23 to all three phosphate wasting disorders.

Figure 5. Summary of three medical conditions, OOM, XLH, ADHR, that all result in elevated serum levels of FGF-23 and phosphate wasting. (Schiavi and Moe 2002)



Under normal conditions FGF-23 activity may be negatively regulated by PHEX.

In OOM, FGF-23 is produced in such excess that FGF-23 levels or activity can not be modulated. In XLH, the defective PHEX is unable to cleave and inactivate FGF-23. Specific mutations render FGF-23 resistant to processing by a yet unidentified pro-convertase enzyme within individuals with ADHR. As PHEX

prefers small molecular weight substrates, it has limited access to the intact non-processed mutant FGF-23 protein. In all the cases, FGF-23 is abundantly and detrimentally available to disrupt phosphate homeostasis. This hypothesis is supported by the recent findings that circulating levels of FGF-23 are elevated in most patients with XLH, ADHR, and OOM (Jonsson *et al.*, 2002, White *et al.* 2002, Yamazaki *et al.* 2002)

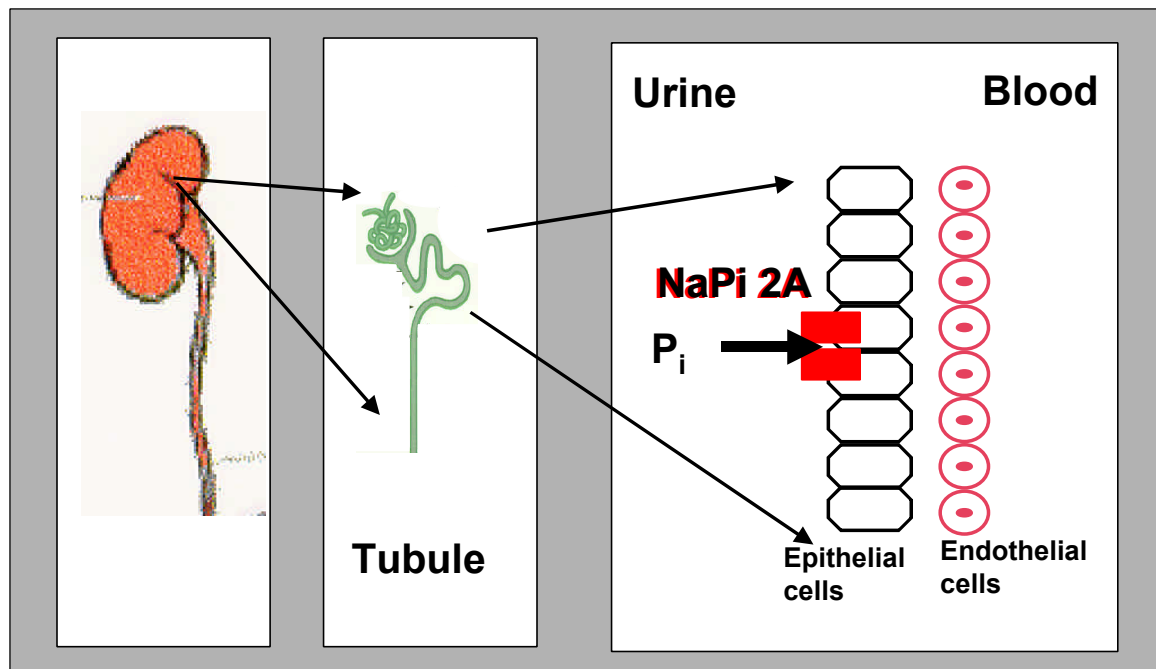
FGF-23 is a phosphate regulating hormone

Linkage of FGF-23 over expression with diseases of phosphate dysregulation suggested a role in phosphate regulation. FGF-23 assayed in subsequent *in vivo* and *in vitro* studies demonstrated that FGF-23 could directly regulate phosphate (Bowe *et al.* 2001, Yamashita 2002, *et al.* 2002, Shimada *et al.* 2002). The major site of phosphate regulation is in the kidney. Approximately 80% of phosphate that is filtered into the kidney is reabsorbed and released back into the blood stream through specific phosphate transporters called the type IIa sodium phosphate transporter (NaPi IIa) (Murer and Biber 1996) (**Figure 6**). NaPi IIa is primarily expressed in the brush border membrane of the renal proximal tubules. The microvilli that express NaPi IIa are located on the apical surface of the tubule. Under normal conditions, if serum phosphate is high, the kidney reabsorbs less phosphate and a greater percentage of phosphate is excreted as a waste product. In the diseased conditions described above, patients have low serum phosphate levels and elevated levels of phosphate in the urine. This scenario raised the possibility that FGF-23 could exert specific actions on the

kidney's control of phosphate. Thus, initial studies have examined FGF-23's ability to regulate phosphate secretion/reabsorption in appropriate *in vitro* and *in vivo* models.

In vitro studies have demonstrated that FGF-23 inhibits phosphate uptake in opossum kidney (OK) cells, a cell line derived from renal proximal tubule cells that continues to express NaPi IIa (Bowe *et al.* 2001, Yamashita *et al.* 2002). The OK cell assay is the classic method of measuring the PTH mediated effect on phosphate uptake. Bowe *et al.* (2001) developed an optimized assay to measure FGF-23 mediated effects. Both wild type and ADHR mutant forms of FGF-23 can produce up to a 60% reduction in phosphate uptake. The *in vitro* role of FGF-23 in phosphate transport provides a possible explanation for hypophosphaturia in OOM patients by reduced renal phosphate reabsorption in the kidney. From the *in vitro* OK assay we know that FGF-23 modulates phosphate uptake. Since human FGF-23 biologically affects opossum kidney cells, it is likely that human kidney cells are also responsive, especially with the clinical evidence linking FGF-23 to phosphate wasting in OOM, ADHR and XLH patients. Additionally, non-published data by Stephen O'Brien (Genzyme Corp.) has demonstrated that FGF-23 causes internalization of the NaPi IIa transporter, making it no longer accessible at the membrane, suggesting a mechanism by which FGF-23 could be blocking reabsorption of phosphate.

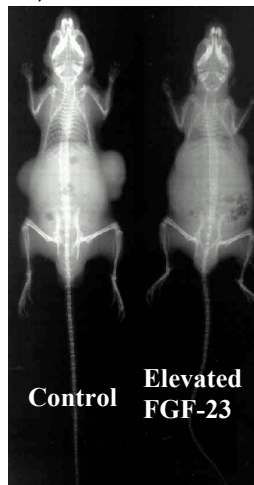
Figure 6. Illustration of phosphate regulation in the kidney. Tubules within the kidney contain NaPi IIa transporters that reabsorb phosphate (Pi) from the urine back into the blood stream.



In vivo experiments also demonstrate that FGF-23 has a role in phosphate regulation. Mice dosed three times in a ten hour period with recombinant FGF-23 exhibited phosphate wasting. Serum $1,25(\text{OH})_2\text{D}_3$ serum levels were low whereas serum calcium and PTH concentrations were unaffected (Shimada *et al.*, 2001, Shimada ASN 2002). Nude mice implanted with FGF-23 expressing CHO cells (Shimada *et al.* 2001), and transgenic FGF-23 knock-in mice (Shimada ASBMR 2001) have profound hypophosphatemia and low circulating levels of $1,25(\text{OH})_2\text{D}_3$. In addition, a significant decrease in bone density was observed in the transgenic compared to control animals at 45 days (figure 7). FGF-23 knockout mice show clinical symptoms of hyperphosphatemia and increased serum $1,25(\text{OH})_2\text{D}_3$ concentrations (Shimada, ASN 2002). Taken together, these

in vitro and *in vivo* results indicate FGF-23 plays an important role in controlling phosphate regulation. Furthermore, *in vivo* studies also suggest that FGF-23 plays a role in the regulation of the vitamin D pathway.

Figure 7. X-ray image of mouse implanted with CHO cells that over express FGF-23 compared to control. Mice exposed to higher than normal levels of FGF-23 have a lower bone density compared to control (Shimada *et al.* 2001).



Mineral Homeostasis

The intestine, kidney, and bone are the primary sites for mineral exchange. The minerals ingested are absorbed through the small intestine, secretion is modulated through reabsorption in the kidney, and the bone is utilized as a reservoir for rapid availability of the necessary minerals. Calcium, phosphorous, and magnesium are the three most abundant minerals that require constant regulation to maintain a proper balance of circulating and intracellular concentrations necessary for normal biological functions. The finding that a novel hormone exists that appears to regulate phosphate levels without causing net changes in calcium is a major advance in our understanding of mineral

homeostasis. Prior to the discovery of FGF-23, it was assumed that phosphate regulation occurred as a secondary action of PTH and Vitamin D₃.

The primary role of PTH and 1,25(OH)₂D₃ (active form of vitamin D) is to maintain calcium homeostasis (Figure 8a). Secretion of PTH occurs in response to low circulating levels of calcium. PTH increases re-absorption of calcium in the kidney while reducing re-absorption of phosphate in the kidney. Elevated levels of PTH increase the synthesis of 1,25(OH)₂D₃ by activating the key catabolic enzyme 1-alpha-hydroxylase (1αOHase) that converts the inert vitamin D (25(OH)D₃) into the active state of 1,25(OH)₂D₃. An elevated level of 1,25(OH)₂D₃ increases intestinal absorption of calcium and phosphate and mobilization of calcium and phosphate from bone stores leading to a normalization of calcium. Thus, these two hormones represent a cyclic feedback system to control calcium and phosphate.

Figure 8a. Ca^{+2} homeostasis via activity of PTH. Low Ca^{+2} in the extracellular fluid (ECF), mediates stimulation of PTH and the subsequent increase in $1,25\text{OH}_2\text{D}_3$ resulting in an increased serum Ca^{+2} by action on the intestine, kidney and bone while Pi wasting is increased through the kidney. Red arrow (low Ca^{+2}) initiates the cellular response, green arrows indicate what PTH act on, black arrows represent the subsequent mineral change.

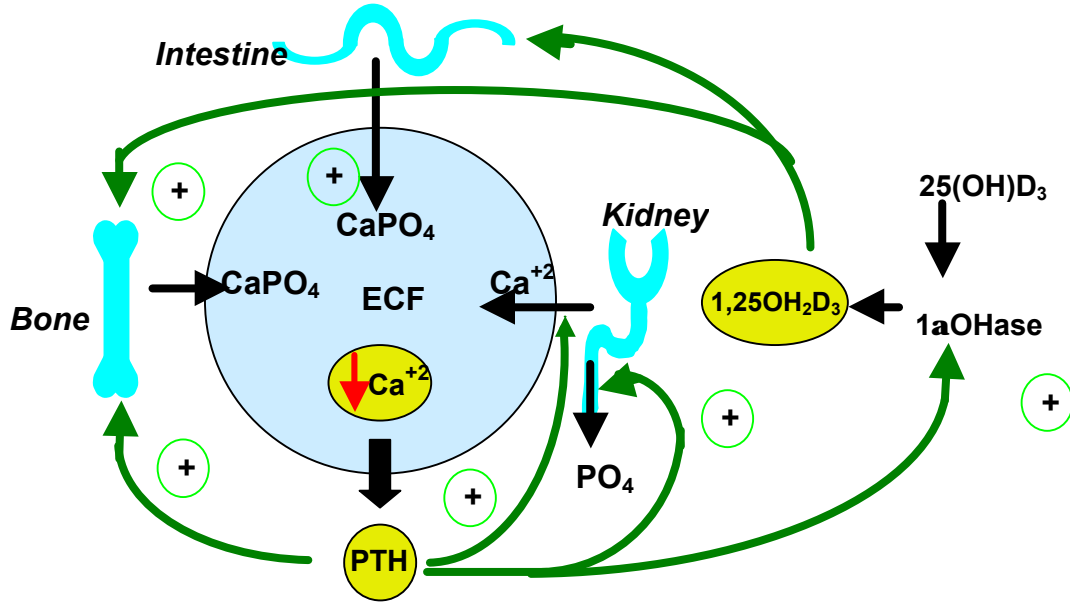
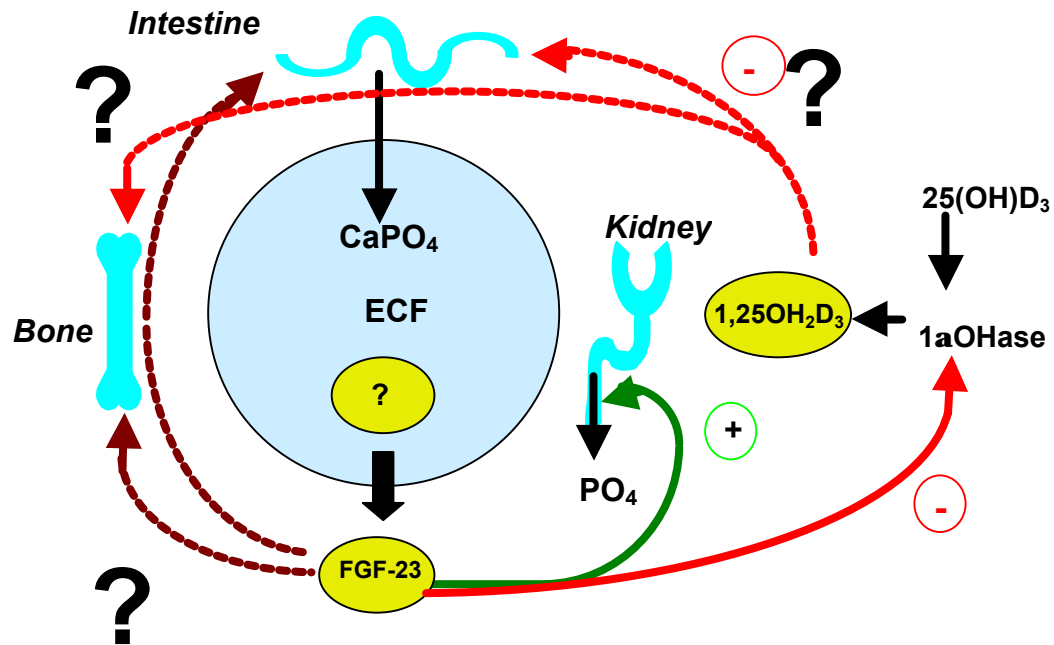


Figure 8b. The effect FGF-23 on PO_4 in the extracellular fluid (ECF). Evidence suggests that FGF-23 can directly act on the kidney and may modulate $1\alpha\text{OHase}$ to possibly reduce $1,25(\text{OH})_2\text{D}_3$ levels. It is uncertain whether FGF-23 can act directly on the small intestine or on the bone but the net effect is phosphate wasting through the kidney. It is uncertain what regulated FGF-23 but *in vivo* data suggest inhibitory action on $1\alpha\text{OHase}$ solid red arrow, and subsequent potential inhibitory action in the intestine and bone (dotted red line). Green arrows indicate positive regulation of PO_4 wasting through the kidney. Black arrows represent the subsequent mineral change. Dotted lines and ? indicate uncertain action.



FGF-23 and PTH appear to have some overlapping and some divergent functions. Both enzymes regulate phosphate reabsorption through the type IIa sodium phosphate transporters in the kidney. In contrast, PTH upregulates $1\alpha\text{OHase}$ expression whereas FGF-23 represses $1\alpha\text{OHase}$ expression. Thus the two hormones appear to differently control $1,25(\text{OH})_2\text{D}_3$. It is not yet clear how the body responds to the actions of these two separate hormones and why there is a need to control $1,25(\text{OH})_2\text{D}_3$ independently from phosphate. There are currently no indications that FGF-23 effects PTH levels or vice versa.

Sites of action for phosphate regulation

FGF-23 is a regulator of phosphate homeostasis. A key question is whether FGF-23 can act at other primary sites for phosphate regulation. Net circulation levels of phosphate are also influenced by regulation at the small intestine and the bone. The bone acts as a reservoir to supply phosphate to the circulatory system as needed to maintain homeostasis. The kidney, as discussed above, regulates the excretion rate of phosphate by modulating reabsorption of phosphate back into the circulatory system whereas entry of phosphate into the body is controlled by absorption in the intestine. In addition to these global regulatory actions of systemic phosphate concentrations, there are likely local control mechanisms that allow independent cells to regulate phosphate entry. FGF-23 may also play a role here. Local phosphate regulation must vary a little because the expression patterns of the phosphate transporters differ between cell types.

There are three members of the Na⁺-dependent Pi cotransporter family. NaPi-1 was the first to be cloned (Werner *et al.* 1991) but the specific physiological and functional role is still not certain (Werner *et al.* 1998). NaPi II has three isoforms. NaPi IIa and IIc are renal specific. Approximately 80% of renal phosphate transport occurs through NaPi IIa. NaPi IIb is located primarily in the intestine. The third family member of the Na⁺ dependent Pi cotransporter is NaPi-3. NaPi-3 cotransporter expression can be detected in osteoblast-like cells and may be important in the control of uptake during bone mineralization. The NaPi-III transporters are ubiquitously expressed and may be important targets controlling local changes or requirements for phosphate. NaPi III transporter function has also been implicated in the process of bone mineralization (Nielsen *et al.* 2001).

As previously discussed, FGF-23 is a secreted factor (White *et al.* 2001) which allows FGF-23 to have both systemic and localized effects. FGF-23 has been shown to have binding specificity for three of the five known FGF receptors (Yamashita *et al.* 2002; Pragnell, Genzyme Corp.). As expression patterns of NaPi transporters vary among cell types, so does the expression patterns of FGF receptors. As shown below, the known receptors that bind with FGF-23 are expressed in cell types representing the three sites of phosphate regulation. Therefore it is possible, but not yet demonstrated, that FGF-23 may affect phosphate transport in the large intestine and bone.

FGF receptors

The 23 known FGFs are believed to induce their specific signaling by binding to one or more of the four functional membrane bound receptors, FGF receptor 1-4 (FGFR) (Powers *et al.*, 2000). A fifth receptor (FGFR-5) has been identified but it is not believed to transmit a signal since it lacks a classic cytoplasmic signaling domain (Kim *et al.* 2001). Although the possibility of the FGFs interacting with novel receptors exists, none have been identified. FGFRs contain three immunoglobulin (Ig)-like repeats. It is likely that the homophilic characteristics of these Ig-like domains (Dackowski *et al.* 2002) within the extracellular domain of the FGFR promote dimerization of the membrane bound receptor. The extracellular portion of the receptor interacts with the FGF ligand, initiating the signaling cascade (Wiedemann and Trueb 2001). Every FGFR has a single hydrophobic membrane-spanning segment and a cytoplasmic tyrosine kinase domain. FGFR's 1-4 have 18-29 exons in each gene resulting in multiple splice variants which helps to explain how 23 FGF ligands can have only four functional receptor genes. For example, the gene that codes for FGFR-1 encompasses 19 exons that allows for complex alternative splicing which may affect ligand affinities to the receptor (Johnson *et al.* 1991). Although the manner by which FGFR expression is regulated within a cell type is not completely understood, it is possible that the alternative splicing may influence the functional expression of a receptor. This mechanism could account for the receptor expression differences among various types of tissues. In addition to the tissue type, the proliferative state of an osteoblast-like cell, SaOS-2, has been shown to

influence receptor expression profiles (Bilbe *et al.* 1996). Multiple isoforms and variable expression of FGF receptors and FGF ligands partially explains how 23 FGF family members can specifically signal through only four receptors.

Receptor mediated signaling by FGFs is also modulated by heparin sulfate proteoglycans (Pellegrini 2001). Classic heparin involvement in FGF signaling is associated to receptor dimer formation necessary for binding and signaling. FGF-23 contains heparin binding domains which suggests that heparin may directly interact with the structural conformation of the protein as well as during receptor dimerization.

FGF-23 signaling pathway

In vitro binding studies have shown that FGF-23 binds to FGFR-2, FGFR-3, and FGFR-4 (M. Pragnell, Genzyme Corp., personal communication). Yamashita *et al.* (2002) also found that FGF-23 binds to FGFR 2 and a splice variant of FGFR-3, FGFR-3c using *in vitro* Biacore binding studies. This study did not investigate the specificity or relative affinities of these interactions, nor did it investigate binding to FGFR4. Yokote (2002 ASBMR) has shown the expression of FGFR-2 and FGFR-4 but not FGFR-1 or FGFR-3 in opossum kidney cells, the most responsive cell line to PTH and FGF-23. Their studies suggest that FGF-23 signals through FGFR-2 and not FGFR-3c. Recent FGF-23/receptor binding studies suggests that heparin strongly affects binding specificity and activity (Pragnell and Bowe, Genzyme Corp., unpublished observations). Conflicting evidence exists suggesting heparin may inhibit (Bowe *et al.*, 2001) or activate FGF-

23's ability to modulate phosphate transport (Yamashita *et al.*, 2002). Further work is required to better understand the role of heparin. However, it is possible that differential expression of specialized heparan proteoglycans within various subclonal lines of OK cells may account for variable efficacy of FGF-23 efficacy in the opossum phosphate uptake assay.

It is unclear which receptor(s) is physiologically relevant but current studies agree that a known FGFR is likely to be involved in the initiation of the tyrosine signaling cascade. SU 5402 is an inhibitor for tyrosine kinases of the FGF receptors. SU 5402, blocks the activity of FGF-23 and subsequently enables phosphate uptake in an *in vitro* opossum kidney cell assay with the presence of FGF-23 was also shown (Yamashita *et al.* 2002). Evidence for FGF-23 induced tyrosine phosphorylation event has also been confirmed at Genzyme (S. O'Brien, personal communication).

To date only limited studies have investigated FGF-23 regulation of gene expression. *In vivo* studies have demonstrated that FGF-23 may reduce mRNA and protein expression of 1α OHase at specific time points post treatment and that type IIa sodium phosphate transporter proteins appear to be post-transcriptionally modified (Shimada, 2001 ASBMR abstract). How FGF-23 elicits these effects is not known. Additional FGF-23 regulated genes haven not yet been identified.

It is assumed that FGF-23 may regulate gene expression similarly to other family members. The binding of FGFs to FGF receptors triggers an autophosphorylation cascade and recruitment of phospholipases such as C-gamma and Crk. Tyrosine phosphorylation promotes associations of SNT1/FRS-2

docking proteins to FGF receptors. These docking proteins activate Ras that in turn activates the Raf-MEK-mitogen-activated protein (MAP) kinase pathway (Park *et al.* 2002). Ultimately, transcription factors such as Jun, Fos, and Myc are phosphorylated and gene transcription is further modulated.

Potential transcriptional regulation by FGF-23

This work is focused on developing a better understanding of FGF-23 induced gene transcription by monitoring transcription levels of thousands of genes using microarrays. Ultimately, the identity of the genes shown to be differentially expressed in response to FGF-23 will be used to infer potential functions of FGF-23 and to determine if the functions are consistent or variable across different sites of phosphate regulation.

Using Serial Analysis of Gene Expression (SAGE), OOM tumors were shown to over express genes involved in bone matrix formation, ion transport, phosphate homeostasis and mineralization (Jan de Beur *et al.*, 2002a). Genes relevant to phosphate homeostasis included two phosphate regulating factors, FGF-23 and frizzled related protein 4 (FRP-4) and the type III sodium phosphate transporter, Glvr1. Due to the large localized concentration of FGF-23 within the tumors, it is possible that FGF-23 may generate an autocrine effect and induce expression of additional genes. Thus, at least a portion of the differentially expressed genes in the OOM tumors represent genes induced directly by FGF-23. It is also important to point out that several additional cytokines, including transforming growth factor beta (TGF- β), insulin-like growth factor II (IGF-II) and

connective growth factor (CTGF), were over-expressed in the OOM tumors. Thus it is likely that these factors may also have participated in the upregulation of some of the OOM associated genes. To further explore genes of particular biological interest, a custom array was designed and generated which contains about 200 genes. Genes were selected based on their previously identified association to OOM tumors by SAGE analysis and/or literature searches of genes involved in phosphate regulation or bone metabolism. In an effort to monitor the maximum number of genes that may be affected by FGF-23, commercial arrays containing 7,200 unique genes were used to analyze samples.

PROJECT PURPOSE

The major goal of this project was to verify that FGF-23 could have a biological effect on the cell lines, Caco-2, HK-2, and SaOS-2, representing the three primary sites of phosphate regulation in the body (small intestine, kidney and bone, respectively). The second goal was to identify specific genes that were regulated by FGF-23 within each cell type and to determine if similar genes were affected across different cell types. We were also interested in learning if FGF-23 was acting as an autocrine factor and upregulating genes identified in the OOM tumor SAGE analysis. The overall goal was to develop a better understanding of how FGF-23 disrupts phosphate homeostasis.

ABBREVIATIONS

25(OH)D₃ pre-active form of vitamin D, 25-dihydroxyvitamin D₃

1αOHase 1-alpha-hydroxylase vitamin D activating enzyme

1,25(OH)₂D₃ 1,25-dihydroxyvitamin D₃, active form of vitamin D via 1αOHase

24OHase 25-hydroxyvitamin D-24 hydroxylase, vitamin D inactivating enzyme

1,24,25(OH)₂D₃ degraded form of active vitamin D via 24-hydroxylase

ADHR autosomal-dominant hypophosphatemic rickets

FGF fibroblast growth factor

FRP frizzled-related protein

PTH parathyroid hormone

OOM tumor- oncogenic osteomalacia

XLH X-linked hypophosphatemia

HK-2 human kidney 2 cells

SaOS-2 *Homo sapiens* osteosarcoma cells

Caco-2 colorectal adenocarcinoma

METHODS AND MATERIALS

FGF-23 purification

E. coli strain BL21 cells containing the PCR2.1-T7-CT-Taq FGF-23 expression vector (constructed by Finnegan (Genzyme Corp.)) were provided by Pragnell (Genzyme Corp). These cells express intracellular FGF-23 containing a carboxyl terminus histidine tag to aid in purification on a talon column and for immunoblot detection via anti-V5 antibody (Invitrogen Cat# 46-0708). 50 ml of LB media containing 50mg/L ampicillin was inoculated and grown for 8 hrs. A 50 ml culture was expanded to 4 liters of LB media with 50mg/L ampicillin and grown overnight at room temperature. Media was centrifuged at 4,500 relative centrifugal force (rcf) for 15 minutes to generate bacterial pellets. Pellets were stored at -80 °C until purification. Pellets were thawed on ice with the addition of H buffer (Buffer H: 50 mM NaPhosphate, 500 mM NaCl, 5 mM Imidazole, 1% glycerol, 0.1% Ipegal pH 7.0, 2 tablets of protease inhibitor per 50 ml buffer Roche Cat# 1873580) and vortexed to produce a cell suspension. Bacterial pellets were sonicated and insoluble bacterial cellular debris was removed from the lysate by centrifuging at 10,000 rcf for 15 minutes. The cell lysate containing solubilized FGF-23 was incubated with Talon beads (Clontech Cat# 8901-4) at room temperature, washed twice for 5 minutes with 10 ml H buffer and once with 100 ml I buffer (Buffer I: 50 mM sodium phosphate, 500 mM NaCl, 5 mM Imidazole pH 7.0). FGF-23 was eluted in 1 ml fractions using imidazole elution buffer

(Imidazole elution buffers: I buffer with the addition of 3M imidazole stock pH 7 diluted to 50 mM, 150 mM, 300 mM, 600 mM and 1 M). Elution fractions were analyzed by a coomassie stained tris glycine electrophoresis. Fractions containing FGF-23 of the appropriate size were pooled. Pooled fractions were diluted with H buffer to a final concentration of 150 mM imidazole and placed over a second column to obtain greater purity. The column was washed again as previously described and eluted. Eluted fractions were analyzed on coomassie gels and by immunoblot. Selected fractions containing high concentrations of FGF-23 with minimal contaminants were pooled, supplemented with 0.1% BSA (Sigma Cat# A-8918) and dialyzed into PBS (Gibco Cat# 20012-027). FGF-23 purity was evaluated with coomassie gel, immunoblot analysis and quantified by an anti-V5 antibody ELISA assay. The anti-V5 antibody ELISA assay, specific to the V5 tag on the wild type FGF-23, was developed and processed by Matijevic (Genzyme Corp.).

Immunoblot analysis

A 10 μ l sample of the FGF-23 elution fraction was electrophoresed using a 4-12% gradient NuPage Bis Tris gel (Invitrogen NP 0321) and 1 X NuPage MOPS SDS running buffer (Invitrogen, Cat# NP 465025). The protein was transferred to a PVDF membrane (Bio-Rad, Cat# 162-0174) using a Bio-Rad Semi-Dry transfer system. A 1X transfer buffer containing 20% methanol, 48 mM Tris and 39 mM glycine was used to transfer the protein from the Bis-Tris gel to the PVDF membrane for 20 minutes at 0.5 Amps. The PVDF membrane was blocked for 30

minutes in buffer containing 5 g dried milk per liter phosphate buffered saline (PBS). PVDF membrane was washed twice with PBS containing 0.05% Tween-20. The PVDF membrane was transferred into 10 ml blocking buffer containing 1:5000 diluted (2 µg) anti-V5-HPR antibody (Invitrogen Cat# R900-50) and incubated at least 1 hour at room temperature with gentle agitation. The PVDF membrane was washed twice with PBS containing 0.05% Tween-20. SuperSignal West Pico (Pierce Cat# 34080) was used for chemiluminescent detection. Kit provided peroxide solution and luminol/enhancer solution was mixed at a 1:1 ratio with a final volume of 3 ml. The PVDF membrane was incubated for 5 minutes, the excess reagent drained and the PVDF membrane was exposed for 10 seconds to X-ray film (Kodak Cat# 165-1579) in a dark room. X-ray film was developed using a Kodak M35A X-OMAT processor.

Cell cultures

HK-2 (HTB-37), Caco-2 (CRL-2102), and SaOS-2 (HTB-85) cell lines were purchased from American Type Culture Collection (ATCC) and grown according to recommended guidelines. The human kidney proximal tubular cell line, HK-2 was grown in Keratinocyte SFM (Gibco Cat# 10724-011) with 5 ng/ml recombinant epidermal growth factor (Cat# 10450-013) and 0.05 mg/ml bovine pituitary extract (Cat# 13028-014). Cells were grown in minimum essential medium Eagle (ATCC Cat# 30-2003) with 2 mM L-glutamine, Earle's BSS with 1.5 g/L sodium bicarbonate, 0.1 mM non-essential amino acids, and 1.0 mM sodium pyruvate, 50 I.U./ml penicillin and 50 µg/ml streptomycin (Gibco Cat# 15140-122),

and 20% fetal bovine (Gibco Cat#16000-044). Caco-2 cells were originally isolated from a primary colonic tumor and possess a large intestine phenotype prior to differentiation. For these studies Caco-2 cells were induced to differentiate into a small intestine phenotype by maintaining the culture at 100% confluence for 10 days while fresh media was replenished 2-3 days (Mariadason *et al.* 2000). SaOS-2 cells are osteoblast-like cells grown in DMEM/F-12 (Gibco Cat# 11330-032), 50 I.U./ml penicillin, 50 µg/ml streptomycin (Gibco Cat# 15140-122), and 10% fetal bovine serum. An SaOS-2 subclone (provided by Ann Bowe, Genzyme Corp) designated as G4A, was selected for array analysis because these cells were isolated based on their ability to maintain mineralization capacity. All cell lines were grown at 37°C in humidified air containing 5% CO₂.

Treatment of cells with FGF-23

Each cell line was expanded to eight T-160 flasks. 48 hours prior to FGF-23 treatment, fresh media containing 0.5% fetal bovine serum was added to the cells. SaOS-2 and HK-2 cells were near 70% confluence and Caco-2 cells had been maintained at 100% confluence for 7 days at the time of FGF-23 treatment. The recommended media for each cell line, with 0.5% FBS, was given to control cells at time zero, and corresponding media supplemented with 50 ng/ml FGF-23 was given to the test samples. At 24 hr, the media was removed from two control T-160 flasks and two FGF-23 treated flasks, cells were washed once with PBS and cells were then harvested after trypsinization (Gibco Cat#15050-065). Cells treated for a total of 72 hours were given the appropriate fresh media at 24 hour

and 48 hr. Following trypsinization, the cells were centrifuged at 3,000 rcf for 5 minutes, supernatant was removed, the cell pellets were flash frozen on dry ice and stored at -80°C until RNA isolation. The cells treated for 72 hours were harvested in a similar fashion as the 24 hour samples and stored at -80°C . Both SaOS-2 and HK-2 cells were less than confluent at the time of harvest.

RNA isolation

Cell pellets from two T-160 flasks, approximately 40 million cells (40×10^6) stored at -80°C were processed with Qiagen RNeasy Midi kit (Cat#74104). Lysis buffer (RLT) containing β -Mercaptoethanol (β -ME) was used to resuspend cells. To ensure complete lysis, cellular homogenate was processed with Qiasheader columns (Qiagen Cat# 79654). The midi kit protocol was followed with the addition of the recommended DNase treatment.

RNA gel electrophoresis

RNA was quantified by spectrophotometry (Beckman DU-600) at 260nm. 260nm/280nm ratios were above 2.0 for all samples. RNA integrity was determined by visualizing non-degraded 28S and 18S bands on denaturing RNA gels. 1% denaturing agarose gel contained 82.5 ml of water, 10 ml of 10X MOPS buffer and 7.5 ml of 12.3 M formaldehyde. 1X MOPS (Amresco Cat# E526) running buffer was used for electrophoresis. 2 μg of total RNA was loaded with denaturing RNA loading solution containing 45 μl 12.3 M formaldehyde, 45 μl 1 M

formamide, 10 µl 10X MOPS buffer (0.4 M MOPS pH 7.0, 0.1 M NaOAc pH 7.0, 10 mM EDTA pH 7.0), 3.5 µl (10 mg/ml) ethidium bromide 0.4 mg/ml, 1.5 µl 0.1M EDTA (pH 7.5) and 8 µl bromophenol blue dye (in 50% glycerol). Samples were heated at 70°C for 10 minutes and cooled on ice before loading onto the gel.

RT-PCR

RNA was isolated using Qiagen RNeasy kit as described above. FGF-23 is believed to signal through FGF receptors. Receptor mRNA expression profiling was completed on the four known functional fibroblast growth factor receptors (FGFR-1 (Accession number NM_015850), FGFR-2 (Accession number NM_022969), FGF-3 (Accession number NM_022965), FGFR-4 (Accession number L03840)) to provide a preliminary indication that the cell lines will be able to respond to FGF-23 treatment. GAPDH (Accession number AK026525) was assessed as a positive control. Forward and reverse PCR primers were designed using the Primer Express software program (PE Applied Biosystems). Thermocycling T_m was designed to be near 60°C and PCR products to be about 340 basepairs (bp) in size. Primers designed for FGF receptor profiling are shown in table 3.

Table 3. Forward and reverse PCR primers for amplification of FGFR 1-4 and GAPDH.

Gene name	Amplicon size	Forward primer 5'-3'	Reverse primer 5'-3'
FGFR-1	370bp	TTTGCCTTCACCCATAAGCC	ACCAGGAGCATCTTACCCGAT
FGFR-2	330bp	TGGCCTTCTGCTTCTGAGTTG	CGGCTATTGCAAAGTGACTGG
FGFR-3	320bp	GTGTGCAGGTTCCGATGTT	AACAAAATCGCACCTGCC
FGFR-4	360bp	TGACACAGTGCTCGACCTTGA	CATTTGCTCCTGTTTTCGGC
GAPDH	226bp	GAAGGTGAAGGTCGGAGT	GAAATCCCATCACCATCTTC

Applied Biosystems Taqman EZ RT-PCR kit (Cat# N808-0234) was used to generate oligo d(T)₁₆ primed cDNA in the reverse transcriptase step from 200 ng of total RNA template per sample. Invitrogen PCR super mix (Cat# 10572-014) was used to generate PCR reaction mix. 50 µl reaction was set up containing 200 nM final concentration of forward and reverse primer. 1 minute denaturing at 94 °C was followed by 30 cycles of 94 °C for 30 seconds, 60 °C for 45 seconds, 72 °C for 1 minute. Cycling was followed by a 10 minute 72 °C extension step was followed by a 4 °C hold until PCR fragments were analyzed by gel electrophoresis.

DNA gel electrophoresis

PCR products were visualized on 1X Tris acetate EDTA (TAE) buffer, 0.4 mg/ml ethidium bromide, 2.5% agarose gels. 60 volts were applied for approximately 30 minutes to allow for 3-4 cm migration of the loading dye front. PCR amplicons were visualized using an ultra violet light.

cDNA Synthesis and Indirect Fluorescent Dye Labeling for Commercial microarrays

To generate fluorescently labeled cDNA probes for Clontech vendor array hybridization, the recommended Atlas Glass Total RNA labeling kit (Cat # K1037-1) was used. This kit provided all reagents described below unless otherwise specified. Manufacturer's recommendations of 20 µg of total RNA from each of

the cell conditions described above was used in generating each labeling reaction. The 20 μg of total RNA was adjusted to 19 μl with deionized water, 5 μl of Random Primer Mix supplied with the array and 1 μl cDNA synthesis control (provided with the kit) was then added to the RNA sample. The mixture was heated at 70°C for 5 minutes and then cooled to 37°C. 25 μl of Master mix containing 10 μl 5X cDNA Synthesis Buffer, 5 μl 10X dNTP Mix, 7.5 μl Deionized H₂O and 2.5 μl MMLV Reverse Transcriptase (200 units/ml) was then added, the sample mixed and the reaction incubated at 37°C for 1 hour. To generate cDNA complex, the reaction was heated to 70°C for 5 min to activate the polymerase, followed by a further incubation at 37°C for one hour. 0.5 μl RNase H (10 units/ml) was added and the 37°C incubation was continued for an additional 15 minutes. To purify the cDNA, 0.5 μl of 0.5 M EDTA (pH 8.0) and 5 μl Quick Clean resin was added to the mixture and was pipetted onto a 0.45- μm Spin Filter and centrifuged at maximum speed in a microcentrifuge for 1 min. The filter was removed and discarded and 5.5 μl of 3M Sodium Acetate was added to the supernatant. 137.5 μl of ice-cold 100% ethanol was added to the sample and vortexed. The cDNA was precipitated by a 1 hour incubation at -20°C and then centrifuged at maximum speed in a microcentrifuge for 20 minutes. The supernatant was discarded and the pellet was washed once in 70% ethanol. 10 μl of 2X Fluorescent Labeling Buffer was added to the cDNA pellet for Indirect Fluorescent Dye Coupling. 0.5 μl Coupling Reaction Control Oligo was added to the cDNA sample and 10 μl of 5 μM fluorescent dye (cy3) and the mixture incubated at room temperature for 30 minutes. Fluorescent dye was kept in the

dark at all times. Fluorescent dye labeled cDNA was precipitated by the addition of 2 μ l 3 M sodium acetate and 50 μ l 100% ethanol and placed at -20°C for 2 hours. The tube was centrifuged at maximum speed in a microcentrifuge for 20 minutes. The supernatant was carefully removed and the pellet washed once in 70% ethanol and air-dried. The pellet was resuspended in 100 μ l deionized H_2O .

Purification of Fluorescent Dye Labeled cDNA

Fluorescent labeled cDNA was purified by a NucleoSpin[®] Column Probe Purification kit (Clontech Cat# K1037-1). All buffers used in the probe purification were provided with the Clontech kit unless otherwise specified. 400 μ l of Buffer NT2 was added to the 100 μ l of cDNA sample applied to the NucleoSpin Extraction Spin Column. The flow-through was discarded and the column was washed 3 times with 700 μ l of NT3 buffer. The column was centrifuged at maximum speed for 1 min between each wash. Purified and labeled cDNA was eluted by the addition of 50 μ l of NE buffer and centrifuged at maximum speed for 1 minute and repeated again to ensure complete elution. The cDNA quantity and cy3 incorporation efficiency was determined by spectrophotometry absorbency (A) at 260nm, 280nm, 450nm, 550nm and 650nm. Nucleic acid purity was determined by calculating the A_{260}/A_{280} ratio. The expected value was between 1.8 and 2.0. Nucleic acid/Cy3 incorporation ratio was calculated the $A_{260}/(A_{550} - A_{650})$ ratio. The expected value was between 8 and 20. Only probes with the expected absorbances and ratios were used for hybridization to the microarrays.

Commercial Microarray Hybridization

Clontech human Atlas glass 3.8I (Cat#7903-1) and 3.8II (Cat#7910-1) microarrays were used for gene expression analysis. The optimal amount of Cy3 labeled cDNA (V_{opt}) to be added to the array hybridization solution was determined by the recommended formula, $V_{opt}(\mu\text{l}) = (10/A550)$. Labeled cDNA was added to 2.1 ml of glass hybridization solution preheated to 50°C. All solutions were provided with the kit unless otherwise specified. The entire solution was mixed and quickly added to the hybridization chamber containing the glass microarray. The hybridization was conducted in the dark for a minimum of 16 hours at 50°C. Without allowing the array to dry, the slide was washed with the provided Clontech GlassHyb wash solution, twice with 1:10 GlassHyb wash and 1X Saline-Sodium citrate buffer (SSC), and once with 0.1 X SSC buffer. The glass array slides were dried by centrifugation at 1,500 rcf for 5 minutes. Arrays were stored in clean, dry and dark containers until image scanning.

Microarray Imaging and Analysis

The ScanArrayLite microarray analysis system by Packard Biosciences was used to scan for Cy3 fluorescence on the microarray. Laser power settings and photomultiplier tube settings were adjusted according to maximal signal without saturation or excessive background levels. BMP files were generated to save pictures of the fluorescence image and TIF files were saved for signal intensity quantification. TIF files were imported into Imagen 5.0 (BioDiscovery Inc.) and signal intensity for each spot, corresponding to every gene was

tabulated. In close proximity to each spot, a background signal was also measured. Microsoft Excel files containing gene identification information spot signal intensity and local background signal intensity were imported into GeneSpring 4.2.1 software (Silicon Genetics Inc.) for data normalization and analysis. Arrays were normalized to total signal intensity across control and sample slides. Signal intensities less than 500 units were considered to be near noise level and were statistically less reliable. Genes were designated as highly unreliable if both control and sample conditions generated signal intensity less than 500 units. Genes that had one or both conditions above 500 units remained in the primary analysis list. From this list, genes that showed a 1.5 differential in control versus the FGF-23 sample were designated as potential genes of interest. See tables 8 - 14 of the results section.

Custom Microarray design and construction

Target genes to be spotted were selected based on previous experimental data, known association to bone mineralization and/or differentiation or phosphate metabolism based on literature searches. Bioinformatics analysis by Liu of Genzyme Corp. identified human homologues to known yeast phosphate related genes. The oligos that were spotted onto the custom array were designed, manufactured, and purchased from Operon. Using Array Designer 2.0 (Premier Biosoft International) hybridization oligos of 68 nucleotides in length, within 1,500 nucleotides of the known carboxyl terminus of the gene sequence and unique to the human genome were designed. The sequences were provided to Operon to

construct the oligos. All of the oligos were approximately 68-mers in length and designed to be the sense strand. The oligos were resuspended and adjusted to a working stock of 500 μM based on measured optical density. The oligos were printed in quadruplicate onto 40 3D-Link slides (Motorola). Quality control validation of correct spotting and negligible carryover was conducted by hybridization with Cy3-labeled random 9-mers to assess general slide quality. The microarrays were stored in a vacuum chamber until used in the experiments.

cDNA Synthesis and Direct Fluorescent Dye Labeling for Custom arrays

Total RNA was isolated as described above. A SpeedVac was used to reduce the 20 μg RNA to a volume of 4 μl (5 $\mu\text{g}/\mu\text{l}$). The volume was verified manually by a pipetman and adjusted accordingly. Total RNA was labeled using FluorScript cDNA labeling kit (Invitrogen Cat# L1013-01). The oligo(dT)12-18 primed direct labeling protocol was followed according to the manufacturer. Labeled cDNA was purified with provided purification kit and materials. 500 μl of loading buffer was added to the Cy3 labeled cDNA mix and added to the purification column. The column was centrifuged at 13,000 rcf and the supernatant removed. The column was washed twice with wash buffer and centrifuged as previously described. The purified and labeled cDNA was eluted in 100 μl of the provided elution buffer. Hybridization, washing, imaging, and analysis was conducted as previously described for the commercial microarray.

Real-time PCR (SYBR Green)

RNA used for array hybridization was also used for real time RT-PCR analysis of selected mRNAs. Nine genes were selected for real time RT-PCR validation based on preliminary array data and literature searches. **Table 4** contains the sequences of the forward and reverse primers. PCR primers were designed for 25-hydroxyvitamin D 1 α OHase Accession number (Acc#) (Acc# NM_000785), Vitamin D receptor-1 (Acc# NM_000376), 24OHase (Acc# NM_000782), Parathyroid hormone receptor-1 (Acc# NM_000316), Parathyroid hormone receptor-2 (Acc# NM_005048), Somatostatin receptor-2 (Acc# NM_001050), Somatostatin receptor-3 (Acc# NM_001051), Somatostatin receptor-4 (Acc# NM_001052), Calcitonin (Acc# NM_001741), Mucin-2 (Acc# NM_002457), APC (Acc# NM_000038), AQP5 (Acc# NM_001651), AQP6 (Acc# NM_001652) CTNNb (Acc# NM_001904) and GAPDH (Acc# AK026525) using the Primer Express software program (PE Applied Biosystems).

Table 4. Primers designed for real-time RT-PCR validation.

Gene name	size	Forward primer 5'-3'	Reverse primer 5'-3'
25-hydro D-1 alpha	72b	GCTGGATGGCCTGAGGAAA	GCCAGCAGCATCAATGAACA
DVR-1	70b	CTGGCTGGCTAACTGGAAGC	TGCCACACATTCCTGCCTT
24-hydro	78b	CAGCACCATCTTCAGGTGCTT	CAGCCTCCCTTTCATGTCATG
PTHr-1	74b	GGCACTGGACTTCAAGCGAA	TTGTGTGGGACACCATGGG
PTHr-2	73b	GGAATCTCTCCGTGGACTGG	ACGGTGGTGAGCACTGAGC
SSTr-2	74b	AAGGTGAGCG GCACAGATG	TCCGTGGTCTCATTGAGCC
SSTr-3	64b	TCCCTCATGTGCCGCT	GGCAGAATATGCTGGTGAAGT
SSTr-4	67b	CTGCGCCAACCCTATTCTCT	GAGAACCCGCTGGAAGGATC
Calcitonin	70b	CTCAGTGAGGACGAAGCGC	CACTGGCCTTCATCTGCACAT
Mucin-2	61	CCCAACTTTGATGCCAGCA	AGCATCCATTGGGCATGAA
APC	82	TGGAGCTCAGTAAAAGTAAAT TCATGTAA	TGTGGGCCTATTATGCTCAATG
AQP5	60	CCCTGCGGTGGTCATGA	ATGGGCCCTACCCAGAAAAC
AQP6	71	GGTGGGATAGAGGAAGGGAG G	GGCAAGCACCTGGGAGG
CTNN beta	73	TGAACTTGCATTGTGATTGGC	GCACTTTCTGAGATACCAGCCC
GAPDH	226	GAAGGTGAAGGTCGGAGT	GAAATCCCATCACCATCTTC

QuantiTect SYBR Green RT-PCR kit (Qiagen, Cat# 204243) was used to quantify gene expression levels. Total RNA isolated from cell culture samples was used for real-time RT-PCR analysis. Each 50 µl reaction contained 50 ng of total RNA and 25 µl of 2x QuantiTect SYBR Green RT-PCR Master Mix, 0.5 µl QuantiTect RT Mix, a final concentration of 0.5 µM of forward and reverse primers. To generate standard curves, final concentrations of 12 ng, 1.2 ng, 12 pg, 120 fg, 12 fg, and 0 fg of corresponding template oligonucleotides were added to 50 µl reactions. The real-time cycling conditions was as follows: 30 minutes at 50 °C for reverse transcription, 15 minutes at 95 °C for initial activation, followed by 40 cycles of 15 seconds at 94 °C, 30 seconds at 60 °C, 30 seconds at 72 °C in a real-time RT-PCR System 7700 (Applied Biosystems). GAPDH was used as the

housekeeping gene for sample normalization. The PCR amplification product was visualized on a 3% agarose ethidium bromide gel to ensure proper amplification of a single band.

Delta CT analysis and GAPDH normalization

Comparative gene expression levels were determined following manufacturer's recommendations. The GAPDH gene was used as a reference and negligible variation was observed across samples. C_T is the threshold cycle value for a sample. C_T values are collected incremental at each cycle but assigned values are extrapolated to best fit the designated threshold value limit assigned for the data analysis and therefore the C_T is often not unit digit. The formula $\Delta C_{FGF} = C_{FGF}(\text{target}) - C_{FGF}(\text{GAPDH average})$ and $\Delta C_{\text{control}} = C_{\text{control}}(\text{target}) - C_{\text{control}}(\text{GAPDH average})$ was used to adjust sample values to a common reference gene. Comparative fold expression levels were calculated with $2^{-\Delta\Delta CT}$ where FGF-23 treated and control cells were normalized to the GAPDH reference gene.

Where: $\Delta\Delta CT = \Delta C_{T \text{ FGF-23 treated}} - \Delta C_{T \text{ control}}$

Quantitative expression levels were obtained by comparison to a standard curve of known spiked target numbers.

RESULTS

Cell Line Selection

The purpose of these experiments was to gain a better understand of how FGF-23 affects phosphate regulation by monitoring gene expression levels in cells believed to be involved in mineral regulation. Three cell lines representing the small intestine, kidney, and bone were selected to monitor FGF-23 induced differential gene expression. As illustrated previously (figure 8a), PTH directly affects calcium/phosphate reabsorption in the kidney and release of calcium and phosphate from the bone. Through its activation of $1,25(\text{OH})_2\text{D}_3$, PTH indirectly affects phosphate absorption in the small intestine. Similarly, FGF-23 may act on all three tissues. FGF-23 has been shown through *in vivo* studies to alter expression of $1\alpha\text{OHase}$ mRNA, which encodes the rate limiting enzyme for the production of $1,25(\text{OH})_2\text{D}_3$ (Shimada, 2002). Other genes are expected to be modulated by FGF-23 in the human epithelial proximal tubule kidney cell line (HK-2) as these cells represent the known functional site of action. Several lines of data suggest that HK-2 cells respond to FGF-23. First, FGF-23 induced tyrosine phosphorylation of several proteins within minutes of addition (Stephen O'Brien, Genzyme). Secondly, all known FGF receptors are expressed in HK-2 cells (figure 9b). Third, FGF-23 inhibited phosphate transport (Ann Bowe, Genzyme). Thus, HK-2 cells appear to be an appropriate cell line to study kidney specific FGF-23 regulation of gene expression.

The most accurate *in vitro* model available for the human small intestine was a differentiation induced colorectal adenocarcinoma (Caco-2) cell line. Prior to differentiation of the Caco-2 cells, they express a large intestine phenotype as demonstrated by the lack the type II NaPi transporter. Following Caco-2 differentiation, the small intestine tissue specific sodium-dependent phosphate transporter variant B of the type II NaPi gene was expressed (Karim-Jimenez *et al.* 2000). Again, tyrosine phosphorylation studies and receptor profiling suggests that FGF-23 was capable of acting on the Caco-2 cells.

The human SaOS-2 cell line represents an epithelial osteosarcoma osteoblast-like cell that expresses NaPi-3. In addition to the NaPi-3 transporters, gibbon ape leukemia virus receptor 1 (Glv-1), also known as solute carrier family 20 (phosphate transporter) member 1 (PiT-1), is another known transporter involved in phosphate regulation. Although Glv-1 is expressed in multiple tissue types, it is the primary phosphate transporter found in bone. Osteoblast-like SaOS-2 cells are used to evaluate the effect of FGF-23 on bone related phosphate regulation. Preliminary western blot and receptor profiling data indicates the FGF-23 can have a biological effect on SaOS-2 cells. It is uncertain which proliferative or differentiated state is optimal for observing the most accurate model for phosphate regulation within the bone. Some of the same genes are expected to be regulated across all cell types but variation was expected to be observed because the physiological functions are different and the primary NaPi cotransporter through which phosphate is transported differs across the three cell types.

RT-PCR analysis of cell lines for FGF receptor expression

As discussed in the background section, FGFR 2,3 and 4 have been shown to interact with FGF-23 *in vitro*. Expression of these receptors by the selected cell lines will support the likelihood of FGF-23 having a biological effect. Forward and reverse PCR primers designed for the C terminal region of FGFR1-4 were used to screen for receptor gene expression in HK-2, Caco-2 and SaOS-2 cells. The PCR products produced were of the expected size based on primer positioning (see methods and material section). The expected sizes for FGFR 1,2,3,4, and GAPDH are 370 bp, 330 bp, 320 bp, 360 bp, and 226 bp, respectively. The total RNA used as a template was DNase treated to ensure no genomic contamination. PCR products were not generated in the absence of reverse transcriptase (RT) indicating that the RNA was indeed free from genomic contamination. Figure 9 shows that all three cell lines express FGFR1-4. In addition, HK-2 cells also express the FGFR-like 1 (FGFRL-1) receptor. Of particular interest was the expression of receptors 2, 3, and 4 in lanes 4, 6, and 8, respectively. It is likely that FGF-23 signals through one or a combination of these receptors and their expression supports the likelihood of FGF-23 having a biological effect on cell types tested. The expression of FGFRL-1 was not tested in Caco-2 cells (figure 9c). FGFRL-1 lacks the cytoplasmic signaling domain and hence is likely not to be directly involved in signal transduction. FGFRL-1 may compete for FGFR-1 ligand binding.

FIGURE 9. Reverse transcriptase (RT)-PCR of FGFR genes. Fig. 9a. SaOS-2 cells, Fig.9b. HK-2 cells. Fig 9c.Caco-2. Lanes: 1.100 bp ladder, 2.FGFR-1, 3.RT negative FGFR-1, 4.FGFR-2, 5.RT negative FGFR-2, 6.FGFR-3, 7.RT negative FGFR-3, 8.FGFR-4, 9.RT negative FGFR-4, 10.FGFR-1, 11.RT negative FGFR-1, 12.GAPDH, 13. RT negative GAPDH. Fig.9c. Lanes 10 GAPDH, 11, TR negative GAPDH.

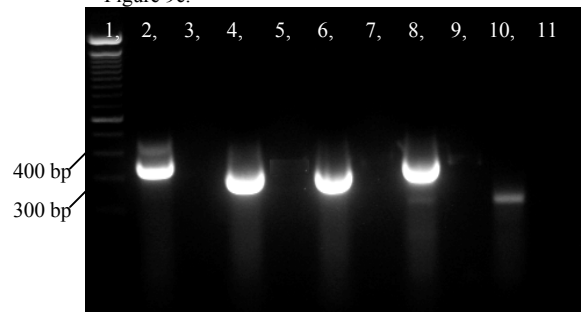
Figure 9a.



Figure 9b.



Figure 9c.



The data from the cell line FGFR RT-PCR profiling indicates that the receptors believed to be required for FGF-23 signaling are expressed in each cell line and the cells are therefore likely to be capable of responding to FGF-23.

To further validate the likelihood that FGF-23 is capable of inducing a signaling event within each cell type, O'Brien of Genzyme Corp tested total protein tyrosine phosphorylation in response to FGF-23 treatment. Cell lines that express FGFR-2 and/or FGFR-4 showed elevated levels of tyrosine phosphorylation using an anti-phosphorylated tyrosine immunoblot strategy, suggesting a classical receptor signaling event. Additionally, a negative control cell line, U937, was also analyzed and as expected did not show FGFR expression via RT-PCR (Data not shown). Consistently, U937 cells did not show

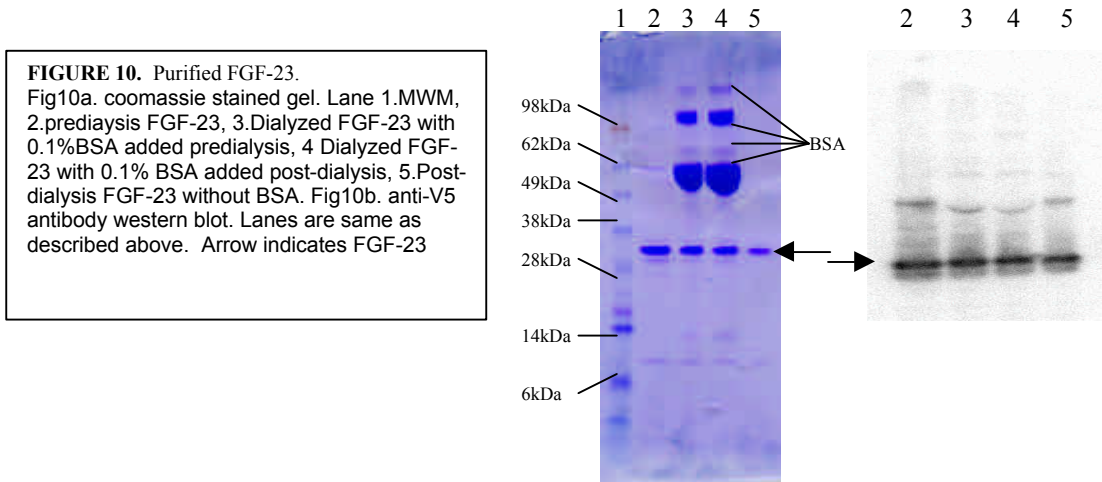
elevated phosphorylation in response to FGF-23 (O'Brien, Genzyme Corp., data not shown).

FGF-23 purification

To generate purified preparations of FGF-23, wild type human FGF-23 was expressed in bacteria (see methods and material section). The intracellularly expressed FGF-23 was purified using a double talon bead purification technique that yielded a highly pure FGF-23 protein. Specific conditions are described in the methods and material section. The recombinant bacterially produced FGF-23 contains a carboxy His tag to aid in purification and an anti-V5 epitope for antibody detection.

FGF-23 was eluted from the talon beads and separated into four homogeneous aliquots. Bovine solution albumin (BSA) was added to one aliquot of FGF-23 for a final concentration of 0.1% to act as a carrier to promote stability of FGF-23 and then dialyzed overnight into phosphate buffered solution (PBS). A second aliquot of FGF-23 was dialyzed into PBS over night and then BSA was added to a portion of the material post dialysis for a final concentration of 0.1%. A aliquot was not supplemented with BSA. Figure 10a illustrates the relative purity of each condition by coomassie gel. Lane two of figure 10a shows the purity of FGF-23 following the elution from the talon beads. Similar purity of FGF-23 is seen in lanes three and four but with the presence of BSA. Figure 10b is an anti-V5 -immunoblot of the same fractions. Anti-V5 immunoblot analysis demonstrated that the anti-V5 tagged FGF-23 was purified with the talon bead

protocol (figure 10b). A minimal amount of additional protein was detected at a higher molecular weight with the anti-V5 antibody.



FGF-23 concentration was determined by bicinchoninic acid (BCA) assay for samples without the addition of BSA. Pre and post dialyzed FGF-23 without BSA yielded 114 $\mu\text{g/ml}$ and 74 $\mu\text{g/ml}$ respectively. An anti-V5 antibody ELISA assay performed by Matijevic (Genzyme Corp.) on all four FGF-23 samples showed a similar 30% loss due to dialysis. FGF-23 with 0.1% BSA added prior to dialysis, with an estimated final concentration of 74 $\mu\text{g/ml}$ was used in subsequent experiments.

The biological activity of anti-V5 and histidine tagged FGF-23 was demonstrated by an opossum kidney phosphate uptake assay (conducted by Bowe, Genzyme Corp.) and by induced gene expression measured by array analysis. FGF-23 for which BSA was added prior to dialysis exhibited a 40%

inhibition of phosphate uptake at 20 ng/ml. Although it is not known whether the three variations from the endogenous form have subtle effects on FGF-23 action, the bacterially produced protein demonstrates potent biological activity in the OK phosphate uptake assay. Appendix A shows the biological activity of the purified FGF-23 used in the subsequent microarray analysis.

Selection of time points/Total RNA isolation from cell culture cells

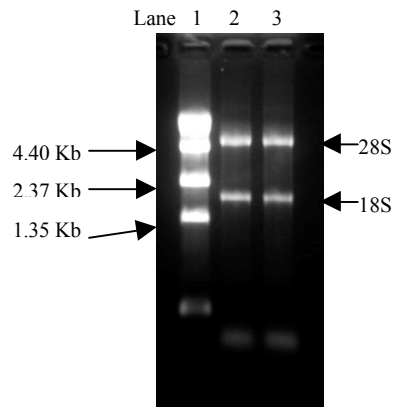
Two time points were selected to collect RNA samples from FGF-23 treated cells. All FGF peptides signal through one or more of the four known functional FGF receptors. As expected based on known signaling pathways for other growth factors, including other FGFs, it is likely that FGF-23 elicits a series of phosphorylation events which lead to rapid regulation of gene transcription within minutes (Greenberg, 1993). The earliest genes to respond to a growth factor are typically transcription factors (immediate early response genes) that induce the subsequent cascade of additional changes in gene expression. Genes encoding functions relevant to specialized changes in the cell are typically regulated after hours or even days of growth factor stimulation. As we were most interested in identifying genes that encode functions specific to FGF-23 within this study, later time points were selected to avoid measurement of early response genes. The earliest time points selected for collecting RNA samples was 24 hours based on initial reports that $1,25(\text{OH})_2\text{D}_3$ was induced in animals that received repeated injections of FGF-23 over a 24 hour period (Shimada *et al.*, 2001).

FGF-23 is linked to clinical phosphate dysregulation (OOM, XLH, ADHR) where patients are exposed to elevated levels of FGF-23 for a prolonged period. A prolonged exposure was also measured at a 72 hour time point. For the cells treated for 24 hours, FGF-23 was added at time zero and cells harvested 24 hours later. For the cells treated for 72 hours, FGF-23 was added at time zero, 24 hours and 48 hours. The repeated dosing was performed in an effort to mimic prolonged FGF-23 exposure while compensating for a limited half life of the protein. A more robust transcriptional response was observed at the 72 hour time compared to the 24 hour time point. A more detailed discussion on the FGF-23 regulated genes can be found below.

Total RNA isolation from cell culture cells

Each cell line was treated with 50 ng/ml FGF-23 for 24 hours or 72 hours. Cells were trypsinized, collected, and stored at -80°C until processed for RNA extraction. The isolated total RNA was DNase treated and the integrity of the RNA was verified using a denaturing RNA gel. The intact 28S and 18S ribosomal RNA bands at approximately 4.5 and 1.9 kb demonstrated that the RNA was not obviously degraded. RNA for HK-2 cells are shown (figure 11), RNA from other cell lines appear similar.

FIGURE 11. Ethidium bromide stained reducing RNA gel. Lane 1. RNA MWM, 2. RNA from HK-2 cells treated with FGF-23, 3. RNA from HK-2 control cells without FGF-23 treatment. 2 µg of total RNA is contained in each sample lane. No RNA degradation is observed.



RNA contamination by protein and/or DNA was assessed by spectrophotometer optical density ratio measurements at 260nm absorbancy/280nm absorbancy which was always greater than 2.0.

RNA labeling for array analysis

Two fluorescent labeling methods were used to detect gene expression quantities using microarrays. The Atlas fluorescent indirect labeling kit recommended by Clontech was used to prepare RNA that was hybridized to the Clontech Atlas arrays. In addition to the manufacturer's recommendation, the atlas labeling technique was used because initially Cy3 and Cy5 incorporation was to be used. Cy3 and Cy5 dyes were to be used so that FGF-23 treated and control labeled RNA could be analyzed in the same microarray, hence reducing inter-microarray variability. Due to a size variation between the two dyes, an indirect labeling method produces a more even incorporation into the probe

representing the gene transcript than a direct labeling method. In the indirect labeling method, following the first-strand cDNA synthesis, a second step was required to couple the fluorescent dye to the amino-modified cDNA. In the direct labeling method, fluorescent labeled dNTPs are directly incorporated during cDNA synthesis. Due to extensive Cy5 detection problems, Cy3 was the only fluorescent dye used for detection. Since dye incorporation variation was no longer an issue, a direct labeling method was used for all custom array analysis. The Invitrogen direct labeling technique required far fewer manipulations of the RNA and hence generated less variability between RNA labeling preparations.

Cell line conditions and microarray strategy

Using the same batch of purified FGF-23, cells were treated with 50 ng/ml FGF-23 in cell culture media for 24 hours or 72 hours. As described in the methods and material section, cells treated for 24 hours were given fresh media containing FGF-23 at time zero and cells were harvested 24 hours later. The cells treated for 72 hours were given fresh media containing FGF-23 at time zero, 24 hours and 48 hours. Control cells were given fresh media without FGF-23 at the same intervals. All cells were handled in as uniform fashion as possible. The entire batch of cells was processed to obtain DNA free total RNA. The same RNA batch was used for each of the three array analyses and subsequent real-time RT-PCR validation, but the fluorescent dye labeling was processed independently for each array hybridization replicate.

Three independent array types (Clontech Vol. I, Clontech Vol. II, and a Custom array) were used to monitor gene expression levels at the two time points. **Table 5** summarizes the number of RNA labeling and microarray hybridization replicates analyzed at each condition. RNA for each cell line collected (24 hour and 72 hour time point) was obtained from a single *in vitro* experiment.

Table 5. Summary of replicate labeling and analysis of cell line conditions using Clontech human atlas microarray volume 1, volume 2 and custom microarray.

Cell Type	Condition	Clontech Vol. I	Clontech Vol. II	Custom Array
HK-2	24 hr +/- FGF-23	3	2	1
HK-2	72 hr +/- FGF-23	1	1	1
Caco-2	24 hr +/- FGF-23	2	2	1
Caco-2	72 hr +/- FGF-23	2	2	1
SaOS-2 –G4	24 hr +/- FGF-23	1	1	1
SaOS-2 –G4	72 hr +/- FGF-23	1	1	1

In an effort to analyze most genes of potential interest prior to further scrutiny, a cumulative list was generated containing all genes that were expressed greater than 1.5 fold (FGF-23 treated / control cells) in both commercial microarray I, II, and custom microarray at both 24 hours and 72 hours. Typically, a two-fold difference in expression is considered to be biologically significant. However, to compensate for the lack of experimental replicates, the inherent variability of the array technology, and the reduced dynamic range of the array technology, it was decided to lower the cut-off limit to 1.5 fold difference. It was hoped that this strategy would identify gene expression trends across cell types, time points, and array types. By incorporating all genes with a 1.5 or greater fold difference, fewer genes of potential biological relevance will be missed. The

consequence of this strategy will also mean that genes will require further validation by another quantification tool to confirm expression levels since the number of false negatives will likely be high. The 1.5 fold up and down regulated lists contained approximately 3200 genes that were differentially expressed at least once (data not shown). To reduce these lists to a more manageable size and to help identify truly differentially expressed genes, emphasis was given to genes that were reproducibly regulated in replicate experiments within one cell type or across more than one cell type. This strategy allowed a preliminary assessment of the ability of FGF-23 to regulate gene expression across the various cell types. Furthermore, we hoped to observe general trends in the types of genes regulated by FGF-23 using this approach.

Microarray data filtering

The unit of relative signal intensity measured by the array imaging system can range from 0 to 100,000. These values are arbitrary because they are dependent on the power setting of the laser photo multiplier tube and gain setting. The imaging settings were adjusted for maximal signal without saturation (near 100,000 units). Values close to 500 are considered to be too close to background signal intensity and require special attention. Genes that generate a signal intensity of less than 500 units in both treated and control condition were discarded because the values are highly unreliable. About 15% of the genes on the commercial array and about 30% on the custom array never generated a signal greater than 500 units. Constant signals, for all tested conditions, below

the level of detection can be explained by poor hybridization specificity, low gene expression, no gene expression, or unknown alternative splicing. Genes that had either the treated or control (but not both) less than 500 units were retained but the calculated fold induction was unreliable. These genes may have an important biological role but since one condition was below the level of accurate detection, an accurate fold induction could not be extracted, only a notable difference between FGF-23 treated and control cells can be identified. Since triplicate microarray analysis was not conducted for all cell types at all time points, a reliable fold induction required the validation by real-time RT-PCR.

Microarray caveats

Microarrays are a powerful tool to measure gene expression profiles. Although this tool allows one to monitor a significantly higher number of genes compared to other methods of mRNA analysis, the capability of the technology is pushed to the limit by demanding greater sensitivity and qualitative answers. Not only is there great variability within the technology itself but the analytical methodologies are still under development and no standard currently exists. There are several sources of variability in processing a microarray. There is inherent variability in the probes, the pins used to spot the probes, array preparation and fluorescent dye labeling of the target, hybridization processes, background noise, spot overshining effect, and image processing (Spruill *et al.* 2002). While microarrays provide valuable insight into transcriptional gene

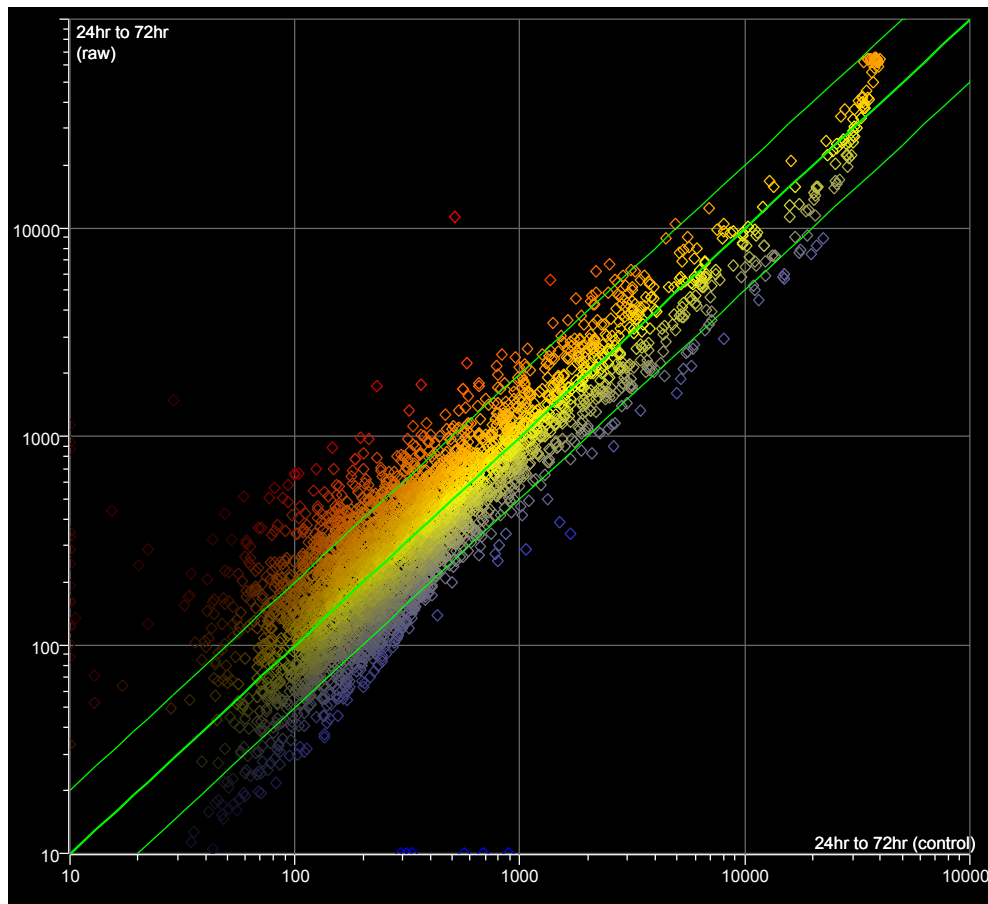
regulation, for the previously mentioned reasons, the expression levels of selected genes of interest should be validated by an alternative method. Alternatively, general information from the expression of families of genes or genes associated with similar functions or pathways may be surmised from microarray analysis, but it is important to utilize the information obtained from non-validated microarray analysis, for the purpose of generating rather than proving a hypothesis.

Array variability assessment

To determine the variability of microarray data and to gain an understanding of the potential degree of false positives and false negative data points, replicate microarray data sets obtained from one biological sample (RNA isolated from non-treated cells) were compared. Under highly reproducible conditions, two data sets normalized to total signal intensity should yield consistent results where all data points would fall onto the middle diagonal line when plotted against each other on the X and Y axis (Figure 12). Each spot on the graph represents a unique gene which is quantified on the microarray by a fluorescent intensity. The fluorescent intensity positioned in the X-axis represents one data set and the Y-axis represents a second data set. Data points that fall above and below the two outside lines indicate a false 2 fold induction. Various sources may cause this variability including the indirect labeling technique recommended by Clontech. Additionally, as the signal intensity decreases, the variability and likelihood of false signaling increases as seen in the lower left-hand

corner of the graph. For all of these reasons, only genes identified to be differentially expressed in at least two separate array experiments were selected. Genes of biologically relevant functions were chosen for validation using real-time RT-PCR.

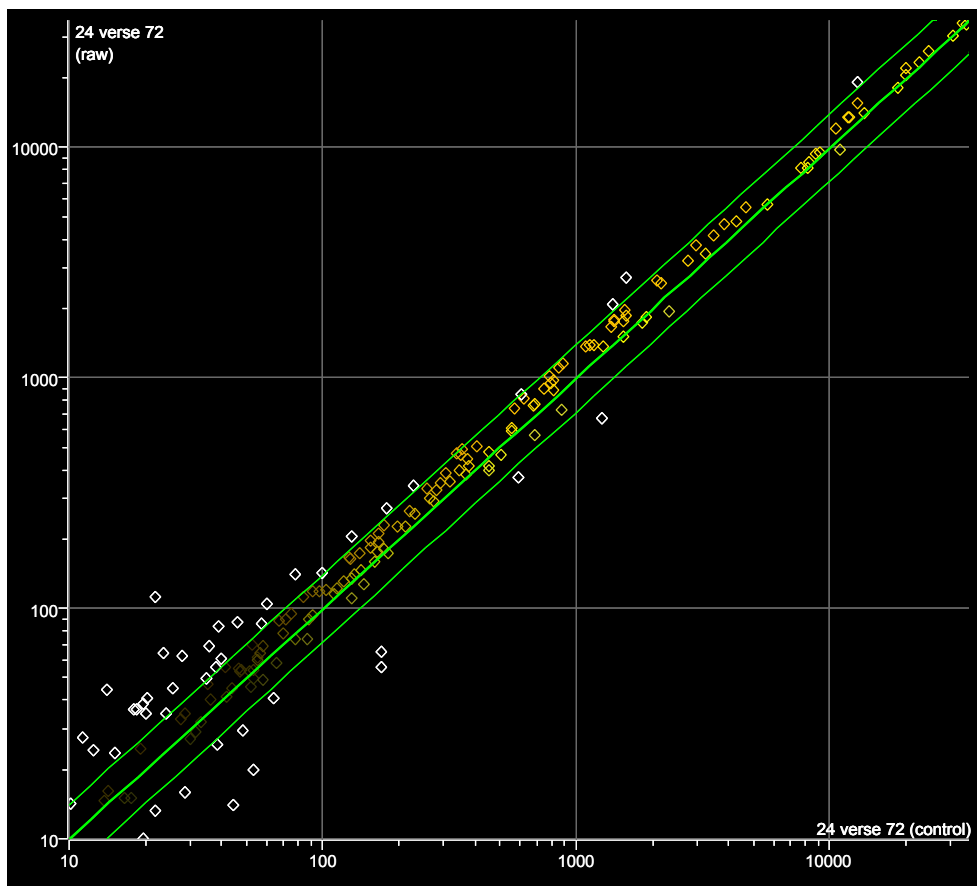
Figure 12. Commercial microarray variability. A comparison of two untreated controls. Red represents an increase and blue corresponds to a decrease in gene expression.



Similar to the above commercial microarray variability assessments, the custom microarrays were also tested for inherent false signaling (Figure 13). One difference between the two array types is that only 200 different genes were

spotted on the custom array compared to 3,700 present on each commercial array. Each gene was spotted four times on the custom array, for a total of 800 spots, compared to only once on the commercial array. The data points were the average of the four gene signal intensities. A direct labeling technique was used instead of the previously discussed Clontech indirect labeling method. Although some variability is still observed, few false data points were seen to change greater than 1.5 fold and these were mostly observed in genes expressed at very low levels (figure 13).

Figure 13. Custom microarray variability. A comparison of two untreated controls. Red represents an increase and blue corresponds to a decrease in gene expression.



Selected genes modulated by FGF-23 as identified by microarray analysis

Table 6 is a brief list of genes generated by cross referencing genes identified to be differentially expressed using microarray analysis that had known functions that are potentially related to FGF-23 function. Expression ratios represent the relative expression level of a particular gene in FGF-23 treated samples relative to untreated samples. Genes with a ratio of 1.5 or greater represent potential candidate FGF-23 induced mRNA. In contrast, genes with expression ratios of less than 0.66 would represent potential candidate FGF-23 repressed mRNAs.

The observation that the two PTH receptors were activated in two cell types is of potential interest as it suggests that FGF-23 may regulate PTH action. The family of parathyroid hormones (PTH) and hence PTH receptors (PTHR) have been associated with calcium and phosphate homeostasis. PTH receptor 1 and 2 is induced 2.1 and 7.65 fold (respectively) after 24 hours of FGF-23 administration in HK-2 cells and 1.7 and 2.3 fold (respectively) after 72 hours of FGF-23 administration in Caco cells (Table 6). An upregulation in PTH receptor number could partially explain why net changes in PTH and calcium are not observed. Long term, an increased number of receptors could lead to increased PTH efficacy without any changes in the actual levels of PTH protein. PTH in turn could counter the FGF-23 controlled down regulation of $1\alpha\text{OHase}$ resulting in a net balance of circulating $1,25(\text{OH})_2\text{D}_3$. Differences in the level of PTH receptors in response to FGF-23 were not observed in the SaOS cells despite the known role of PTH in bone metabolism.

Another class of receptors of potential relevance is the somatostatin receptors. Somatostatin (SST) receptor-2 is a marker for osteosarcoma tumors of which OOM is a subclass (Jan de Beur *et al.* 2002b). All the members of the SST receptor family appear to be upregulated in the HK-2 cells between 1.7 and 2.7 fold (Table 6).

Differential expression of several aquaporin (AQP) transporters was observed in two cell types. Induction ratios for AQP-5 and AQP-6 mRNA were 2.2 and 1.6 in the 72 hour SaOS samples, and 2.1 and 2.9 in the 24 hour HK-2 samples. Of relevance is the observation that although AQP-5 and AQP-6 appeared to be induced at 72 hours in SaOS cells the ratios suggested a repression by FGF-23 at 24 hours. In addition, both genes appeared to be repressed in Caco cells at 72 hours based on the observed ratios of 0.60 and 0.36. These apparent differential responses across cell types may indicate that a different cellular response occurs in Sao-2 cells compared to HK-2 and Caco-2 cells. Alternatively, it may reflect the inherent variability of the microarray technique and suggest that the apparent difference in the expression of these genes in all or a subset of the three cell types represent false positives. It is uncertain whether the Saos-2 respond in a completely different manner or whether the cells were not in the appropriate cell state to robustly respond to FGF-23 treatment. However, it is apparent that the Saos-2 are transcriptionally less responsive than the other two cell lines studied because fewer genes appear to be differentially regulated. Recent reports indicate that heparin sulfates modulate FGF receptor/ligand specificity (Guimond and Turnbull 1999). Current

studies suggest that the various forms of heparin may affect FGF-23 specificity differently under specific conditions. Three forms of genes encoding heparin proteoglycans were down regulated in HK-2 and Caco-2 cells but are not significantly modulated in Saos-2 cells (table 6).

The biological significance of mucin-2 is unclear but it was observed to be up regulated between 1.5 fold to 3.2 fold in all but one condition tested. The consistency of apparent upregulation across three cell types increases the likelihood that mucin gene or mRNA is indeed a target for regulation by FGF-23. One of several functions with which mucin-2 is associated is abnormal cell growth. This function is consistent with other growth related and anti-apoptosis genes modulated by FGF-23 throughout the various cell types and time points.

Expression of FRP-4 mRNA is a potentially repressed gene based on the observed ratio of 0.61 in Caco cells treated for 72 hours. SAGE analysis demonstrated that FRP-4 upregulation is associated with OOM tumors (Jan de Beur *et al.* 2001). Similar to FGF-23, FRP-4 has also been demonstrated to regulate phosphate transport *in vitro* (Bowe *et al.* 2001) and *in vivo* (Berndt *et al.* ASN 2002). FRP-4 has been linked to apoptosis in cartilage (Shimada *et al.* 2001) and similar to other FRP family members may inhibit Wnt action (Schiavi and Moe 2002). Each gene specifically mentioned in this section was chosen for further validation using real time RT-PCR (see below).

The categorization of the genes listed in tables 6-13 represent general functions currently associated with the gene that were obtained from Clontech Atlas gene lists (BD Biosciences Cat# PT2593-CD), GeneSpring software (SiliconGenetics) and/or National Center for Biotechnology Information (revised October 10, 2001). The genes may possess additional functions that are not represented by the assignment of the categorization and the basic gene functions. The assigned functions have not been individually confirmed through direct literature review.

Table 6. Selected genes of interest up and down regulated greater than 1.5 fold from all cell lines, both time points and both array times but values may not be statistically significant due to limited replication of experiment.

Gene name	Accession	SaOS 24hr	SaOS 72hr	HK-2 24hr	HK-2 72hr	Caco 24hr	Caco 72hr	Basic function
Wnt related genes		Average fold expression versus control						
adenomatosis polyposis coli	NM_000038			0.49		0.66		Binds beta-catenin, involved in Wnt signaling
beta catenin -1	NM_001904				12.15		1.45	cell adhesion, signal transduction in the Wnt pathway
Frizzled Related Protein-4	NM_003014						0.61	Phosphatonin, associated with phosphate wasting, and Wnt signaling
May be involved in receptor binding								
heparan sulfate (glucosamine) 3-O-sulfotransferase 1	NM_005114				0.54		0.58	generating numerous distinct heparan sulfate fine structures that may play a role in FGF-23 specificity
heparan sulfate (glucosamine) 3-O-sulfotransferase 3A1	NM_006042				0.62		0.58	generating numerous distinct heparan sulfate fine structures that may play a role in FGF-23 specificity
heparan sulfate proteoglycan 2 (perlecan)	M85289			0.61	0.62	0.56		generating a myriad of distinct heparan sulfate fine structures that may play a role in FGF-23 specificity
Calcium and phosphate related								
24-OHase	NM_000782					2.07		Involved in calcium homeostasis, catalyzes vitamin D into the active state.
cadherin 15, M-cadherin (myotubule)	NM_004933				1.8	0.37		calcium binding, calcium-dependent cell adhesion molecule
FGF 23	NM_020638				0.23			Phosphatonin, associated with phosphate wasting, growth factor
PTH receptor 1	NM_000316			2.1			1.70	Involved in serum calcium level modulation
PTH receptor 2	NM_005048			7.65	0.65	1.5	2.3	Involved in serum calcium level modulation
somatostatin receptor 1	NM_001049			1.7				Expressed in tubules and glomeruli of human kidney, known to modulate tubular cell function and growth
somatostatin receptor 2	M81830				1.7	0.45	1.73	Receptor involved in calcium and phosphate regulation. OOM tumor marker
somatostatin receptor 3	NM_001051			2.7			0.63	Receptor involved in blood sugar modulation and cell growth
somatostatin receptor 4	NM_001052			2.6				Reported to be express in the human kidney
Membrane channels and transporters								
aquaporin 5	NM_001651	0.65		2.2	2.1		0.60	water channel, primarily expressed in salivary glands
aquaporin 6, kidney specific	NM_001652	0.63		1.6	2.88		0.36	Nitrate specific water channel
cross cell type expression								
mucin 2, intestinal/tracheal	NM_002457	2.3	1.7	3.2	1.5	2.2		Associated with abnormal growth and protection against infection

As illustrated in table 5, the HK-2 24 hour condition was the only sample analyzed three times using a single type of microarray. Table 7 is a selected compilation of up and down regulated genes that were reproducibly identified to be differentially expressed in triplicate repeat experiment using a single sample. When averaging multiple array data points with signal intensity values above the noise level (500 units of signal) 38 genes were identified to be consistently regulated up or down. As shown in table 7, several genes, in the 24 hour HK-2 samples, are involved in transcription (i.e. T-box 10 and paired-like homeodomain transcription factor 1), differentiation (Beclin 1, Myeloid differentiation response gene), and general changes in cellular metabolism (cytochrome P450, tubulin specific chaperone). No apoptosis inducing genes are seen. The consistent regulation across triplicate analysis strengthens the likelihood that the genes represented in Table 7 are indeed targets of FGF-23 action. As described below, real-time RT-PCR analysis was performed on two genes listed in table 7, aquaporin 5 and somatostatin 2. As expected, results confirmed aquaporin 5 and somatostatin 2 mRNAs are induced in HK-2 cells after 24 hours of treatment with FGF-23 (figure 20 and figure 30 respectively).

Table 7. Triplicate commercial microarray analysis of HK-2 genes up and down regulated 24 hours.

Gene Name	Accession	Ave fold	Basic function
General cell change			
adenylate cyclase 8 (brain)	NM_001115	2.5	Enzyme involved in energy production
cytochrome P450, subfamily I	NM_000499	0.34	Protein involved in the metabolism and synthesis of cholesterol, steroids and lipids
G protein-coupled receptor 8	NM_005286	2.6	has similarity to somatostatin receptors may regulate transport channels
pancreatic polypeptide	NM_002722	2.2	Regulator of pancreatic functions
proline-rich protein BstNI subfamily 4	NM_002723	2.5	Function unknown, may interact with concavalin-A binding proteins
Ribosomal protein L13a	X56932	2.0	component of large 60S ribosomal subunit
signal recognition particle 14kD	NM_003134	2.6	Subunit of protein targeting complex
somatostatin receptor 3	NM_001051	2.7	G protein-coupled receptor, signals through an inhibitory G-protein
synapsin I	NM_006950	1.7	Associated with neuronal growth and signaling
Tubulin-specific chaperone d	NM_005993	43.9	Involved in tubulin formation/cellular movement
ubiquitin-conjugating enzyme E2E 1	NM_003341	2.2	may catalyze cellular proteins before degradation
Cell differentiation			
Carcinoembryonic antigen-related cell adhesion molecule 3	NM_001815	2.3	May function in cell adhesion
cholinergic receptor, nicotinic, gamma polypeptide	NM_005199	2.1	clustering of acetylcholine receptors (AChRs) is an early sign of postsynaptic differentiation
Beclin 1	NM_003766	2.0	Anti-apoptosis
ES1 (zebrafish) protein, human homologue of	NM_004649	6.2	Similar to E. coli SCRIP-27A believed to be involved in differentiation
myeloid differentiation primary response gene (88)	NM_002468	2.0	Involved in myeloid differentiation
paired-like homeodomain transcription factor 1	NM_002653	2.3	Transcription factor that controls cell differentiation
pre-B-cell leukemia transcription factor 2	NM_002586	2.1	very strongly similar to murine Pbx2 known to be involved in differentiation
zinc finger protein 151 (pHZ-67)	NM_003443	2.3	Function unknown contains zinc-fingers
Cell division			
growth differentiation factor 10	NM_004962	0.46	TGF-beta family of growth factors member
RAD9 (S. pombe) homolog	NM_004584	2.0	may function as a cell cycle checkpoint protein during DNA synthesis
T-box 10	NM_005995	2.3	Polymerase II promoter transcription factor
TGFB inducible early growth response 2	NM_003597	3.7	Activates gamma-globin gene promoters
transcription factor 21	NM_003206	1.9	Expressed in kidney glomerular epithelial cells
TTK protein kinase	NM_003318	3.1	Essential for spindle assembly maintenance
wingless-type MMTV integration site family, 5A	NM_003392	0.48	Member of the Wnt family of cell signaling proteins, involve in oocyte growth
X-ray repair complementing defective repair in Chinese hamster cells 4	NM_003401	5.9	DNA synthesis and recombination
nuclear receptor subfamily, member 1	NM_000475	0.62	Inhibitor of growth by negative regulator of transcription
Membrane channels and transporters			
amiloride-sensitive cation channel 1, neuronal (degenerin)	NM_001094	4.2	sodium channel permeable to lithium and potassium ions
aquaporin 5	NM_001651	2.2	water channel
calcium channel, voltage-dependent, beta 2 subunit	NM_000724	2.1	voltage-dependent calcium channel
solute carrier family 1, member 6	NM_005071	2.0	High affinity aspartate/glutamate transporter
solute carrier family 10, member 2	NM_000452	3.8	sodium/bile acid cotransporter family
Metabolism enzymes			
arylsulfatase A	NM_000487	2.7	Lysosomal arylsulfatase A; hydrolyzes cerebroside sulfate
Phosphofructokinase, muscle	NM_000289	2.9	enzyme required for glycolysis
phospholipase A2, group IB (pancreas)	NM_000928	6.9	hydrolyzes the phospholipid sn-2 ester bond, involved in signal transduction
serum deprivation response	NM_004657	0.63	substrate for protein kinase C which is involved in cell signaling and calcium binding
Unclassified function			
small proline-rich protein 2B	NM_006945	1.9	Small proline rich protein

To obtain triplicate identification of up regulated genes across the three cell types, experimental results were cross referenced. The total number of times each cell line condition was analyzed was previously shown in Table 5. Genes identified to be above the noise level and significantly up regulated in the five HK-2 24 hour microarrays analysis experiments were combined. The four 24 hour microarrays analysis experiments for the Caco-2 cells were also combined and the two SaOS-2 microarray analysis experiments were combined. This provided a conservative strategy, again in attempt to retain true positives that might have arisen through averaging replicate experiments. The smallest number of genes identified as differentially expressed are in Saos cells partly due to the limited number of replicate microarray data sets. As shown in Figure 14a, 38 genes appeared to be commonly up regulated in all three cell types at 24 hours and Figure 14b shows 13 genes were universally up regulated at 72 hours.

Figure 14. Venn diagram of up regulated genes on both Clontech microarray 1 and 2 at 24 hours and 72 hours.

Figure 14a. 24 hour time point.

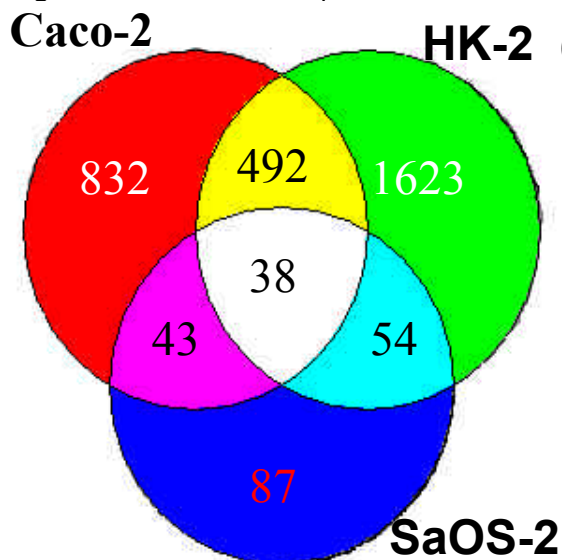
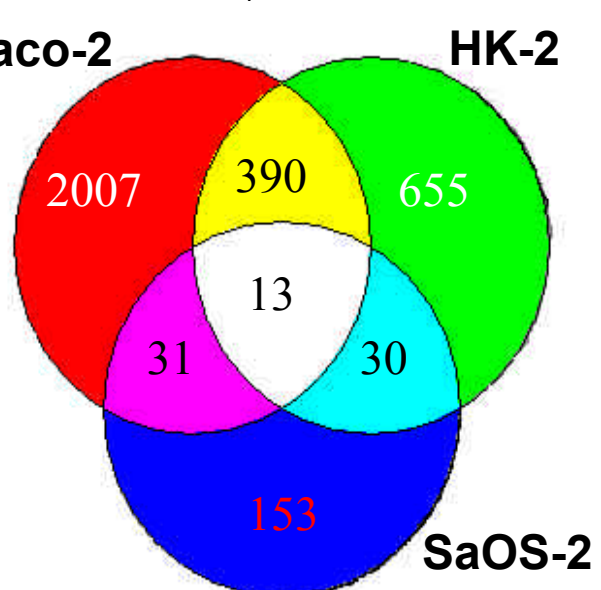


Figure 14b. 72 hour time point.



As shown in Figure 14b, 38 genes are up regulated at 24 hours in all three cell types as identified by commercially array analysis. Table 8 lists the 38 genes and the average fold induction as compared to the appropriate control. The genes observed to be up regulated across all three cell types at the 24 hour time can be categorized into similar biological classification as in the HK-2 24 hour triplicate analysis discussed previously. Genes in table 8 are generally associated with cellular growth and differentiation through transcription and cellular communication. None of the genes in table 8 are currently known to be associated with phosphate regulation or FGF-23 function. However, protein kinase C-like appeared to be upregulated an average of 3.13 fold and mucin-2 appeared to be upregulated an average of 2.57 fold. Protein kinase C like-1 may be associated with FGF ligand/receptor phosphorylation signaling and mucin-2 appeared to be most prominently upregulated by FGF-23 in all but one condition tested. It is not surprising that genes specifically associated with phosphate regulation may not be contained on this list because different mechanisms and pathways are believed to be involved in the method of phosphate regulation in the three tissue types represented by the three cell lines.

Table 8. Genes up regulated an average of 1.5 fold or greater in all 3 cell types at 24 hours by commercial microarray analysis.

Gene Name	Accession	Ave.	Basic function
General cell change			
Cbp/p300-interacting transactivator	NM_004143	2.25	may be a transcriptional activator
hepatocyte nuclear factor 3, alpha	NM_004496	2.66	transcription activators of liver-specific genes
immunoglobulin mu binding protein 2	NM_002180	2.44	involved in pre-mRNA processing and activation of transcription
integrin beta 4 binding protein	NM_002212	2.24	Links beta 4 integrin to intermediate filament cytoskeleton
intercellular adhesion molecule 4, Landsteiner-Wiener blood group	NM_001544	2.06	participate in cell adhesion as well as cell-surface mediated signaling
intercellular adhesion molecule 5, telencephalin	NM_003259	1.69	participate in cell adhesion as well as cell-surface mediated signaling
ladinin 1	NM_005558	2.48	may be an anchoring filament
leukemia inhibitory factor receptor	NM_002310	3.14	Involved in transmembrane signaling through receptor activation
major histocompatibility complex, class II, DR beta 5	NM_002125	2.30	complex binds peptides and presents them to CD4+ T lymphocytes
methionine-tRNA synthetase	NM_004990	2.15	functions in protein biosynthesis
mitogen-activated protein kinase 11	NM_002751	1.97	activated by stress and proinflammatory cytokines
mitogen-activated protein kinase 13	NM_002754	2.27	activated by stress and proinflammatory cytokines
mitogen-activated protein kinase 10	NM_002446	2.45	APT mediated catalytic activity
mucin 2	NM_002457	2.57	Associated with abnormal growth and protection against infection
myeloid differentiation primary response gene (88)	NM_002468	2.65	Involved in immune response signaling pathway
polymerase (RNA) II (DNA directed) polypeptide G	NM_002696	2.31	RNA polymerase II subunit
protein kinase C-like 1	NM_002741	3.13	Involved in phosphorylation mediated cell signaling
protein phosphatase 1, regulatory (inhibitor) subunit 8	NM_002713	2.33	Activator of RNA decay
RAB5C, member RAS oncogene family	NM_004583	2.59	Protein trafficking peptide
receptor-interacting serine-threonine kinase 2	NM_003821	2.33	Enhances CASP-8-mediated apoptosis
RNA (guanine-7-) methyltransferase	NM_003799	2.07	Involved in RNA capping
ubiquitin-conjugating enzyme E2E 1	NM_003341	2.23	may catalyze ubiquitination of cellular proteins prior to degradation
ubiquitin-conjugating enzyme E2I	NM_003345	1.81	ubiquitinates cellular proteins and marks them for degradation
v-ral simian leukemia viral oncogene homolog B	NM_002881	4.45	May be involved in transmembrane signaling
Cell differentiation			
homeo box B2	NM_002145	2.10	may regulate gene expression, morphogenesis, and differentiation
homeo box B3	NM_002146	2.43	may regulate gene expression, morphogenesis, and differentiation
myogenic factor 3	NM_002478	2.13	transcriptional activator involved in skeletal muscle differentiation
transforming growth factor, beta 3	NM_003239	1.73	cytokine family member , may be required for normal development
Cell division			
kinesin family member C3	NM_005550	3.44	may function in intracellular transport and mitosis
lectin, galactoside-binding, soluble, 7 (galectin 7)	NM_002307	2.51	Cell adhesion associated with normal cell growth and differentiation.
pancreatic polypeptide	NM_002722	2.35	mature peptide inhibits pancreatic exocrine function
semaphorin 3B	NM_004636	3.58	involved in neuronal growth
tumor necrosis factor superfamily, 14	NM_003807	2.36	Growth modulator
Membrane channels and transporters			
solute carrier family 10 member 2	NM_000452	2.92	important for reabsorption of bile acids from small intestine
iduronidase, alpha-L-	NM_000203	2.64	catalyzes degradation of disaccharides heparan
Unclassified function			
immunoglobulin superfamily containing leucine-rich repeat	NM_005545	2.13	may play a role in cell adhesion

As described above, Figure 14b illustrates the number of genes appeared to be commonly up regulated across three cell types at 72 hours as identified by commercial microarray analysis. Table 9 lists the 13 genes that appeared to be commonly up regulated under these 72 hour conditions and the average fold expression compared to control conditions. The genes listed below belong to various classifications but maintain a common theme of cellular growth and differentiation. Again, mucin-2 is observed to be potentially up regulated an average fold of 2.19 in the three cell types at 72 hours. Additionally, B lymphoid tyrosine kinase appeared to be seen up regulated 3.79 fold. The expression and function of B lymphoid tyrosine kinase is consistent with the activation of FGFRs by FGF-23 which results in a tyrosine phosphorylation cascade. The function of the genes in table 9 are not known to be directly linked to calcium and or phosphate regulation but expression of paired gene box 4 and mucin-2 are known to be involved in cancer growth.

Table 9. Genes up regulated an average of 1.5 fold or greater in all 3 cell types at 72 hours by commercial array analysis.

Gene name	Accession	Ave.	Basic function
General cell change			
B lymphoid tyrosine kinase	NM_001715	3.79	involved in tyrosine phosphorylation
mucin 2	NM_002457	2.19	Associated with abnormal growth and protection against infection
Cell differentiation			
ATPase, H+/K+ exchanging, beta polypeptide	NM_000705	2.23	Involved in transport
sialyltransferase 6	NM_006279	1.84	metabolism enzymes
UDP-Gal:betaGlcNAc beta 1,4- galactosyltransferase, polypeptide 5	NM_004776	3.03	metabolism enzymes
Cell division			
glutathione S-transferase theta 2	NM_000854	2.20	anti-apoptosis
hyaluronoglucosaminidase 1	NM_007312	2.16	cell growth and differentiation
metargidin, domain 15 (metargidin)	NM_003815	2.20	cell growth; cell-matrix adhesion
myeloid/lymphoid or mixed-lineage leukemia 2	NM_003482	1.68	transcription factor
paired box gene 4	NM_006193	1.60	transcription factor
RNA binding motif protein 3	NM_006743	1.78	Involved in RNA binding
Unknown function			
chromosome X open reading frame 5	NM_003611	2.09	Protein coding region
DNA segment on chromosome 21 (unique) 2056 expressed sequence	NM_003683	2.28	Protein coding region

To obtain triplicate identification of down regulated genes across the three cell types, experimental results were cross referenced in a similar manner as described previously for up regulated genes. The total number of times each cell line condition was analyzed is described in Table 5. Genes identified to be above the noise level and significantly down regulated in the five HK-2 24 hour microarray analysis experiments were combined. The four 24 hour microarrays analysis experiments for the Caco-2 cells were also combined and the two SaOS-2 microarray analysis experiments were combined. As shown in Figure 15, 15 genes appeared to be commonly up regulated in all three cell types at 24 hours, and 15 genes appeared to be down regulated at 72 hours.

Figure 15. Venn diagram of down regulated genes on both Clontech microarrays 1 and 2 at 24 hours and 72 hours.

Figure 15a. 24 hour time point.

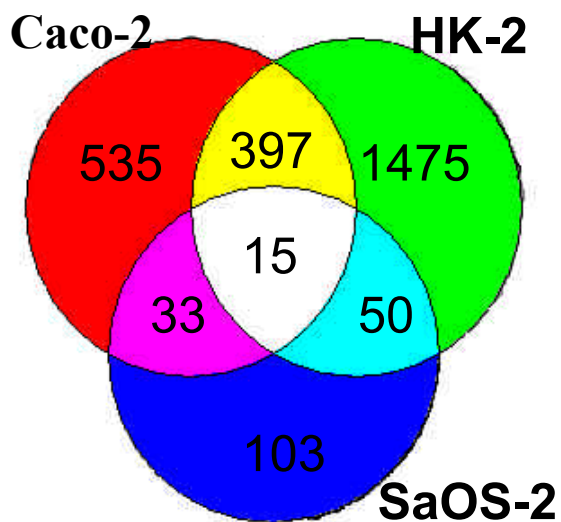


Figure 15b. 72 hour time point.

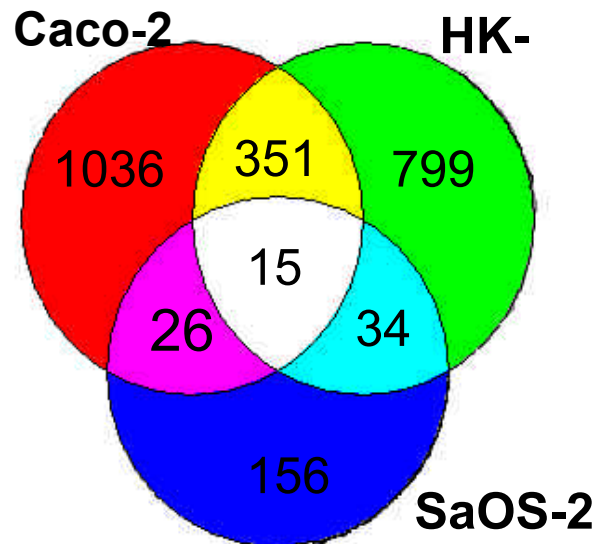


Table 10 lists the gene names and the average fold down regulation at 24 hours as shown in figure 15a. Genes associated with inhibition of transcription, apoptosis, and differentiation are potentially down regulated at 24 hours. The expression level of D-aspartate oxidase appeared to be down regulated 6.25 fold, the greatest at 24 hours. This gene was also identified as down potentially regulated in OOM tumors compared to non-OOM mesenchymal tumors in SAGE analysis conducted by Genzyme Corp. This parallel observation observed between two technologies and four biological samples, one of which represents a relevant *in vivo* condition, supports the likelihood that this gene is indeed an important target for FGF-23 regulation. Furthermore, the observation that this gene appears to be repressed *in vitro* by FGF-23 and *in vivo* in tissues over-expressing FGF-23 relative to histologically similar samples not expressing FGF-23, supports the hypothesis that some of the OOM associated genes are regulated directly by autocrine actions of FGF-23 in these tumors.

Table 10. Down regulated genes an average 1.5 fold or greater in all 3 cell types at 24 hour
A value of 0.666 or smaller indicates a significant down regulation of 1.5 fold or greater.

Gene name	accession #	Fold down	Fold up	Basic function
General cell change				
D-aspartate oxidase	NM_004032	6.25	0.16	Aspartic acid catabolism, repressed in OOM
dysferlin, limb girdle muscular dystrophy 2B (autosomal recessive)	NM_003494	2.04	0.49	involved in membrane regeneration and repair
eukaryotic translation initiation factor 3, subunit 5 (epsilon, 47kD)	NM_003754	3.85	0.26	stabilizes translation initiator subunits
Fas (TNFRSF6)-associated via death domain	NM_003824	3.23	0.31	Required for apoptosis signaling
interleukin 18 receptor 1	NM_003855	2.44	0.41	immune response, signal transduction
JAK binding protein	NM_003745	2.86	0.35	suppressor of cytokine signaling
KH-type splicing regulatory protein (FUSE binding protein 2)	NM_003685	2.44	0.41	Specific mRNA splicing of integrin signaling to the cytoskeleton.
mitogen-activated protein kinase-activated protein kinase 3	NM_004635	4.00	0.25	integrative element of signaling in both mitogen and stress responses
olfactory receptor, family 3, subfamily A, member 1	NM_002550	2.56	0.39	olfaction, signal transduction
small inducible cytokine subfamily A, member 13	NM_005408	3.13	0.32	immune response
syntaxin binding protein 2	NM_006949	2.22	0.45	intracellular protein traffic, and binds neurotransmitters that are released during calcium-regulated exocytosis
Membrane channels and transporters				
sodium channel, voltage-gated, type I, beta polypeptide	NM_001037	1.75	0.57	ion and sodium transport
Cell division				
histone acetyltransferase 1	NM_003642	3.85	0.26	DNA packaging, S-phase of DNA replication
numb homolog	NM_003744	4.17	0.24	generating asymmetric cell division during neurogenesis
Unknown function				
Ric	NM_002930	2.50	0.40	Calmodulin binding protein, function unknown

Table 11 contains the genes that are potentially down regulated at 72 hours as shown in figure 19b and the average fold expression compared to the control condition. Transcription and translation related genes appear to be down regulated at 72 hours. Interferon alpha 13 was seen to be potentially down regulated the greatest at a 2.86 average fold compared to the control condition. Tumor suppressor oncogene homolog B, which is associated with tumor suppression and calmodulin binding, appeared to be down regulated 2.27 fold. Calmodulin is involved in regulation of serum calcium levels and provides an

additional association of FGF-23 to calcium homeostasis similar to PTH related genes.

Table 11. Genes down regulated 1.5 fold or greater in all 3 cell types at 72 hour
A value of 0.666 or smaller indicates a 1.5 fold or greater down regulation.

Gene name	Accession #	Fold down	Fold up	Basic function
General cell change		regulated		
actin, gamma 1	NM_001614	2.27	0.44	mediators of internal cell motility
interferon, alpha 13	NM_006900	2.86	0.35	defense response
mesenchyme homeo box 2	NM_005924	1.96	0.51	transcription regulation
phosphodiesterase 6D,	NM_002601	2.27	0.44	solubilizes the normally membrane-bound holoenzyme
protein phosphatase 1, regulatory subunit 8	NM_002713	2.22	0.45	mRNA splicing, RNA catabolism
protein tyrosine kinase 9	NM_002822	2.27	0.44	protein amino acid phosphorylation
pyrimidinerbic receptor P2Y	NM_004154	2.00	0.50	mediates cellular signaling responses to nucleotides
retinoic acid receptor, alpha	NM_000964	2.38	0.42	stimulates transcription in a ligand-dependent manner
ribosomal protein L3	NM_000967	1.72	0.58	protein biosynthesis
ribosomal protein S16	NM_001020	2.70	0.37	protein biosynthesis
small nuclear ribonucleoprotein polypeptide F	NM_003095	1.69	0.59	mRNA splicing
v-ral simian leukemia viral oncogene homolog B	NM_002881	2.27	0.44	oncogenes and tumor suppressors, differential binding of calmodulin
Cell division				
POU domain, class 2, associating factor 1	NM_006235	2.63	0.38	Involved in translational regulation of growth inhibitor in response to stress
procollagen C-endopeptidase enhancer	NM_002593	2.13	0.47	cell growth and/or maintenance

Custom microarray analysis of FGF-23 induced genes

As described above, approximately 200 genes were selected which encode biological functions in pathways postulated to be regulated by FGF-23 and analyzed by custom array. Every gene was spotted four times on each custom microarray. The average signal intensity for the four spots was calculated for RNA obtained from cells treated with FGF-23 and the fold induction was determined by comparison to signal intensity generated by RNA obtained from untreated cells. A 1.5 fold difference was used as a criterion for identifying

potentially significant gene regulation differences. Table 12 contains the names and fold expression of genes observed to be increased in expression by custom microarray analysis and table 13 contains genes observed to be decreased in expression.

Table 12. Genes up regulated greater than 1.5 fold on custom arrays.

Gene name	accession	SaOS 24hr	SaOS 72hr	HK-2 24hr	HK-2 72hr	Caco 24hr	Caco 72hr	Basic function
Apoptosis								
Protein kinase C inhibitor protein-1 (14-3-3)	NM_003406				3.57			Interacts with kinase mediate signal transduction
Bone mineralization related								
Bone morphogenetic protein 4 (BMP4)	NM_001202			1.68				ossification
Glvr2 (Pit-2)	NM_006749	1.46						phosphate transport
Osteocalcin	NM_000711	1.56		1.47				Binds strongly to calcium, ossification
PTH receptor 1	NM_000316						1.70	Involved in serum calcium level modulation
House keeping								
alpha Tubulin	NM_006082				15.26		1.46	microtubule-based movement
Cyclophilin -A	NM_021130				11.06			Involved in immunosuppressant activity
GAPDH	NM_002046				5.15			Second phase of glycolysis
Human homologues to Yeast Phosphate genes								
CATD_HUMAN Cathepsin D precursor	NM_001909				4.00			Required for intracellular protein breakdown
IMB3_HUMAN Importin beta-3 subunit (Karyopherin beta-3 subunit)	Y08890					1.85		plays a role in nuclear import of some ribosomal proteins
Sodium-dependent high-affinity dicarboxylate transporter	NM_022829		1.50					sodium-dependent dicarboxylate transporter
OOM related								
Alpha-actinin mRNA	NM_004924				6.74			Intravellular structural/bundle protein
Apolipoprotein J mRNA	NM_001831				1.41		1.59	Function uncertain but may have anti-apoptosis role
BTF 3b mRNA	NM_001207			1.62				transcription regulation, transcription, from Pol II promoter
CD74 antigen	NM_004355				3.11			Involved in immune response initiation and antigen presentation
diacylglycerol kinase, zeta	NM_003646				8.95	1.47	1.81	intracellular signaling cascade, protein kinase C activation
EST (hypothetical protein MGC2491)	NM_024040				2.141			Protein coding sequence
EST (Kruppel-like factor 13)	AL390127					1.59	1.90	Transcription repressor
EST(hypothetical protein MGC4022)	NM_033420				2.87			Protein coding sequence
Fibronectin-1	NM_002026				10.33			cell adhesion and migration processes
HSMN P1	NM_018478						1.7	Chromosome 20 open reading frame
IGF-2 (insulin-like growth factor	NM_000597						1.43	regulation of cell growth

binding protein 2)							
Jumping Translocation breakpoint	NM_006694				2.19		Linked to oncogenesis
Lamin C mRNA	NM_005572				2.28		Thought to provide for nuclear envelope structure, cell shape and cell size control
Leukemia Virus Receptor (Glv-1)	NM_005415				1.48		Sodium dependant phosphate transporter
oligomeric matrix protein	NM_000095				2.87	1.48	cell adhesion, cartilage matrix and skeletal development
Prepro Alpha-1 Collagen mRNA	NM_000088	1.66					Bone mineralization and skeletal development
RTP mRNA	NM_006096		1.50				Associated with cell differentiation, may have growth inhibitory role
TGF beta	NM_000660				1.70		anti-apoptosis, cell growth, cell-cell signaling, developmental processes, TGF beta receptor signaling pathway
Osteoblast Markers							
JunD	NM_005354				9.70		play a critical role in terminating cell proliferation in granulocytic differentiation
Wnt Related							
beta catenin -1	NM_001904				12.15	1.45	cell adhesion, signal transduction in the Wnt pathway
sFRP-5	NM_003015		1.39	1.87		2.25	May modulate Wnt protein function associated with oncogenesis and several developmental processes

GAPDH was observed to be upregulated 5 fold in HK-2 cells (table 12) but when measured with real-time RT-PCR (data not shown) no change in expression was observed, suggesting a false positive. Similarly, FRP-4 was observed to be downregulated 1.6 fold (table 13) but no significant change was observed when test by real-time RT-PCR (figure 19) suggesting a false negative. Detection of false positives and false negatives by custom microarray analysis is not surprising because the samples were only tested once due to limited mRNA availability and a lack of robust signal. For these reasons, the apparent differential expression of house keeping genes alpha Tubulin (table 12 and 13) and Cyclophilin -A (table 12) are not of notable concern but should not be simply dismissed. Five genes with novel association to phosphate, as identified by bioinformatics homology analysis

to known yeast phosphate genes were also identified to be differential expressed. Additional validation of these genes is required to determine validity of fold expression. A greater than 1.5 fold differential expression of sodium-dependent high-affinity dicarboxylate transporter (table 12) and PIX1 pituitary homeobox 1 (table 13) was measured. The level of expression, as measured by unit fluorescence, for FGF-23 treated and control cells was robust and therefore more likely to represent an accurate fold change in expression. The sodium transporter and PIX1 should be the first of the yeast phosphate genes to be validated by real-time RT-PCR.

Table 13. Genes decreased in expression greater than 1.5 fold on custom microarrays.

Gene name	Accession	SaOS 24hr	SaOS 72hr	HK-2 24hr	HK-2 72hr	Caco 24hr	Caco 72hr	Basic function
Bone related								
Bone morphogenetic protein 2 (BMP2)	NM_001200			0.67				cell-cell signaling, ossification
gremlin	NM_013372	0.66						Blocks bone morphogenic protein signaling
Paired box gene 3 (PAX-3)	BC008826					0.54		genes play critical roles during fetal development and cancer growth
vitamin D (1,25-dihydroxyvitamin D3) receptor	NM_000376				0.59			signal transduction, involved in maintenance of calcium homeostasis
House keeping								
alpha Tubulin (ubiquitous)	NM_006082	0.6						microtubule-based movement
Human homologues to Yeast Phosphate genes								
PIX1_HUMAN Pituitary homeobox 1 (Hindlimb expressed homeobox protein)	NM_002653				0.37			may regulate gene expression and control cell differentiation
Sodium-dependent high-affinity dicarboxylate transporter	NM_022829				0.38			sodium transport
OOM related								
23810 Osteopontin	NM_000582				0.55			cell adhesion, ossification
ANK	NM_054027				0.32			Involved in phosphate level modulation, possible mechanism regulating tissue calcification
Calmodulin	NM_006888				0.64			Calcium binding protein involved in growth and cell cycle
CD44 Splice variant w/in coding (zinc finger protein 6 (CMPX1))	AJ251595				0.29			may play an important role in the pathogenesis of human tumors
Chondroitin-6-sulfotransferase	AB017915			0.65	0.5			Extracellular matrix maintenance
CSR-1	NM_016240				0.15			Protects against stress response
double Leman coiled-coil protein (was NME)	NM_016201				0.51			Unknown function
EST (FKSG14) AF5alpha	NM_022145				0.53			leucine zipper binding protein

EST (Kruppel-like factor 13)	AL390127				0.36			Transcription repressor
EST(hypothetical protein MGC4022)	NM_033420					0.64		Protein coding sequence
EST/distal-less homeobox protein (DLX3)	AF028233				0.65			developmental processes, skeletal development
FGF 23	NM_020638				0.23			Phosphatonin, associated with phosphate wasting
FGF acidic	NM_004214				0.49			cell-cell signaling, induces various morphogenic changes and differentiation
Frizzles Related Protein-4	NM_003014						0.62	Phosphatonin, associated with phosphate wasting, signal transduction
hSHIP	NM_005541				0.17			May be involved in inhibition of apoptosis
Human O-linked GlcNAc transferase	NM_003605						0.01	Involved in O-linked glycosylation
HVEB mRNA	NM_002856					0.64		mediates entry of some alphaherpesvirus mutants, involved in cell to cell spreading of the virus
Hypothetical protein FLJ10199	NM_018022			0.64				Protein coding sequence
integrin alpha 10	AF112345				0.19			Involved in cell adhesion as well as cell-surface mediated signaling
Jumping Translocation breakpoint	NM_006694						0.67	Linked to oncogenesis
Lamin C mRNA	NM_005572						0.6	Thought to provide for nuclear envelope structure, cell shape and cell size control
leucine rich repeat (in FLII) interacting protein 2 (candidate20)	NM_006309				0.41			candidate20
MEF-2A	NM_005587				0.33			May be involved in growth factor-related transcription
Milk Fat Globule-EGF 8 Protein	NM_005928				0.56			cell adhesion, oncogenesis
MRG-1 protein	AF109161				0.3			transcription regulation
Neurogranin RC3 mRNA	NM_006176				0.49		0.59	Binds to calmodulin in the absence of calcium
Novel gene hom. to sulfatase Novel (Candidate 46) or KIAA1077 protein	AB029000				0.39			Protein coding sequence
Plectin (PLEC-1 mRNA)	NM_000445				0.42		0.54	cytoskeletal anchoring
Prostaglandin I2 Synthase	NM_000961						0.58	inhibitor of platelet aggregation
Selenoprotein P	NM_005410				0.16			Heparin binding protein
Serine Protease 11 (IGF Binding)	NM_002775			0.59				regulation of cell growth
THC 3' 286255 ninjurin 2)	BC015737				0.38			neuronal cell adhesion
TIAM-1 variant	NM_003253				0.23			Involved in intracellular signaling cascade
transcription factor 7-like 2	NM_030756				0.49			transcription regulation
Osteoblast Markers								
alkaline phosphatase	NM_000478			0.5				post-translational membrane targeting, linked directly to hypophosphatasia, a disorder that is characterized by hypercalcemia and includes skeletal defects
CSF-1	M37435		0.58		0.48			antimicrobial humoral response, positive control of cell proliferation
double Rank ligand (OPG, TR1, OCIF) product osteoprotegerin	NM_002546						0.56	This protein is an osteoblast-secreted decoy receptor that functions as a negative regulator of bone reabsorption
Wnt Related								
APC	NM_000038			0.54		0.66		cell adhesion, binds beta-actin

Real-time RT-PCR technology used to validate leads generated by arrays

Taqman™ is a real-time polymerase chain reaction (PCR) quantification technology patented by Perkin-Elmer. As microarrays are useful for screening a large variety of genes for expression patterns, real-time RT-PCR is lower throughput but allows for accurate validation of selected gene expression. Traditional sequence specific forward and reverse primers were used to amplify the target sequence. Through temperature cycling, double stranded product is generated. Real-time detection and quantification of the amplified fragment is achieved by a SYBR green fluorescent dye. Qiagen has developed a user-friendly kit to be used on a real-time PCR technology. Buffer conditions are optimized so that the SYBR green dye efficiently binds to double stranded DNA generated by the amplification process. SYBR green dye fluoresces only upon double stranded DNA incorporation. The Qiagen QuantiTect SYBR Green RT-PCR kit is used on the Perkin-Elmer real-time RT-PCR system to validate leads identified by array analysis. Several genes of interest identified from initial array data and literature were selected for real-time RT-PCR validation. Their published functional properties associate each gene with either calcium or phosphate related regulation.

Calculation of standard deviation

Standard deviation was calculated for real-time RT-PCR analysis. The formula used is:

$$\text{Stdev} = \frac{(n\sum x^2 - (\sum x)^2)}{(n(n-1))}$$

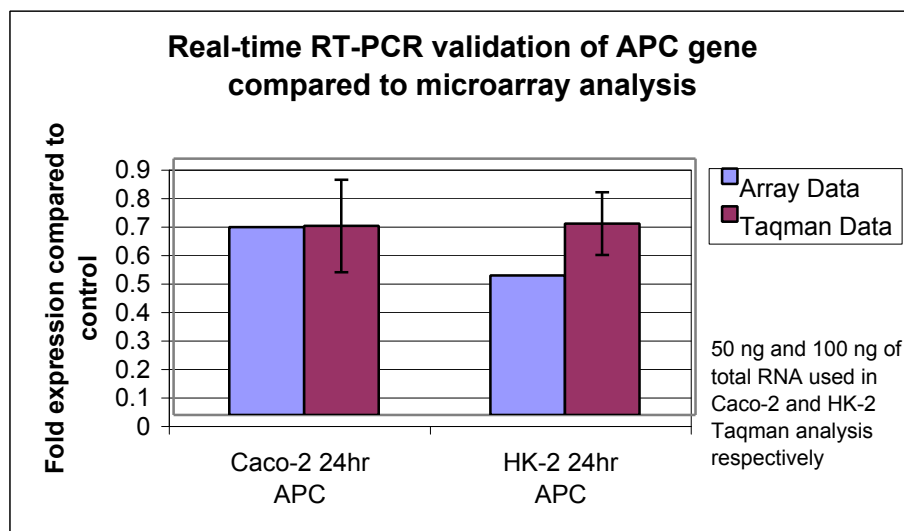
Where n is the number of replicates and x is the value of the data point signal intensity. Samples were analyzed in triplicate so n is equal to 3 for all real-time RT-PCR analysis unless otherwise noted.

Real-time RT-PCR validation

Real-time RT-PCR validation was conducted on selected genes identified from microarray analysis. Standard curves were generated using known concentrations of template oligos for all genes tested except aquaporin-5 to ensure that the analysis was performed in the linear range of the assay (figures 21-26). Furthermore, agarose gel electrophoresis analysis was performed to confirm absence of contaminating bands. Adenomatosis polyposis coli (APC) was selected for validation by real-time RT-PCR because of the observed 1.5 fold reduced expression by microarray analysis in two cell types and the association of APC to the Wnt signaling pathway. The Wnt pathway is of relevant interest because the family members of FRP-4 (another phosphatoin) is know to interact with WNT signaling and may create a synergistic effect on phosphate regulation (Anderson *et al.* 2002). Although a dramatic change in expression was not observed in either microarray or real-time RT-PCR analysis, both methods

showed a consistent 1.5 fold down regulation of APC. A down regulation of APC is associated with activation of the Wnt pathway and is consistent with the potential upregulation of beta-catenin observed by microarray analysis of HK-2 and Caco-2 cells at 72 hours. It is difficult to assess whether a 1.5 fold repression is biologically relevant, but the consistency of the data would suggest that this gene should be further assessed in other cell types or within experiments that monitor a broader range of FGF-23 treatment times.

Figure 16. APC expression analysis of Caco-2 and HK-2 cells treated with FGF-23 for 24 hours by microarray and real-time RT-PCR.



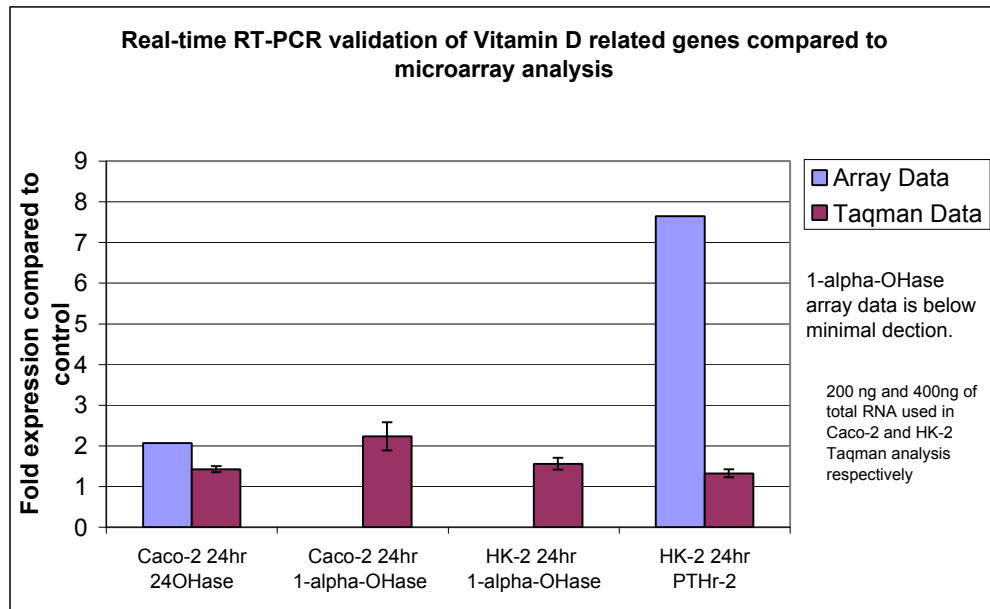
The parathyroid hormone (PTH) signals through the PTH receptor (PTHR) 1 and 2. In response to low serum calcium levels, PTH is increased (Juppner *et al.* 1999). An increase in PTH reduces the reabsorption of phosphate in the kidney hence resulting in phosphate wasting. The association of PTHr-2 to phosphate homeostasis prompted the desire for RT-PCR validation of the

observed microarray upregulation in HK-2 cells at 24 hours. However, it is important to point out that although PTHr-2 appeared to be induced in the first array analysis of this mRNA sample, a reproducible induction was not observed in replicate array analysis. Based on this result, it was not surprising to observe that upregulation of PTHr-2 was not supported by the RT-PCR data (figure 17).

PTH also modulates calcium and phosphate homeostasis through regulation of vitamin D levels. An increase in PTH increases $1\alpha\text{OHase}$ which is the key metabolic enzyme that converts the inert vitamin D ($25(\text{OH})\text{D}_3$) into the active state of 1,25-dihydroxyvitamin D ($1,25(\text{OH})_2\text{D}_3$). 24-hydroxylase (24OHase) degrades the active $1,25(\text{OH})_2\text{D}_3$ to an inert $1,24,25(\text{OH})_2\text{D}_3$ form allowing for tight regulation of vitamin D activity and hence calcium homeostasis (Holick 1999). FGF-23 has been shown to repress renal expression of $1\alpha\text{OHase}$ *in vivo* (Shimada *et al.* 2002). Changes in expression of this gene were not observed by array analysis because all signals fell below the background level of 500. However, consistent with a predicted repression of the anabolic $1\alpha\text{OHase}$, array analysis suggested FGF-23 may induce expression of the catabolic enzyme, 24-OHase as an expression ratio of 2.07 was observed in Caco-2 cells at 24 hours. RT-PCR results showed that in the intestinal Caco-2 cells at 24 hours, FGF-23 treatment increased $1\alpha\text{OHase}$ 2 fold, while no change was observed in 24OHase (figure 17). The RT-PCR result would suggest that production of $1,25(\text{OH})_2\text{D}_3$ would increase. Direct measurement of $1,25(\text{OH})_2\text{D}_3$ would be required to validate this conclusion. These results (figure 17) are opposite from *in vivo* studies (Yamazaki 2002, Shimada ASBMR 2002) by a decrease in renal

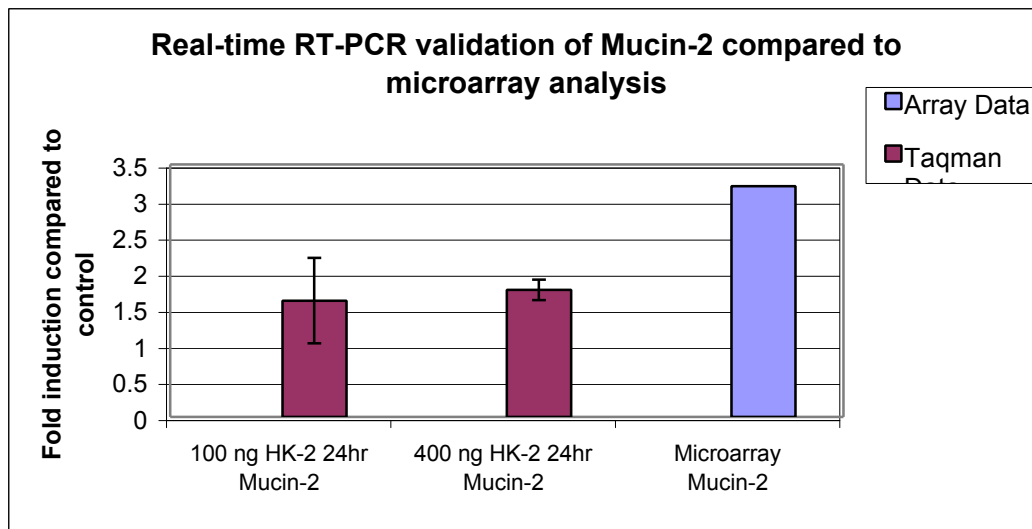
1 α OHase was observed at 1-9 hours after FGF-23 treatment, but expression level at 24 hours was not analyzed in that study. Patients with OOM tumors have a low level of 1,25(OH)₂D₃ and return to normal upon removal of the tumors (Yamazaki *et al.* 2002). The Caco-2 24 hour *in vitro* results are inconsistent with the Yamazaki *in vivo* data. Perhaps a prolonged treatment of Caco-2 cells with FGF-23 would result in a measured decrease in 1 α OHase levels. Alternatively, measurement of 1 α OHase levels at a more optimal time point (1-9 hours post-FGF-23 treatment) would result in measured decrease. Alternatively, these results may support a differential role in the regulation of 1,25(OH)₂D₃ in the intestine compared to the kidney. A third possibility is that the observed changes at 24 hours may be a reflection of an FGF-23 induced feedback on the maintenance of 1,25(OH)₂D₃. It is also interesting to note that specific changes observed in the renal cell line, HK-2 despite the existing *in vivo* data. These results may reflect the inherent inability of the cells to maintain a true renal epithelial cell phenotype under culture conditions.

Figure 17. Vitamin D related gene expression analysis of Caco-2 and HK-2 cells treated with FGF-23 for 24 hours by microarray and real-time RT-PCR.



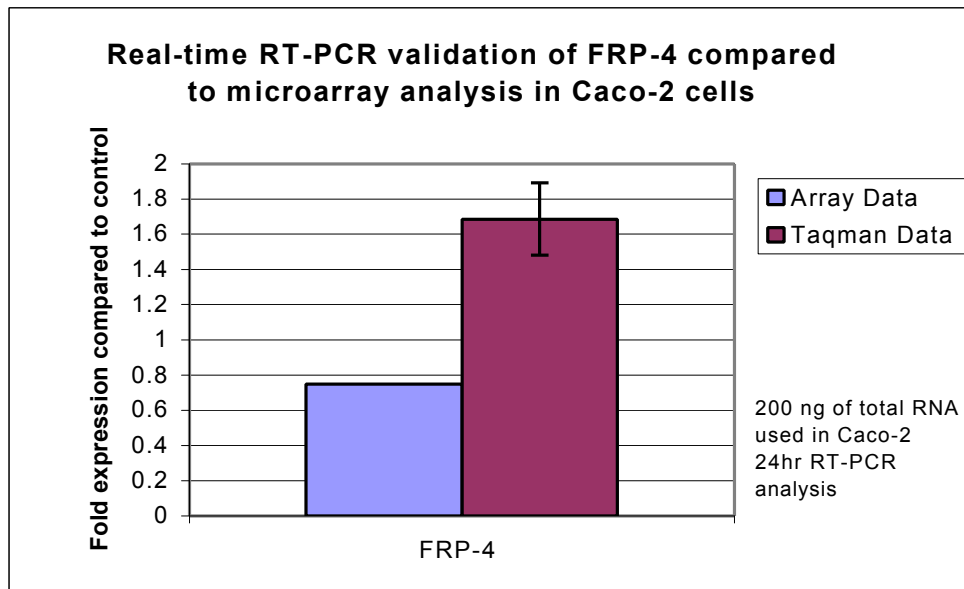
Mucin-2 was observed to be consistently expressed 1.5 fold greater in FGF-23 treated cells than the control condition (figure 18). Both 100 ng and 400ng of starting total RNA for the real-time RT-PCR template yielded similar fold induction but with better reproducibility with more template. Tables 6, 7, and 8 (shown previously) show the putative upregulation of mucin-2 in all the tested conditions except for Caco-2 at 72 hours. Real-time RT-PCR validation of the HK-2 cells treated for 24 hours showed a change in expression and that was slightly less than 2X and was less robust than indicated by microarray analysis (figure 18). Again, analysis of this gene across different FGF-23 exposure times would be valuable to identify maximum induction of this gene by FGF-23

Figure 18. Mucin-2 expression analysis of HK-2 cells treated with FGF-23 for 24 hours by microarray and real-time RT-PCR.



FRP-4 was previously identified to be upregulated in OOM tumors by SAGE analysis (Jan de Beur *et al.* 2002a), and since then has been demonstrated to be a phosphatonin. Microarray analysis suggested that FRP-4 might be downregulated in Caco cells at 72 hours since the expression level was 0.6 (Table 6). A modest reduction that did not approach the 1.5X cut-off was observed at 24 hours (ratio 0.75). Due to the limited availability of the 72 hour sample, real-time RT-PCR validation was conducted on Caco-2 RNA collected at 24 hours (figure 19). Real-time RT-PCR analysis showed conflicting results of a 1.68 fold expression compared to 0.6 by array (Figure 19). These results did not support regulation of FRP-4 by FGF-23 and suggested that the observed changes may be due to inherent variability of the array technology or lack of biological replicates.

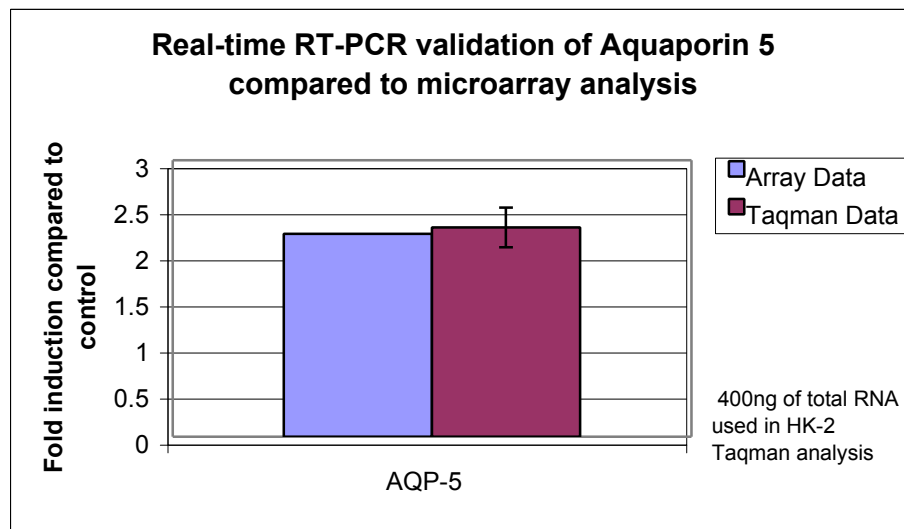
Figure 19. FRP-4 expression analysis of Caco-2 cells treated with FGF-23 for 24 hours by microarray and real-time RT-PCR.



Aquaporins (Aqp) are a family of extracellular membrane bound water channels expressed in various organs. Aqp-5 and Aqp-6 were identified to be upregulated in HK-2 cells after 24 hours of FGF-23 treatment (Table 6). Although Aqp-5 is structurally similar to the other family members, it is unique because it is expressed intracellularly and is primarily an ion channel and not a water channel as are the other Aqps (Ikeda *et al.* 2002). Aqp-5 has high specificity for nitrate instead of water in renal collecting ducts. Elevated levels of nitrate have been reported to inhibit H⁺-ATPase activity (Valles and Manacha 2000) and inhibition of H⁺-ATPase activity is associated with obstruction of kidney collecting ducts. The microarray data indicated a 1.5 fold upregulation of Aqp-5 and the real-time RT-PCR validated the upregulation by showing close to a 2.25 fold increase in expression when cells were treated with FGF-23 compared to control conditions

(Figure 20). A standard curve not generated for this analysis. However, the absence of contamination as accessed by agarose gel electrophoresis and CT values falling between 27.5 and 29.5 suggests that the analysis falls within the linear range. This data confirmed that FGF-23 induces expression of Aqp-5.

Figure 20. Aquaporin 5 expression analysis of HK-2 cells treated with FGF-23 for 24 hours by microarray and real-time RT-PCR.



Real-time RT-PCR standard curves and amplification product

To demonstrate the reliability of the real-time RT-PCR analysis, a standard curve was generated for each analyzed gene (with the exception of aquaporin-5) by diluting an oligo template representing the region amplified for each gene of interest. The oligo template served as a positive control for amplification product and was used to establish a linear range of the SYBR green fluorescent intensity that correlated to the double stranded PCR amplification product. For each gene analyzed, the threshold cycle (Ct) of all the RNA samples are between the highest

and lowest template control (Figures 21-28). The zero template negative control yielded a value near or at 40 Ct corresponding to no double stranded DNA. Some of the PCR primers generated a primer dimer amplicon but by measuring the Ct at higher temperatures, the short amplicon disassociates producing no signal while the larger amplicon remains double stranded and produces a fluorescent signal (FRP-4, mucin-2 and PTHr-2). Figure 21 is the real-time RT-PCR amplification data for FRP-4. Figure 22 is the real-time RT-PCR amplification data for 1 α OHase. Figure 23 is the real-time RT-PCR amplification data for Adenomatosis polyposis coli (APC). Figure 24 is the real-time RT-PCR amplification data for 24-OHase. Figure 25 is the real-time RT-PCR amplification data for mucin-2. Figure 26 is the real-time RT-PCR amplification data for parathyroid hormone receptor-2 (PTHr-2). Figure 27 is the real-time RT-PCR amplification data for GAPDH by HK-2 24 hour RNA dilution. Figure 28 is the real-time RT-PCR amplification data for GAPDH by Caco-2 24 hour RNA dilution. Figure 29 is the real-time RT-PCR amplification data for Aquaporin 5 RT-PCR amplification of HK-2 cells. These results confirm that each real-time RT-PCR analysis was performed within the linear range of the assay. In addition, a portion of amplicon produced by each real-time RT-PCR reaction was assessed by gel-electrophoresis. Each amplicon was consisted with the expected size and no additional bands were observed in negative controls or experimental samples (Figure 21b-28b, figure 29). When amplicons are observed in the negative control lane, they are a result of primer dimer formation and are smaller in size than the expected amplicon sized.

Although dramatic changes are not measured by real-time RT-PCR analysis, the observed changes in expression for the genes selected to be validated via RT-PCR generally paralleled the microarray results. Genes that were found to be induced across replicate experiments within a single cell type (HK-2)(aquaporin 5) or across all three cell types (mucin-2) were validated by real-time RT-PCR analysis whereas genes (i.e. PTHr-2 and FRP-4) that were not observed to be consistently regulated across replicate array experiments were not validated. Real-time RT-PCR analysis validated genes found to be induced in HK-2 cells (AQP-5 and mucin-2) and Caco-2 cells (1 α OHase). This indicates that FGF-23 did induce a biological response in HK-2 and Caco-2 cells but a less robust response was measured than anticipated (summarized in table 14). Due to limited amounts of RNA, Saos-2 samples were not validated via real-time RT-PCR. Therefore, these results cannot confirm whether these cells truly responded to FGF-23.

Table 14. Fold expression of house keeping genes spotted on the custom microarray.

Cell type and time point	Gene name	Microarray Data	RT-PCR Data	Consistent expression
		Fold expression	normalized to GAPDH	
Caco-2 24 hr	24-OHase	2.07	1.43	similar
Caco-2 24 hr	1AlphaOHase	LS	2.23	No data
HK-2 24 hr	1AlphaOHase	LS	1.56	No data
HK-2 24 hr	PTHr-2	7.65	1.33	similar
Caco-2 24 hr	APC	0.66	0.66	yes
HK-2 24 hr	APC	0.49	0.67	yes
Caco-2 24 hr	FRP-4	0.75	1.69	no
100ng HK-2 24 hr	Mucin-2	3.20	1.61	yes
400ng HK-2 24 hr	Mucin-2	3.20	1.76	yes
HK-2 24 hr	AQP-5	2.20	2.27	yes
Caco-2 72 hr	SSTR-3	1.80	1.73	yes

Figure 21. A. Standard curve of FRP-4 template versus threshold cycle (Ct) as determined by real-time RT-PCR analysis. B. Table representation of Ct values and standard deviation. C. Ethidium bromide stained 3% agarose gel template, sample, and zero template control.

Figure 21 A.

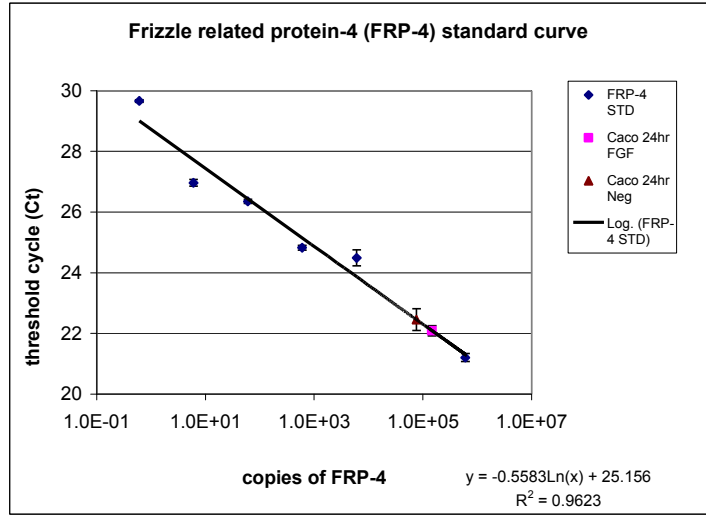


Figure 21 B.

Sample type and template	average Ct	Ct STDev
Caco 24 hr FGF	22.1	0.17
Caco 24 hr Neg	22.5	0.36
FRP-4 zero	39.0	0.16
FRP-4 1pM STD	21.2	0.13
FRP-4 10 fM STD	24.5	0.26
FRP-4 1 fM STD	24.8	0.08
FRP-4 100 aM STD	26.4	0.07
FRP-4 10aM STD	27.0	0.11
FRP-4 1 aM STD	29.7	0.04

Figure 21 C.

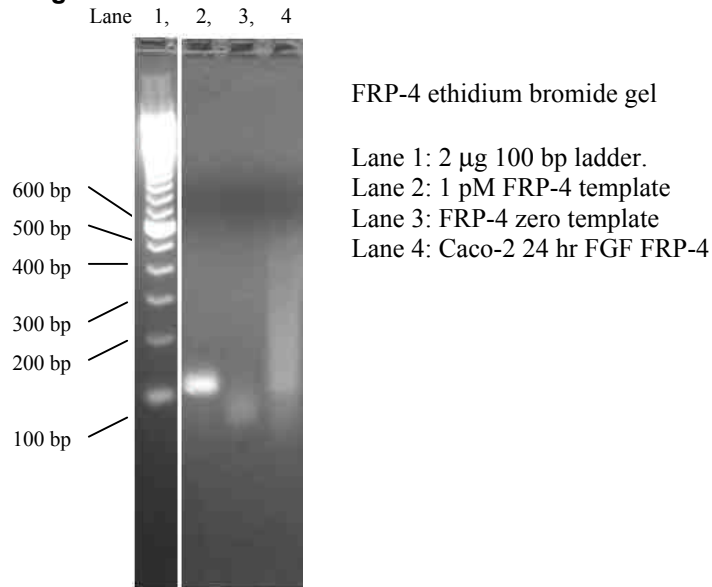


Figure 22. A. Standard curve of 1 α OHase template versus threshold cycle (Ct) as determined by real-time RT-PCR analysis. B. Table representation of Ct values and standard deviation. C. Ethidium bromide stained 3% agarose gel template, sample, and zero template control.

Figure 22 A.

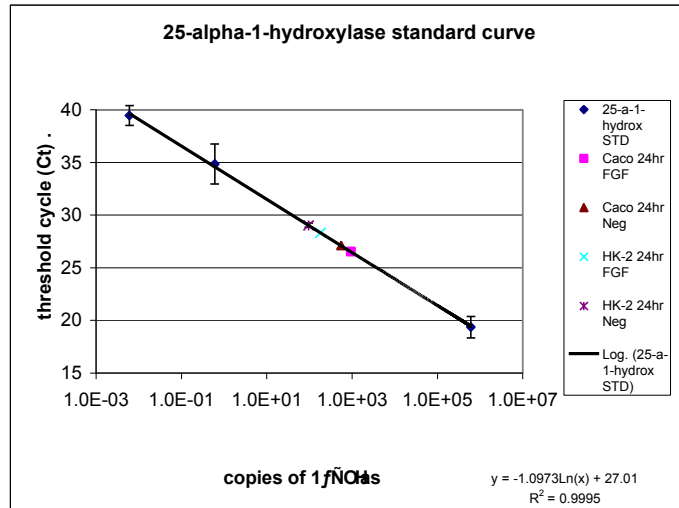


Figure 22 B.

Sample type and template	average Ct	Ct Stdev
Caco 24 hr FGF	26.5	0.27
Caco 24 hr Neg	27.1	0.09
HK-2 24 hr FGF	28.3	0.07
HK-2 24 hr Neg	29.0	0.20
1 α OHase zero	40.0	0.00
1 α OHase 1 pM STD	19.4	1.02
1 α OHase 1 aM STD	34.8	1.89
1 α OHase.01 aM STD	39.5	0.95

Figure 22 C.

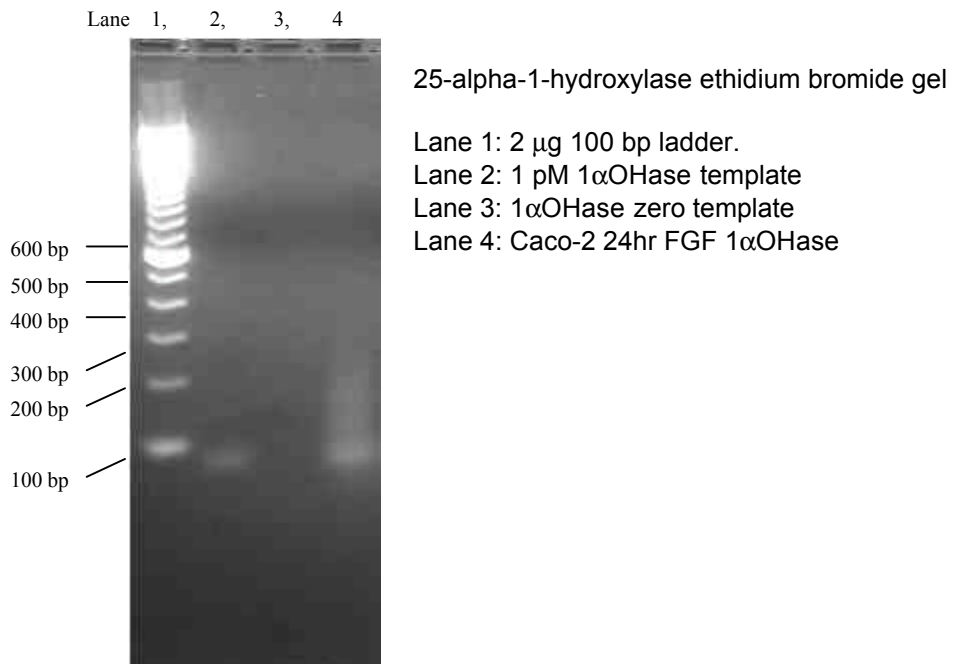


Figure 23. A. Standard curve of Adenomatosis polyposis coli (APC) template versus threshold cycle (Ct) as determined by real-time RT-PCR analysis. B. Table representation of Ct values and standard deviation. C. Ethidium bromide stained 3% agarose gel template, sample, and zero template control.

Figure 23 A.

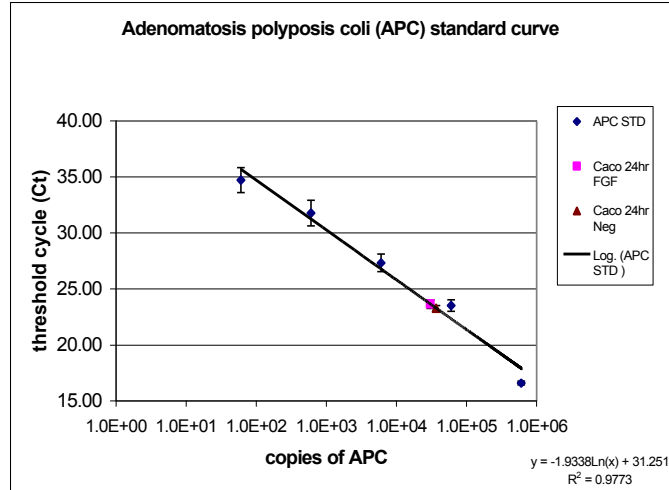
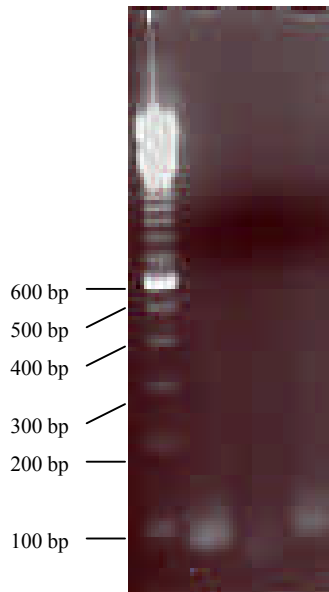


Figure 23 B.

Sample type and template	average Ct	Ct Stdev
Caco 24 hr FGF	23.7	0.38
Caco 24 hr Neg	23.3	0.23
APC zero	40.0	0.00
APC 1 pM STD	16.6	0.17
APC 100 fM STD	23.5	0.51
APC 10 fM STD	27.3	0.80
APC 1 fM STD	31.8	1.14
APC 100 aM STD	34.7	1.12

Figure 23 C.

Lane 1, 2, 3, 4



APC ethidium bromide gel

Lane 1: 2 µg 100 bp ladder.
 Lane 2: 1 pM APC template
 Lane 3: APC zero template
 Lane 4: Caco-2 24 hr FGF APC

Figure 24. A. Standard curve of 24OHase template versus threshold cycle (Ct) as determined by real-time RT-PCR analysis. B. Table representation of Ct values and standard deviation. C. Ethidium bromide stained 3% agarose gel template, sample, and zero template control.

Figure 24 A.

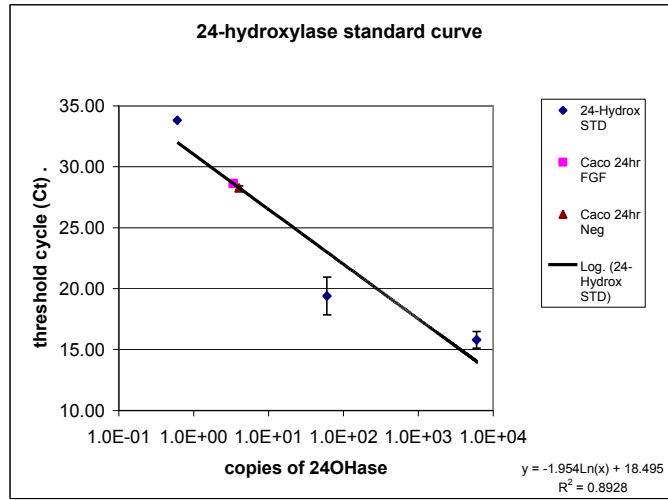


Figure 24 B.

Sample type and template	average Ct	Ct Stdev
Caco 24 hr FGF	28.6	0.16
Caco 24 hr Neg	28.3	0.13
24OHase zero	39.9	0.17
24OHase 10 fM STD	15.8	0.08
24OHase 100 aM STD	19.4	0.68
24OHase 1 aM STD	33.8	1.54

Figure 24 C.

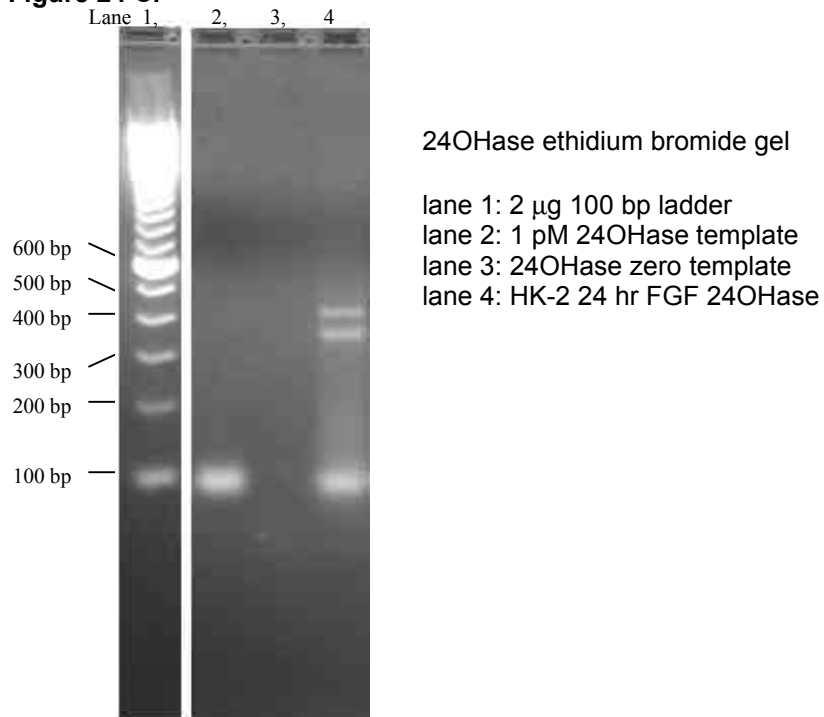


Figure 25. A. Standard curve of mucin-2 template versus threshold cycle (Ct) as determined by real-time RT-PCR analysis. B. Table representation of Ct values and standard deviation. C. Ethidium bromide stained 3% agarose gel template, sample, and zero template control.

Figure 25 A.

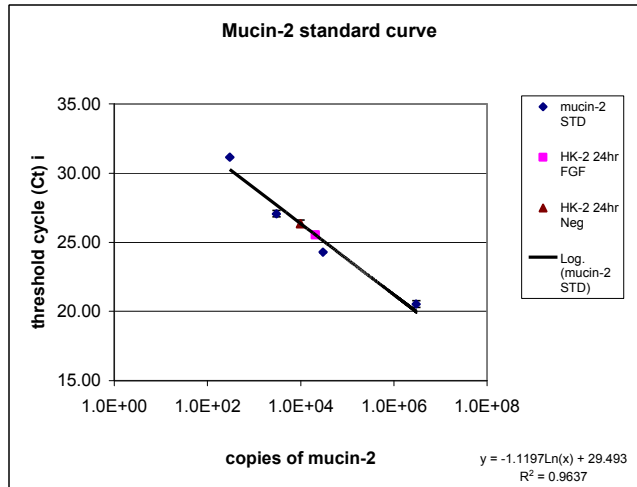


Figure 25 B.

Sample type and template	average Ct	Ct Stdev
HK-2 24 hr FGF	25.5	0.12
HK-2 24 hr Neg	26.4	0.26
M-2 zero	39.0	1.68
mucin-2 5 pM STD	20.5	0.25
mucin-2 50 fM STD	24.3	0.15
mucin-2 5 fM STD	27.1	0.04
mucin-2 500 aM STD	31.2	0.23

Figure 25 C.

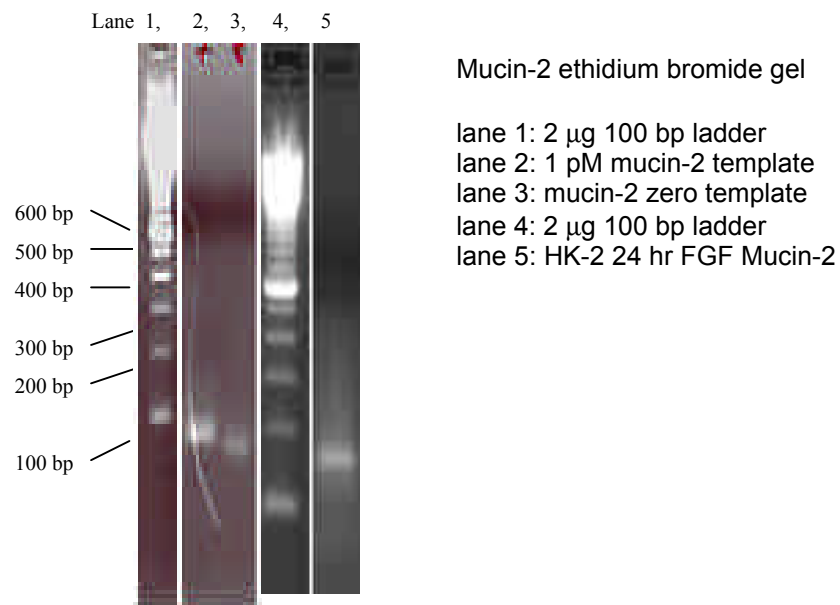


Figure 26. A. Standard curve of parathyroid hormone receptor-2 (PTHr-2) template versus threshold cycle (Ct) as determined by real-time RT-PCR analysis. B. Table representation of Ct values and standard deviation. C. Ethidium bromide stained 3% agarose gel template, sample, and zero template control.

Figure 26 A.

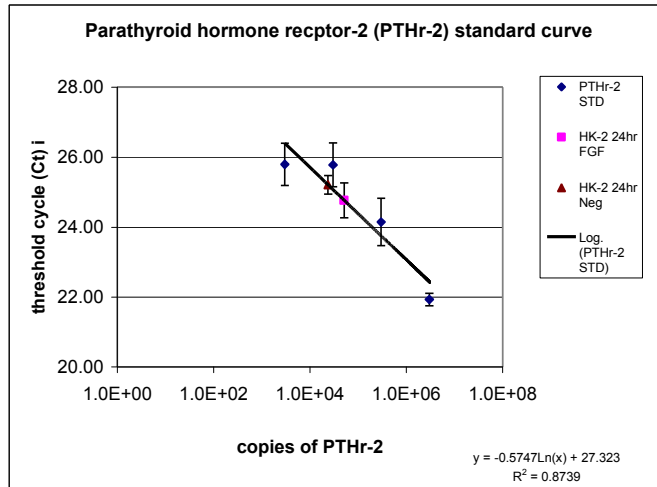


Figure 26 B.

Sample type and template	average Ct	Ct Stdev
HK-2 24 hr FGF	24.8	0.50
HK-2 24 hr Neg	25.2	0.27
PTHr-2 zero	39.4	1.11
PTHr-2 5 pM STD	21.9	0.18
PTHr-2 500 fM STD	24.1	0.68
PTHr-2 50 fM STD	25.8	0.63
PTHr-2 5 fM STD	25.8	0.60

Figure 26 C.

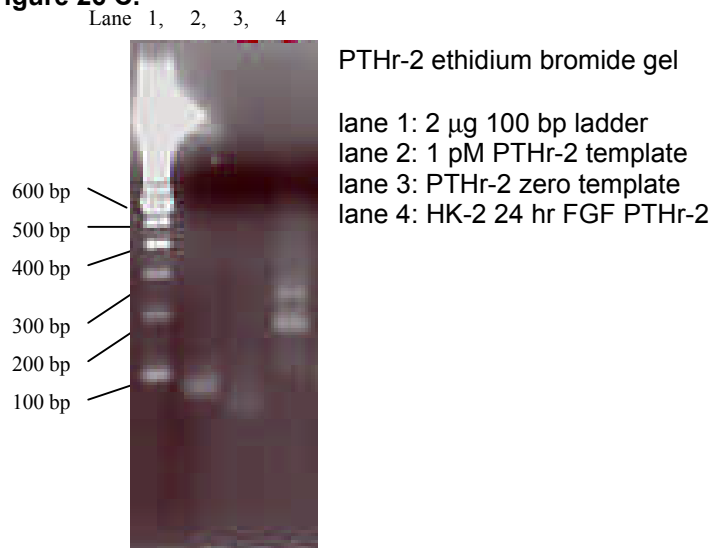


Figure 27. A. HK-2 24 hour RNA dilution for GAPDH expression analysis versus threshold cycle (Ct) as determined by real-time RT-PCR analysis. B. Table representation of Ct values and standard deviation. C. Ethidium bromide stained 3% agarose gel sample and zero template control.

Figure 27 A.

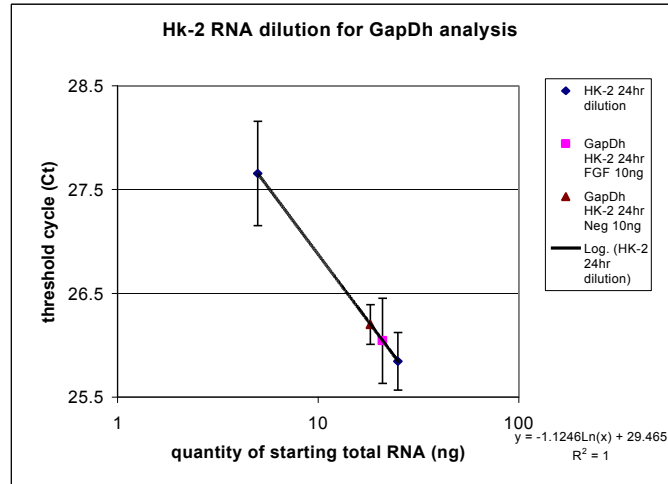


Figure 27 B.

Sample type and RNA conc.	average Ct	Ct Stdev
GAPDH HK-2 24 hr FGF 10 ng	26.0	0.19
GAPDH HK-2 24 hr Neg 10 ng	26.2	0.41
GAPDH zero	40.0	0.00
GAPDH HK-2 FGF 24 hr 25 ng	25.8	0.28
GAPDH HK-2 FGF 24 hr 5 ng	27.7	0.50

Figure 27 C.

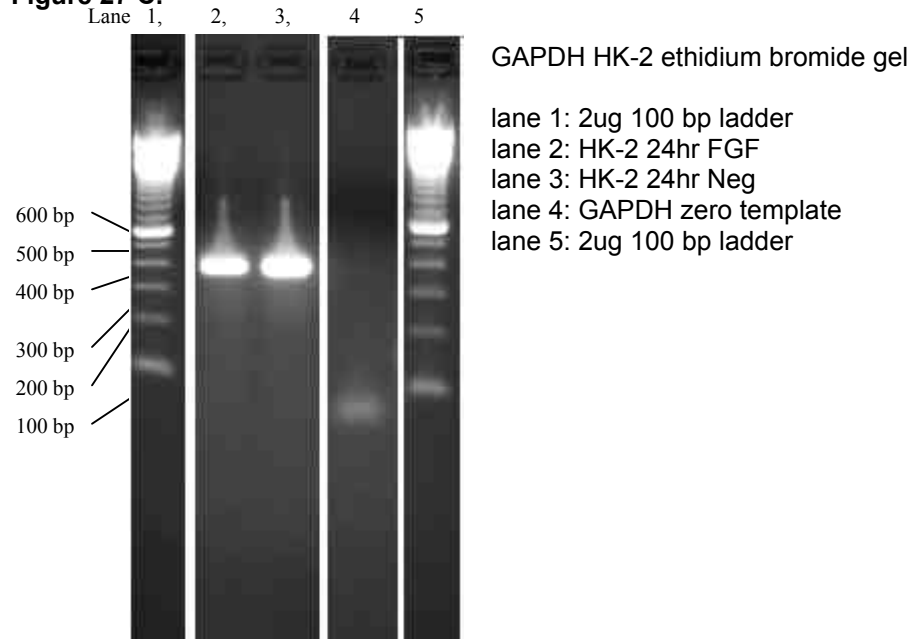


Figure 28. A. Caco-2 24 hour RNA dilution for GAPDH expression analysis versus threshold cycle (Ct) as determined by real-time RT-PCR analysis. B. Table representation of Ct values and standard deviation. C. Ethidium bromide stained 3% agarose gel sample and zero template control.

Figure 28 A.

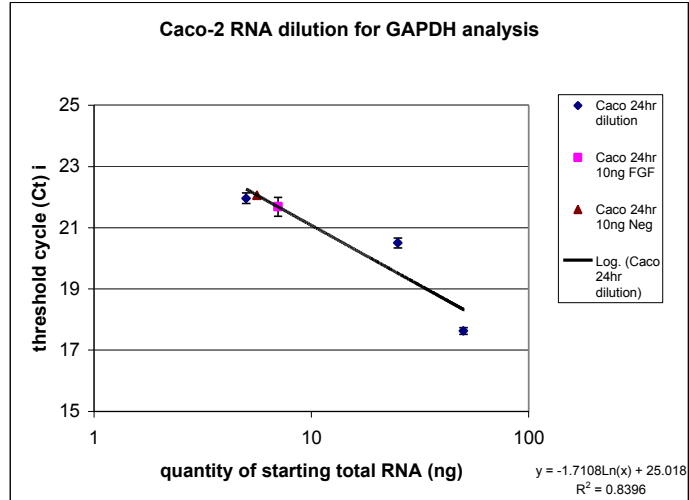
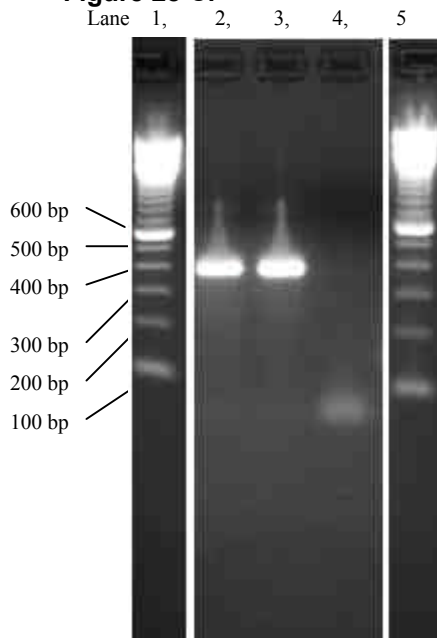


Figure 28 B.

Sample type and RNA conc.	average Ct	Ct Stdev
Caco 24 hr 10 ng FGF	21.7	0.30
Caco 24 hr 10 ng Neg	22.1	0.06
GAPDH zero	40.0	0.00
GAPDH Caco 24hr 50 ng	17.6	0.11
GAPDH Caco FGF 24 25 ng	20.5	0.16
GAPDH Caco FGF 24 5 ng	22.0	0.17

Figure 28 C.

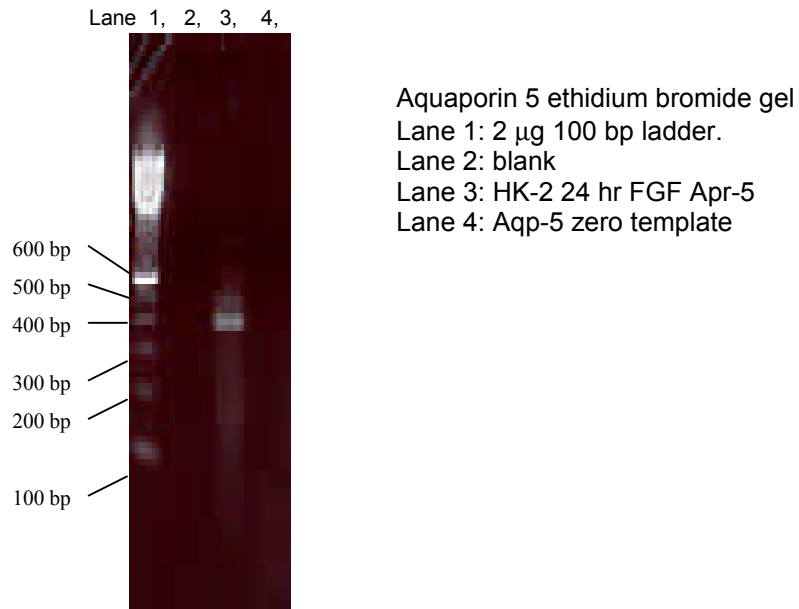


GAPDH -Caco-2 ethidium bromide gel

- lane 1: 2ug 100 bp ladder
- lane 2: Caco-2 24hr FGF treated
- lane 3: Caco-2 24hr Neg control
- lane 4: GAPDH zero template
- lane 5: 2ug 100 bp ladder

Figure 29 shows the amplification of a single band by aquaporin 5 primers for the HK-2 24 hour RNA sample as a template in lane 3. Lane 4 is a template free negative control to demonstrate that the reaction is contamination free.

Figure 29. Ethidium bromide stained 3% agarose gel of Aquaporin 5 RT-PCR amplification of HK-2 cells treated with FGF-23 for 24 hours and zero template control.



Expression levels of house keeping genes were measured on the custom microarray. The RT-PCR data described above was normalized to GAPDH for HK-2 and Caco-2 cells measured at 24 hours. Similar to the real-time RT-PCR data (figure 27b, 28b) custom microarray data (table 15), no significant change in mRNA expression was observed for FGF-23 treated and control cells.

Table 15. Fold expression of house keeping genes spotted on the custom microarray.

Low Signal intensity(LS)			caco	HK-2	Saos
EF-1	NM_001959	24hr	0.80	LS	LS
		72hr	LS	LS	LS
beta-Actin	AF111848	24hr	0.82	0.83	LS
		72hr	LS	LS	LS
alpha Tubulin	NM_006082	24hr	1.26	1.25	0.60
		72hr	1.47	15.26	0.98
Cyclophilin-A	NM_021130	24hr	1.18	1.26	0.98
		72hr	1.12	11.06	0.84
GAPDH	NM_002046	24hr	1.08	1.07	0.87
		72hr	1.05	5.16	0.96
STAT1	NM_007315	24hr	LS	LS	LS
		72hr	LS	LS	LS
beta-glucuronidase	NM_000181	24hr	LS	LS	LS
		72hr	LS	LS	LS

DISCUSSION

RT-PCR receptor profiling

In vitro binding studies by Yamashita *et al.* (2002) and Pragnell (unpublished) indicate that FGF-23 binds to FGF receptors 2, 3 and 4. To determine the possibility of FGF-23 acting on selected cell lines, RT-PCR analysis was conducted for FGF receptor gene expression. Several cell lines predicted to play a role in phosphate uptake were screened for gene expression. Previously validated GAPDH PCR primers were used as a positive control, and reactions without the addition of reverse transcriptase (RT) demonstrated that there were no detectable levels of genomic contamination when no bands were visualized in the RT omitted control lanes. The PCR amplification products were of the expected size and migrated correctly in comparison to each other based on the positioning of the designed primers. The RT-PCR receptor profiling of Caco-2, HK-2, and SaOS-2 cells demonstrate that of all three FGF receptors believed to be relevant to FGF-23 signal are expressed. This result indicates that FGF-23 may be capable of inducing a biological response in model cell lines selected to represent sites of phosphate regulation. However, amplification of correct sized amplicons only indicates gene expression, but does not ensure proper translation, localization, availability/accessibility, and protein stability to ensure the receptor is available for ligand signaling. In addition to these variables, it is also possible that additional, yet to be identified, novel receptor(s) may be involved in FGF-23 signaling and the cell specific expression of that receptor is subsequently

unknown. To our best knowledge, the receptors required for FGF-23 signaling are present in the target cell lines used in these experiments.

Furthermore, Saos-2 and HK-2 cells were tested to respond to FGF-23 treatment by a phosphate uptake assay (Bowe, Genzyme Corp) (Appendix figure 33). A 40% phosphate uptake inhibition was observed in both cell lines (Appendix figure 32b). Saos-2 and HK-2 cells were also tested for biological response to FGF-23 by increased tyrosine phosphorylation of receptor related signaling. Both cell lines showed an increased phosphorylation when treated with FGF-23 compared to control (O'Brien, Genzyme Corp, Data not shown). Caco-2 cells were tested once for a response to FGF-23 treatment by phosphate uptake. Caco-2 cells did not demonstrate an inhibition of phosphate uptake when treated with FGF-23 (data not shown).

Biological relevance of identified genes

Examination of protein function of genes suggested to be differentially regulated by array analysis revealed multiple cellular functions that may be regulated by FGF-23. The majority of the identified expression changes fell into six general classifications. These categories were the following: general cell change, differentiation, division, membrane channels and transporters, metabolic enzymes, and unknown functions. Most of the upregulated genes are associated with cell growth, differentiation, and various cellular changes. Table 9, of the results section, shows apparent upregulation of genes such as glutathione S-transferase theta 2 and hyaluronoglucosaminidase 1, which are required for anti-

apoptotic activity and enhanced cellular growth. The downregulated genes are also involved in similar cellular function but with an opposite function. Table 10 shows genes like TNFRSF6, required for apoptosis to be down regulated and other genes involved in stress and immune responses. In general, the cells viability did not seem to be compromised based on the observed genes that appeared to be differentially expressed with FGF-23 treatment.

The three cell types appeared to respond to FGF-23 by modulating various transcription factors, receptors, and membrane channels/transporters. The HK-2 cell line, which is of kidney epithelial origin and the Caco-2 cell line, which is derived from a small intestine epithelial cells, had more common genes induced than SaOS-2 cells. Several genes associated with calcium and/or phosphate regulation were similarly modulated in the HK-2 and Caco-2 cell lines. Table 6 of the result section highlights some of these genes. This finding is not surprising in that the intestinal and renal cell lines are both of epithelial origin and are derived from tissues whose main functions are to regulate transport of metabolites. The SaOS-2 cell line is osteoblast-like, of mesenchymal origin, and represents a tissue with distinct functions compared to epithelial cells.

The commercial arrays provided an opportunity to survey multiple genes without bias to obtain a basic understanding of FGF-23 actions. The observation that most potentially regulated genes have generalized functions related to cell changes suggests that in addition to control of phosphate homeostasis, FGF-23 might play a role during embryogenesis, development and/or differentiation of specific cell types. Additional studies will be required to confirm this hypothesis.

The custom array approach was an opportunity to ask specialized questions regarding specific genes whose functions might be related to the known functions of FGF-23. Significant emphasis was placed on selection of appropriate genes through review of the literature. The observation that two-thirds of the oligos spotted had signals representing general expression of selected genes confirmed and established this approach. These arrays will form the basis of further analysis and can be expanded using gene candidates identified through the commercial arrays.

Data from the custom microarray analysis suggested that several genes identified through OOM SAGE analysis were regulated by FGF-23 (table 12 and 13). This result supported the hypothesis that some OOM associated genes represent genes whose expression was induced by the autocrine actions of FGF-23. The expectation was that most differentially regulated genes would have been upregulated but many OOM genes appeared to be downregulated by FGF-23. Given that a single experiment was performed for each cell condition, this discrepancy may reflect a high number of false negatives.

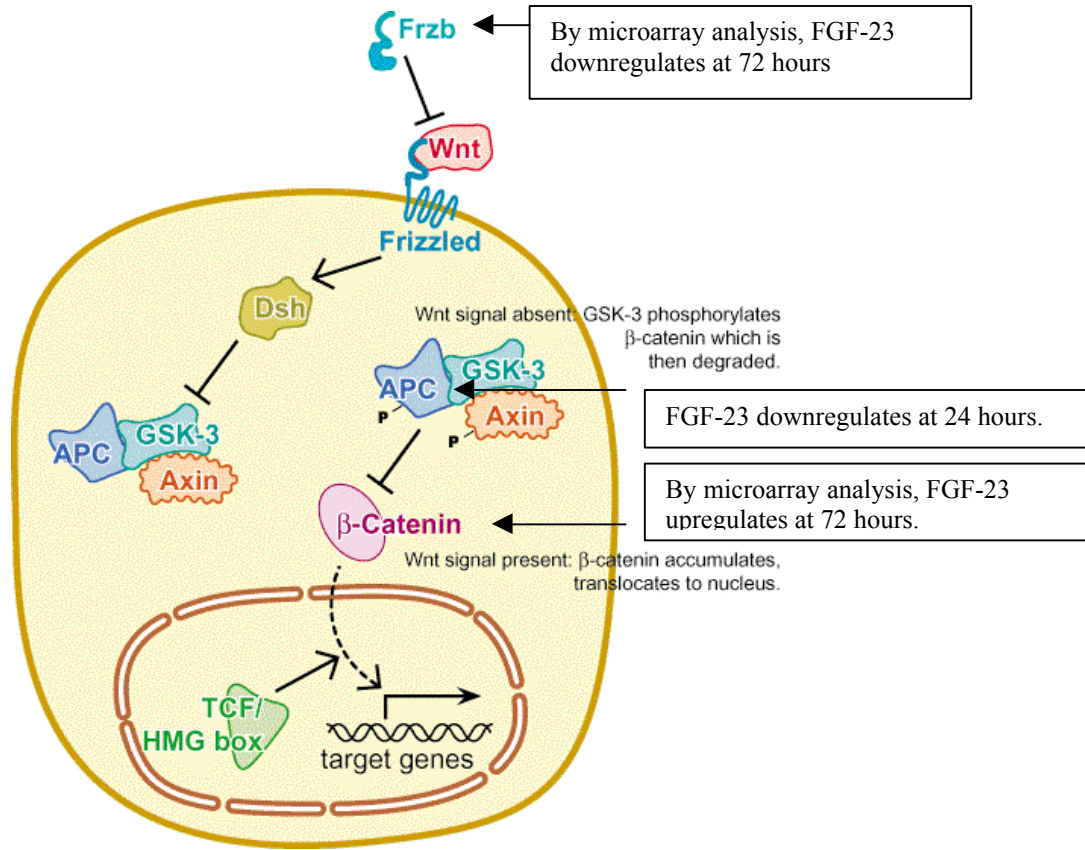
Additionally, several human homologues to yeast phosphate related genes were also identified to be differentially expressed (Table 13 and 14). A phosphate regulated pathway has been well studied in yeast yet little is known regarding a similar pathway in mammalian cell types. However, multiple human homologues of yeast proteins within this pathway have been identified (Dong Yu, Genzyme Corp.). These homologues were spotted on the custom microarray to determine if FGF-23 may influence expression of genes. Cathepsin D precursor was seen to

be upregulated 4 fold, while pituitary homeobox 1 and sodium dependant high-affinity dicarboxylate transporter was down regulated 2.5 fold. Although the signal intensity for each gene on the custom microarray is an average of four spots, it is still a single microarray analysis and would require replicate analysis from multiple samples and real-time RT-PCR validation before the fold changes could be considered to be statistically significant. The sodium-dependant high-affinity dicarboxylate transporter produced the greatest signal in both FGF-23 treated and control cell RNA samples, making the fold induction more reliable. Future work should monitor FGF-23 induced repression via real-time RT-PCR of the sodium dependent high-affinity dicarboxylate transporter.

FGF-23 appears to regulate two key genes of the Wnt signaling pathway by microarray analysis. By microarray analysis, FGF-23 reduced adenomatosis polyposis coli (APC) expression 1.5 fold in both HK-2 and Caco-2 cells at 24 hours. Real-time RT-PCR analysis showed a similar weak down regulation in Caco-2 cells at 24 hours. Additionally, Beta catenin-1 was upregulated at 72 hours in both cell types, but RT-PCR validation was not conducted on beta catenin-1. These two genes are known to be integral components of the Wnt signaling pathway (Slusarski *et al.* 1997). When the Wnt signaling pathway is inactive, APC is a key component in the pathway responsible for beta-catenin degradation. The degradation of beta-catenin results in WNT signaling inhibition. Upon Wnt activation, APC disassociates from beta-catenin so beta-catenin is not degraded and is allowed to enter the cell nucleus for transcriptional activation of several oncogenes and cellular growth genes (figure 30). There is no evidence

that directly links the Wnt signaling pathways to calcium or phosphate regulation. However, some FRPs are known to modulate Wnt signaling (Jones and Jomary 2002, Bergwitz *et al.* 2001, Jones and Jomary 2002, Robitaille *et al.* 2002). Based on homology between the phosphatonin, FRP-4 and other FRP family members, it is reasonable to speculate that FRP-4 might also interact with the Wnt signaling pathway. It is difficult to assert the specific biological significance of the FGF-23 induced down regulation of APC and the upregulation of Beta-catenin but it is possible that this may activate the Wnt pathway resulting in subsequent gene transcription. The potential down-regulation of FRP-4 observed by microarray analysis was not validated by real-time RT-PCR analysis. However, the concept that FGF-23 might regulate FRP-4 expression and WNT pathway members is intriguing. Relationships between Wnt and FGF pathways have already been established in development systems (Jones *et al.* 2002). Clearly additional and quantitative studies will be required to understand this potential relationship.

Figure 30. Generalized Wnt/ β -Catenin signaling pathway (Slusarski *et al.* 1997). Upon Wnt binding to membrane bound frizzled, APC disassociates from Beta-catenin allowing for entry into the cell nucleus and transcription of various genes related to growth. Down regulation of APC and up regulation of Beta-catenin by FGF-23 may have a similar activating function. FRPs (Frzb) are known to inhibit Wnt signaling.



PTH receptor

Parathyroid hormone receptor -1 (PTHr-1, NM_000316) and PTHr-2 (NM_005048) appeared to be upregulated by FGF-23 by microarray analysis. However, real-time RT-PCR analysis of PTHr-2 showed no change in expression. Expression of PTHr-1 was not tested by real-time RT-PCR but microarray analysis suggested a potential 2.1 fold increase in HK-2 cells at 24 hours post FGF-23 treatment. PTHr-1 is most abundantly expressed in the kidney, bone,

and liver. Mutations in PTHr-1 are associated with murk-jansen and blomstrand type of abnormal bone growth. Clinical symptoms of these two types of chondrodysplasia are a rare form of short limb dwarfism associated with hypercalcemia and low to normal levels of the two parathyroid hormones. Since PTHr-1 and PTHr-2 both bind the parathyroid hormone that is the primary method of calcium homeostasis, it would be valuable as a future experiment to validate the increased expression level of PTHr-1 in the HK-2 cells by real-time RT-PCR.

1-alpha-hydroxylase and 24-hydroxylase

As depicted in figure 31, in response to low serum calcium levels, PTH elevates active vitamin D levels which subsequently causes an increase in calcium serum levels, and also induces phosphate wasting through the kidney by reducing the reabsorption rate. The production of active vitamin D is achieved through $1\alpha\text{OHase}$ activity in the kidney. Although $1\alpha\text{OHase}$ expression levels were below the lower limit of detection of the microarrays, a 2 fold increase was measured by real-time RT-PCR analysis of the Caco-2 cells at 24 hours. A slight but non-significant increase was detected in the HK-2 cells measured at the 24 hour time point. No other conditions were tested for $1\alpha\text{OHase}$ expression via real-time RT-PCR. These results are contradictory to $1\alpha\text{OHase}$ expression levels observed in the *in vivo* mouse kidney studies (Shidmada *et al.* 2002). Several reasons may explain why $1\alpha\text{OHase}$ was observed to be induced in Caco-2 cells by real-time RT-PCR and a non-significant response was observed in HK-2 and Saos-2 cells. The first and most significant difference is that $1\alpha\text{OHase}$ was down

regulated *in vivo* where additional factors are present that may be required for $1\alpha\text{OHase}$ mRNA levels to be affected such as the presence of heparin, vitamin D and/or other yet to be discovered factors. Currently there are no human renal cell lines known to respond to FGF-23 by a change in $1\alpha\text{OHase}$ mRNA levels and currently the best model to validate FGF-23 biological activity by measuring phosphate uptake is using an opossum cell line and not a human cell line.

Second, $1\alpha\text{OHase}$ was observed to be affected within the *in vivo* experiments within 1 hour and maximal reduction of $1,25(\text{OH})_2\text{D}_3$ was seen between 8-13 hours, suggesting that $1\alpha\text{OHase}$ and/or 24-hydroxylase maybe modulated prior to the 24 hour time point at which mRNA levels were measured in our experiment. It is possible that $1\alpha\text{OHase}$ was regulated in a similar manner as in the *in vivo* studies but a non-optimal time point was selected to observe this response. The 24 hour time point was selected to measure a sustained FGF-23 exposure response and not to measure initial transcriptional genes that may be indicative of general growth factors and not necessarily specific to FGF-23. It is also possible that FGF-23 plays a different role in controlling $1,25(\text{OH})_2\text{D}_3$ production in intestinal tissue compared to renal tissues. The bulk of circulating $1,25(\text{OH})_2\text{D}_3$ is believed to be produced in the kidney and levels of $1\alpha\text{OHase}$ are significantly greater in renal versus intestinal tissues. It is possible that differential regulation at the intestine might result in local changes in $1,25(\text{OH})_2\text{D}_3$ rather than systemic.

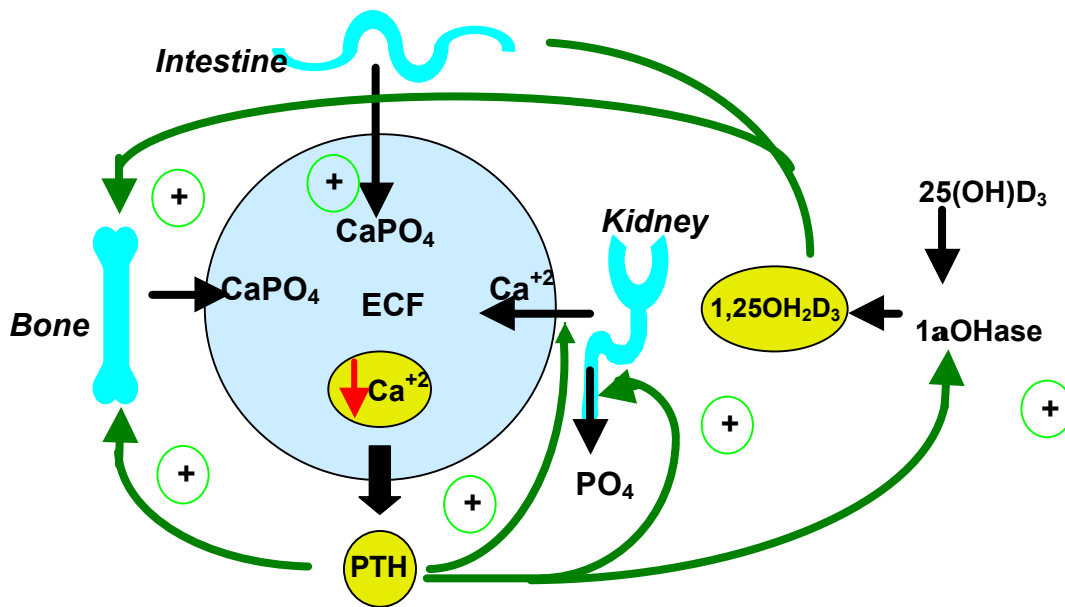
Additionally, no significant transcriptional changes to 24-OHase, the enzyme that degrades active vitamin D, was observed by real-time RT-PCR analysis in Caco-2 cells at 24 hours. This real-time RT-PCR result conflicts with

the microarray results where a two fold expression was observed in the Caco-2 24 hour time point cell sample.

There are indications that the Caco-2 cells responded to FGF-23 treatment at 24 hours with an increase in $1\alpha\text{OHase}$ mRNA but with a non-significant change in 24-OHase . It is likely that there is an accumulation of active vitamin D but to be certain $1,25\text{-dihydroxyvitamin D}_3$ would have to be directly measured.

$1\alpha\text{OHase}$ is expressed in a wide variety of cells including renal, monocytes, skin cells (Holick 1999) and intestine (Zehnder *et al.* 2001).

Figure 31. Known effect of PTH in response to low serum calcium levels. An increase in $1\alpha\text{OHase}$ increases active vitamin D ($1,25\text{OH}_2\text{D}_3$) levels.



Somatostatin receptors

The somatostatin hormone is distributed throughout the body. There are two primary forms of somatostatin, somatostatin –14 and somatostatin –28. These two forms of somatostatin bind to five known somatostatin receptors

(SSTr) that are involved in a variety of important endocrine and nervous system regulatory functions.

Several of the somatostatin receptors (SSTR) were observed to be potentially differentially expressed in HK-2 and Caco-2 cells treated with FGF-23. Of the five known SSTRs, SSTR1-4 appeared to be upregulated at various time points. Of particular interest is the apparent up regulation of SSTR-2 at 72 hours in both HK-2 and SaOS-2 cells. SSTR-2 is expressed in the brain, kidney, intestine, liver and is a marker for oncogenic osteomalacia tumors (Jan de Beur *et al.* 2002b), which as previously discussed, over express FGF-23 and induce phosphate wasting. Although the specific binding and signaling interaction of the two forms of SST to the five SSTRs is not completely understood, SSTR-2 expression and signaling has been associated with a rapid increase in intracellular calcium levels and availability of phosphate (Roskopf *et al.* 2002). SSTR-2 was observed to be upregulated 1.7 fold by microarray analysis and 1.8 fold by real-time RT-PCR analysis. A standard curve was not generated for this gene, hence the results are presented in the appendix section.

Aquaporins

Aquaporins (Aqp) are a family of extracellular membrane bound water channels expressed in various organs. Aqp-5 and Aqp-6 appeared to be upregulated in HK-2 cells by microarray analysis. Aqp-5 was seen to be potentially upregulated 2 fold in HK-2 cells at 24 hours by both microarray and real-time RT-PCR analysis (Figure 20). Reabsorption in the kidney's proximal

tubules involves Aqp-2 and 3, which are not observed to be modulated by FGF-23.

Although Aqp-6 was also suggested to be upregulated by FGF-23 in HK-2 cells by microarray analysis, real-time RT-PCR validation was inconclusive due to a high amount of non-specific RT-PCR amplification (appendix figure 2). Although Aqp-6 is structurally similar to the other family members, it is unique because it is expressed intracellularly and is primarily an ion channel and not a water channel as are the other Aqps (Ikeda *et al.* 2002). Even though the residues critical for water transport are highly conserved with only few changes, Aqp-6 has high specificity for nitrate instead of water in renal collecting ducts. Elevated levels of nitrate have been reported to inhibit H⁺-ATPase activity (Valles and Manucha 2000) and inhibition of H⁺-ATPase activity is associated with obstruction of kidney collecting ducts.

Custom microarray

Of the 205 genes spotted on the custom array, 87 genes produced a signal intensity less than 500 units under all conditions tested and 64 genes produced a signal intensity less than 300 units. Table 1 of the appendix section contains a list of these genes. Several reasons may explain why 30 percent of the genes produced a signal at or below the sensitivity of the microarray. Many of the gene families such as bone morphogenic proteins (BMPs), matrix metalloproteinase (MMPs), TRAILR and many others, may only be expressed under specific bone differentiated states and would not be expected to be expressed by the cells

under the conditions tested. Additionally, these genes and their sequences are available in the publicly available gene databases such as National Center for Biotechnology Information (NCBI) yet many were not spotted on the Clontech commercial microarray. It is possible that these genes possess a unique secondary structure that makes the design of efficient hybridization probes more difficult and were not included in the commercial microarray because they failed the extensive quality control tests.

Seven house keeping genes were selected to be placed on the custom microarray. STAT1 and beta-glucuronidase always produced a signal intensity less than 500 units of fluorescence. An approximate 1.5 fold change in expression was observed for alpha tubulin in Saos-2 72 hour and HK-2 72 hour, Cyclophilin-A HK-2 72 hour, and GAPDH HK-2 72 hour. Analysis of HK-2 72 hour sample by real-time RT-PCR did not verify any significant change (table 12).

Summary

In conclusion, microarray analysis suggests that all three cell lines representing the three known sites of phosphate regulation may be responded to FGF-23 treatment but the FGF-23 induced mRNA expression response was weaker than expected. Genes involved in the Wnt signaling pathway, parathyroid receptor signaling, somatostatin receptor signaling, and aquaporin channels were among the genes modulated by FGF-23. A more robust and similar response was observed in HK-2 and Caco-2 cells than in SaOS-2 cells. For rapid modulation of phosphate or calcium, similar mechanisms could be used to block

intestinal mineral absorption and renal reabsorption to lower serum levels or enhance transport to elevate serum levels. Both these sites require a monodirectional transport and the transport rate is modulated to maintain serum homeostasis. The SaOS-2 cells, representing bone, may not have been in the optimal bone differentiation state to best respond to FGF-23, and phosphate regulation may be modulated through an alternative pathway. It is likely that phosphate transport is achieved in different tissues using distinct methods because the primary renal phosphate transporter is NaPi2a, while GLVR-1 is the primary bone phosphate transporter.

In general, few genes were observed to be drastically affected by FGF-23 treatment across the three cell types. The purified FGF-23 used in these microarray studies was demonstrated to be biologically active by an opossum kidney cell phosphate uptake assay (A. Bowe, Genzyme Corp.). All cell types tested appeared to respond to FGF-23 treatment, but the measure of potency by microarray and, in particular, real-time RT-PCR was less than expected. Although a dampening of relative induction levels obtained by array analysis is well established, more robust and reliable inductions are typically observed using real time RT-PCR. There are several factors that may have contributed to the non-potent response. Various forms of heparin may affect the binding specificity of FGF-23. The effect of heparin on FGF-23 binding to FGF receptors is currently being studied to better understand the role of heparin on ligand/receptor binding to potentially help optimize FGF-23 potency. The half-life of FGF-23 may vary when exposed to different cell types. The optimal window to measure mRNA

responses to FGF-23 treatment may have been missed. Further *in vitro* and *in vivo* studies will help to better understand the stability of FGF-23. The cell types treated with FGF-23 may not have been in the optimal cell cycle or differentiated state to best respond to FGF-23 treatment. A non-homogenous cell population within one culture may have caused some cells to be less responsive, thereby masking the FGF-23 induced transcriptional response and hence the mRNA levels measured by the microarray and real-time RT-PCR. Monitoring mouse *in vivo* and/or *in situ* expression levels of the genes identified in this study, as well as additional microarray analysis of RNA isolated from tissue samples may provide insight into the complex regulation of phosphate as affected by FGF-23.

One caveat of this study that may have influenced the relative fold-induction observed by real-time RT-PCR is the choice of genes selected for analysis and the fact that most genes were not selected based on statistical analysis of repeat experiments with multiple biological samples. Assuming this was done, the expectation is that some genes would be identified that were induced to a greater degree and consistently by FGF-23.

In conclusion, HK-2 and Caco-2 cells responded to FGF-23 treatment by modulating mRNA expression as measured by microarray and real-time RT-PCR analysis. FGF-23 may have also induced changes in gene expression as measured by microarray analysis but fewer genes in Saos-2 cells were affected than HK-2 or Caco-2 cells. Since real-time RT-PCR validation was not conducted on Saos-2 cell mRNA, it can not be determined whether the genes observed by microarray analysis are truly modulated genes. Additionally the

limited number of biological and technical replicates limit the statistical certainty of the currently identified genes. Future *in vitro* experiments should include real-time RT-PCR measurement of 1 α OHase and consistently modulated genes like mucin-2 and aquaporin family members in a time course experiment. This may lead to the identification of a more optimal time point to identify FGF-23 induced mRNA expression. The selected time point should be tested by biological and technical replicates. Alternatively, *in vivo* tissue mRNA studies of mice treated with FGF-23 may provide a more accurate model for the biological function of FGF-23 where yet to be identified additional factors required for signaling are present as validated by the observed phosphate wasting.

APPENDIX

Figure 32a. Opossum kidney phosphate uptake assay demonstrated the biological activity of FGF-23 used in all microarray experiments. (Bowe, Genzyme Corp.)

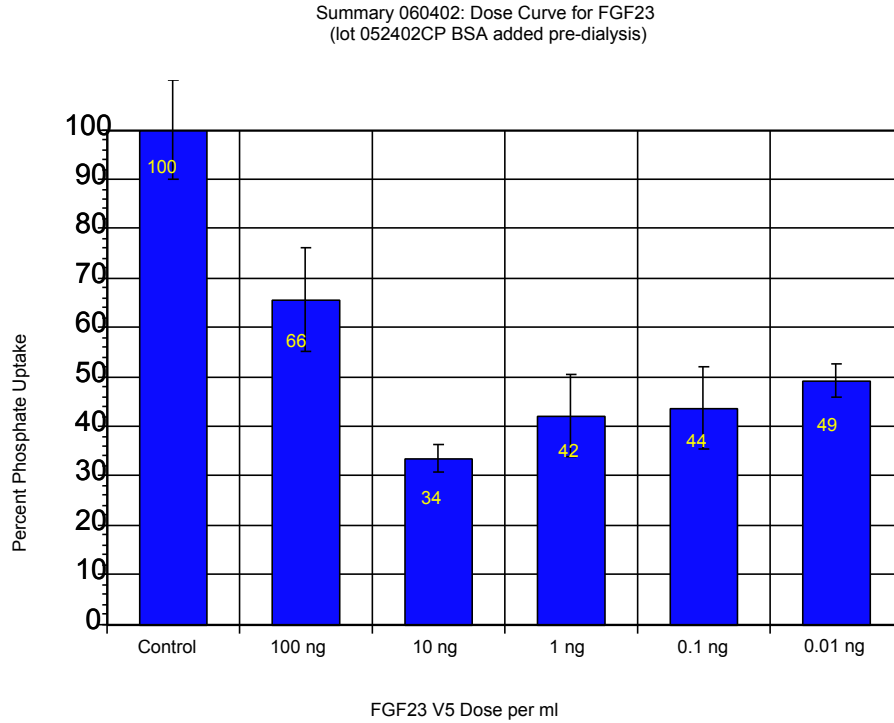


Figure 32b. Phosphate uptake assay demonstrates biological response of Saos-2 and HK-2 to FGF-23 treatment. (Bowe, Genzyme Corp.)

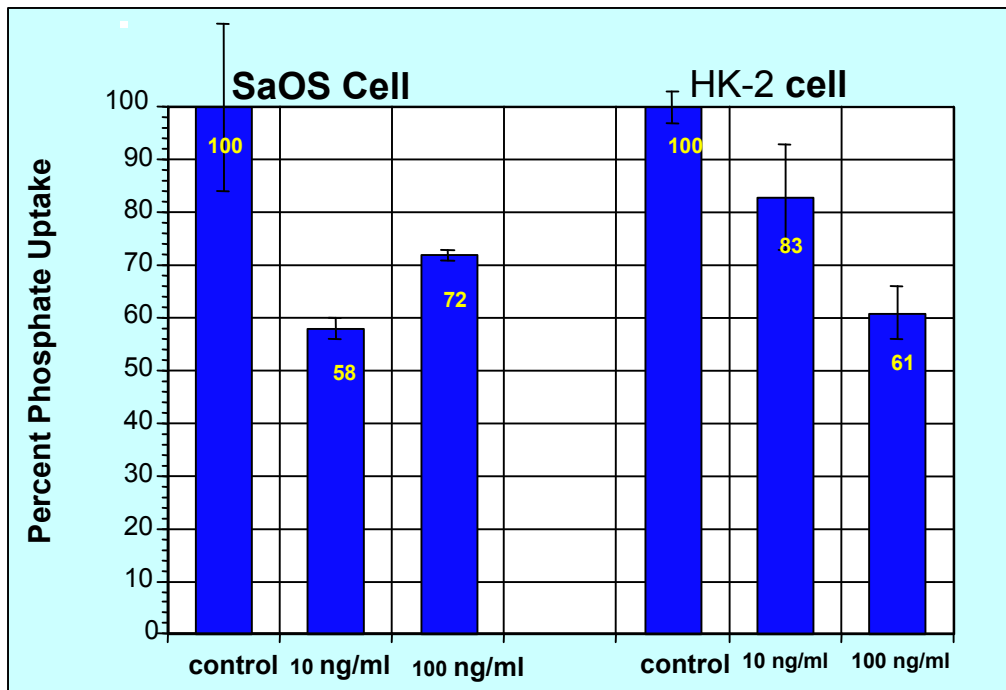


Figure 33. Real-time RT-PCR analysis without standard curve and without ethidium bromide gel analysis.

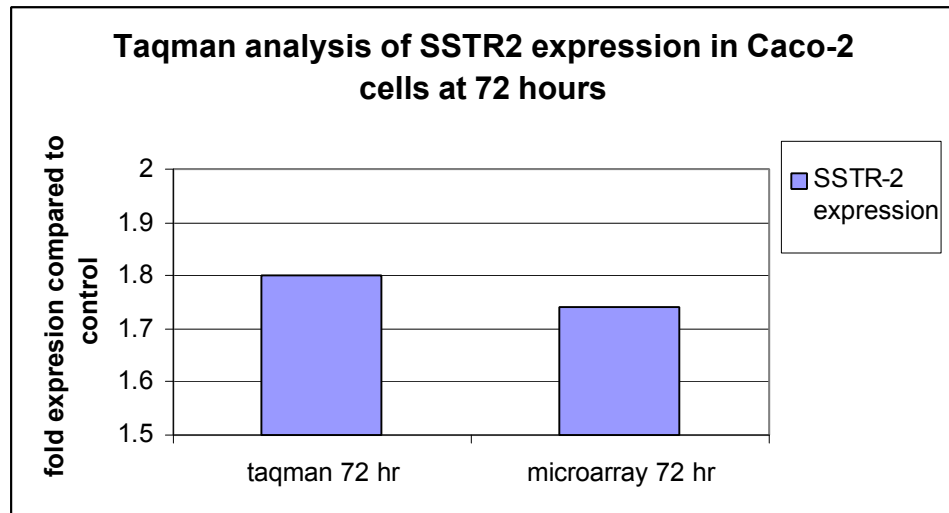


Figure 34. Ethidium bromide gel of Aquaporin 5 and 6 RT-PCR amplification. Non-specific amplification is seen for Aquaporin 6 and primer dimer formation in the negative control.

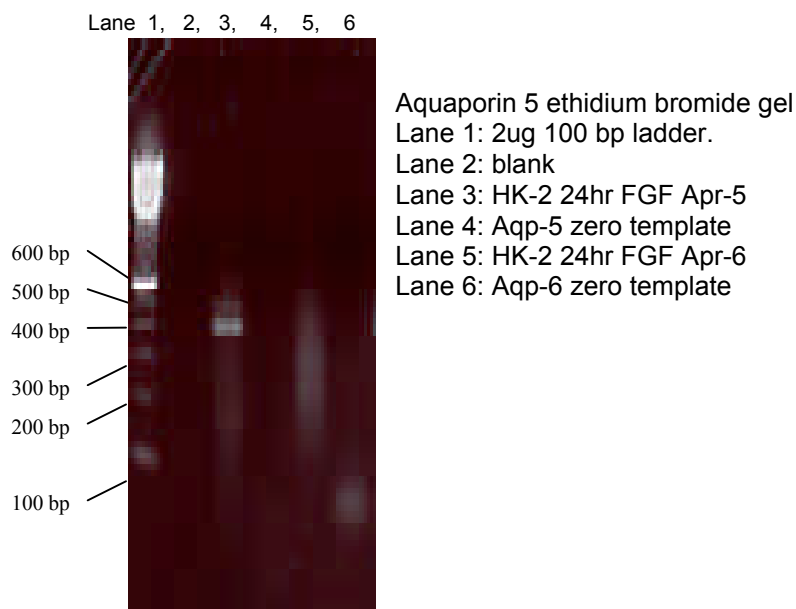


Table 16. List of genes spotted on the custom microarray but expressed a signal intensity less than 500 unit in all conditions tested. * Gene signal intensity greater than 300 units but less than 500 units.

accession	gene name
NM_000181	beta-Glucuronidase
NM_015675	growth arrest and DNA-damage-inducible, beta
AK023607	Homo sapiens cDNA FLJ13545 fis, clone PLACE1006867
NM_002838	LCA protein tyrosine phosphatase, receptor type, C
AK024230*	14-3-3 gamma
AL031228	a2-Collagen Type XI
NM_001148	ANK2_HUMAN Ankyrin 2
NM_017680	Asporin
NM_004324	Bax
NM_020396	BCL2-like 10 (apoptosis facilitator)
AF111848*	beta-Actin
NM_033637	beta-trcp
NM_005811	bone morphogenetic protein 11 (BMP11)
NM_001200	Bone morphogenetic protein 2 (BMP2)
NM_001201	Bone morphogenetic protein 3 (BMP3)
NM_001719	Bone morphogenetic protein 7 (osteogenic protein 1)
NM_004967	Bone Sialo protein (BSP)
NM_004348	CBFA1/RUNX2
NM_001798*	CDK2_HUMAN Cell division protein kinase 2
NM_003465*	chitinase 1
NM_001892	ck1 (casein kinase 1)
NM_001895*	ck2 (casein kinase 2)
NM_001854	collagen 11
NM_001850	collagen 8 alpha1
NM_000493	collagen type IX
NM_000493	Collagen Type X
NM_003254*	collagenase inhibitor mRNA/TIMP-1
NM_001901	Connective Tissue Growth Factor
NM_000962	Cox1
NM_003649	D-aspartate oxidase variant 1
NM_001920	DCN
NM_005221	Dlx5
NM_001959*	EF-1
NM_016357	epithelial protein lost in neoplasm beta
NM_058229	EST
NM_024732	EST AA625899
NM_022450*	EST(hypothetical protein FLJ22357 similar to epidermal growth factor receptor-related protein) eukaryotic translation elongation factor 1 alpha 1
AJ420488	Exportin 5
AF298880	Exportin 5
NM_005117	FGF-19
NM_000138	fibrillin 1
NM_001999	fibrillin 2
NM_002021	Flavin containing monooxygenase 1
NM_006894	Flavin containing monooxygenase 3
NM_005479	frat-1
NM_000557	GDF5
NM_001537	heat shock factor binding protein 1

NM_002856* HVEB mRNA
 AK022929* hydroxysteroid (17-beta) dehydrogenase 7
 NM_000619 IFN gamma
 NM_000600 IL-6
 NM_007315* ISGF-3 (STAT1)
 NM_005354* JunD
 NM_020196 KIAA 1177 protein
 U50748 leptin receptor
 NM_002427 matrix metalloproteinase 13(MMP13)
 NM_004995 matrix metalloproteinase 14 (MMP14)
 NM_004530* matrix metalloproteinase 2 (MMP2)
 NM_004994 matrix metalloproteinase 9 (MMP 9)
 NM_020203* MEPE
 NM_000900 MGP (matrix gla protein)
 NM_024165* milk PDH finger protein 1
 NM_002449 Msx-2
 NM_004897 Multiple inositol polyphosphate phosphatase
 NM_005074 Napi1 (SLC17A1)
 NM_003052* Napi2a
 NM_013436* Nck-associate protein 1
 NM_005450 Noggin
 NM_003058 Organic cation transporter
 NM_004418* PAC-1(protein tyrosine phosphatase)
 BC008826* Paired box gene 3 (Waardenburg syndrome 1) PAX-3
 NM_002609 PDGF-BB
 NM_000444* PEX or PHEX
 NM_002845 protein ty phosphatase rec type M
 NM_002668 Proteolipid protein 2
 NM_005048* PTH receptor 2
 NM_002775* Serine Protease 11 (IGF Binding)
 NM_001463 sFRP-3
 NM_014474 Similar to acid sphingomyelinase-like
 phosphodiesterase
 NM_000627 TGFb Binding Protein
 NM_000594 TNF
 NM_003844 TRAILR-1
 AF016266 TRAILR-2
 NM_003841 TRAILR-3
 NM_003840 TRAILR-4
 NM_003287 tumor protein D52-like 1
 AF089744 Xenotropic and polytropic murine retrovirus receptor

BIBIOGRAPHY

ADHR Consortium (No Author), (2000). Autosomal dominant hypophosphataemic rickets is associated with mutations in FGF-23. *Nat Genet.* Nov;26(3):345-8.

Anderson C.B., Neufeld K.L., White R.L. (2002) Subcellular distribution of Wnt pathway proteins in normal and neoplastic colon. *Proc Natl Acad Sci U S A.* Jun 25;99(13):8683-8.

Bergwitz C, Wendlandt T, Kispert A, Brabant G. (2001). Wnts differentially regulate colony growth and differentiation of chondrogenic rat calvaria cells. *Biochim Biophys Acta.* Apr 23;1538(2-3):129-40.

Bilbe G, Roberts E, Birch M, Evans DB. (1996). PCR phenotyping of cytokines, growth factors and their receptors and bone matrix proteins in human osteoblast-like cell lines. *Bone.* Nov;19(5):437-45.

Boileau G, Tenenhouse HS, Desgroseillers L, Crine P. (2001) Characterization of PHEX endopeptidase catalytic activity: identification of parathyroid-hormone-related peptide107-139 as a substrate and osteocalcin, PPI and phosphate as inhibitors. *Biochem J.* May 1;355(Pt 3):707-13.

Bowe A.E., Finnegan R., Jan de Beur S.M., Cho J., Levine M.A., Kumar R., Schiavi S.C. (2001) FGF-23 inhibits renal tubular phosphate transport and is a PHEX substrate. *Biochem Biophys Res Commun.* Jun 22;284(4):977-81.

Broadus A.E., (1999). *Primer on the Metabolic Bone Disease and Disorder of Mineral Metabolism.* 4th edition, Lippincott Williams and Wilkins P74-80.

Dackowski W.R., Luderer H.F., Manavalan P., Bukanov N.O., Russo R.J., Roberts B.L., Klinger K.W., Ibraghimov-Beskrovnaya O. (2002) Canine PKD1 Is a Single-Copy Gene: Genomic Organization and Comparative Analysis. *Genomics.* Jul;80(1):105-12.

Econs M.J., McEnery P.T., Lennon F., Speer M.C. (1997) Autosomal dominant hypophosphatemic rickets is linked to chromosome 12p13. *J Clin Invest.* Dec 1;100(11):2653-7.

Gallieni M., Cucciniello E., D'Amaro E., Fatuzzo P., Gaggiotti A., Maringhini S., Rotolo U., Brancaccio D. (2002). Calcium, phosphate, and PTH levels in the hemodialysis population: a multicenter study. *J Nephrol.* Mar-Apr;15(2):165-70.

Guimond S.E., Turnbull J.E. (1999) Fibroblast growth factor receptor signalling is dictated by specific heparan sulphate saccharides. *Curr Biol.* Nov 18;9(22):1343-6.

Holick M.F. (1999). Primer on the Metabolic Bone Disease and Disorder of Mineral Metabolism. 4th edition, Lippincott Williams and Wilkins P92-98.

HYP Consortium. (1995). A gene (PEX) with homologies to endopeptidases is mutated in patients with X-linked hypophosphatemic rickets. Nat Genet. Oct;11(2):130-6.

Ikeda M., Beitz E., Kozono D., Guggino W.B., Agre P., Yasui M. (2002) Characterization of Aquaporin-6 as a Nitrate Channel in Mammalian Cells. Requirement of pore-lining residue threonine. J Biol Chem. Oct 18;277(42):39873-9.

Jan de Beur SM, Finnegan RB, Vassiliadis J, Cook B, Barberio D, Estes S, Manavalan P, Petroziello J, Madden SL, Cho JY, Kumar R, Levine MA, Schiavi SC. (2002a) Tumors associated with oncogenic osteomalacia express genes important in bone and mineral metabolism. J Bone Miner Res. Jun;17(6):1102-10.

Jan de Beur S.M., Streeten, E.A. Civelek C.A., McCarthy E.F., Uribe L., Marx S.J., Onobrakpeya O., Raisz L.G., Watts N.B., Sharon M., Levine M.A. (2002b) Localisation of mesenchymal tumors by somatostatin receptor imaging THE LANCET. Mar 2;359(9308):761-3.

Johnson DE, Lu J, Chen H, Werner S, Williams LT. (1991). The human fibroblast growth factor receptor genes: a common structural arrangement underlies the mechanisms for generating receptor forms that differ in their third immunoglobulin domain. *Mol Cell Biol.* Sep;11(9):4627-34.

Jones SE, Jomary C. (2002). Secreted Frizzled-related proteins: searching for relationships and patterns. *Bioessays.* Sep;24(9):811-20.

Juppner M.D., Brown E.M. Kronenberg H.M., (1999). *Primer on the Metabolic Bone Disease and Disorder of Mineral Metabolism.* 4th edition, Lippincott Williams and Wilkins P80-91.

Karim-Jimenez Z, Hernando N, Biber J, Murer H. (2000) Requirement of a leucine residue for (apical) membrane expression of type IIb NaPi cotransporters. *Proc Natl Acad Sci U S A.* Mar 14;97(6):2916-21.

Kim I, Moon S, Yu K, Kim U, Koh GY. (2001). A novel fibroblast growth factor receptor-5 preferentially expressed in the pancreas(1). *Biochim Biophys Acta.* Mar 19;1518(1-2):152-6.

Kumar R. (2000). Tumor-induced osteomalacia and the regulation of phosphate homeostasis. *Bone.* Sep;27(3):333-8.

Kumar R. (2002). New insights into phosphate homeostasis: fibroblast growth factor 23 and frizzled-related protein-4 are phosphaturic factors derived from tumors associated with osteomalacia. *Curr Opin Nephrol Hypertens.* Sep;11(5):547-53.

Kumar R. labs unpublished Department of Internal Medicine, Mayo Clinic and Foundation, Rochester, Minnesota 55905, USA. rkumar@mayo.edu

Liu S, Guo R, Tu Q, Quarles LD. (2002). Overexpression of PheX in osteoblasts fails to rescue the Hyp mouse phenotype. *J Biol Chem.* Feb 1;277(5):3686-97.

Mariadason J.M., Rickard K.R., Barkla D.H., Augenlicht L.H., and Gibson P.R., (2000). Divergent Phenotypic Patterns and Commitment to Apoptosis of Caco-2 Cells During Spontaneous and Butyrate-Induced Differentiation. *Journal of Cellular Physio* 183:347–354.

Mehrotra R., Nolph K.D. (1999). Low protein diets are not needed in chronic renal failure. *Miner Electrolyte Metab.* Jul-Dec;25(4-6):311-6.

Meyer RA Jr, Meyer MH, Gray RW. (1989) Parabiosis suggests a humoral factor is involved in X-linked hypophosphatemia in mice. *J Bone Miner Res.* 1989 Aug;4(4):493-500.

Murer H, Biber J. (1996). Molecular mechanisms of renal apical Na/phosphate cotransport. *Annu Rev Physiol.* 58:607-18.

Nielsen LB, Pedersen FS, Pedersen L. (2001) Expression of type III sodium-dependent phosphate transporters/retroviral receptors mRNAs during osteoblast differentiation. *Bone.* Feb;28(2):160-6.

Park E.K., Warner N., Mood K., Pawson T., Daar I.O. (2002) Low-molecular-weight protein tyrosine phosphatase is a positive component of the fibroblast growth factor receptor signaling pathway. *Mol Cell Biol.* May; 22(10): 3404-14.

Pellegrini L. (2001). Role of heparan sulfate in fibroblast growth factor signalling: a structural view. *Curr Opin Struct Biol.* Oct;11(5):629-34. Review.

Powers C.J., McLeskey S.W., Wellstein A. (2000). Fibroblast growth factors, their receptors and signaling. *Endocr Relat Cancer.* Sep;7(3):165-97.

Pragnell M., Genzyme Corporation Framingham MA 01701 USA

marlon.pragnell@genzyme.com

Robitaille J, MacDonald ML, Kaykas A, Sheldahl LC, Zeisler J, Dube MP, Zhang LH, Singaraja RR, Guernsey DL, Zheng B, Siebert LF, Hoskin-Mott A, Trese MT,

Pimstone SN, Shastry BS, Moon RT, Hayden MR, Goldberg YP, Samuels ME. (2002). Mutant frizzled-4 disrupts retinal angiogenesis in familial exudative vitreoretinopathy. *Nat Genet.* Oct;32(2):326-30.

Roskopf D., Schurks M., Manthey I., Joisten M., Busch S., Siffert W. (2002). Signal transduction of somatostatin in human B lymphoblasts. *Am J Physiol Cell Physiol.* Sep 18

Schiavi S.C., Moe O.W. (2002). Phosphatonins: a new class of phosphate-regulating proteins. *Curr Opin Nephrol Hypertens.* Jul;11(4):423-30.

Shimada T., Mizutani S., Muto T., Yoneya T., Hino R., Takeda S., Takeuchi Y., Fujita T., Fukumoto S., Yamashita T. (2001). Cloning and characterization of FGF-23 as a causative factor of tumor-induced osteomalacia. *Proc Natl Acad Sci* May 22;98(11):6500-5.

Shore R.M., (1999) *Primer on the Metabolic Bone Disease and Disorder of Mineral Metabolism.* 4th edition, Lippincott Williams and Wilkins P134-146.

Slusarski D.C., Yang-Snyder J., Busa W.B., Moon R.T. (1997) Modulation of embryonic intracellular Ca²⁺ signaling by Wnt-5A. *Dev Biol.* Feb 1;182(1):114-20.

Spruill SE, Lu J, Hardy S, Weir B. (2002) Assessing sources of variability in microarray gene expression data. *Biotechniques*. Oct;33(4):916-20, 922-3.

Tulassay T., Tulassay Z., Rascher W., Szucs L., Seyberth H.W., Nagy I. (1991) Effect of somatostatin on kidney function and vasoactive hormone systems in health subjects. *Klin Wochenschr*. Aug 1;69(11):486-90.

Valles P.G., Manucha W.A. (2000). H⁺-ATPase activity on unilateral ureteral obstruction: interaction of endogenous nitric oxide and angiotensin II. *Kidney Int*. 2000 Oct;58(4):1641-51.

Werner A., Moore M.L., Mantei N., Biber J., Semenza G., Murer H. (1991) Cloning and expression of cDNA for a Na/Pi cotransport system of kidney cortex. *Proc Natl Acad Sci* Nov 1;88(21):9608-12.

Werner A., Dehmelt L., Nalbant P. (1998) Na⁺-dependent phosphate cotransporters: the NaPi protein families. *J Exp Biol*. Dec;201 (Pt 23):3135-42.

White K.E., Jonsson K.B., Carn G., Hampson G., Spector T.D., Mannstadt M., Lorenz-Depiereux B., Miyauchi A., Yang I.M., Ljunggren O., Meitinger T., Strom T.M., Juppner H., Econs M.J. (2001). The autosomal dominant hypophosphatemic rickets (ADHR) gene is a secreted polypeptide overexpressed

by tumors that cause phosphate wasting. *J Clin Endocrinol Metab.* Feb;86(2):497-500.

Wiedemann M., Trueb B. (2001) The mouse *Fgfr1* gene coding for a novel FGF receptor-like protein *Biochimica et Biophysica Acta* 1520 247-250.

Yamashita T, Yoshioka M, Itoh N. (2000). Identification of a novel fibroblast growth factor, FGF-23, preferentially expressed in the ventrolateral thalamic nucleus of the brain. *Biochem Biophys Res Commun.* Oct 22;277(2):494-8.

Yamashita T., Konishi M., Miyake A., Inui K., Itoh N. (2002) Fibroblast growth factor (FGF)-23 inhibits renal phosphate reabsorption by activation of the mitogen-activated protein kinase pathway. *J Biol Chem.* Aug 2;277(31):28265-70.

Yamazaki Y, Okazaki R, Shibata M, Hasegawa Y, Satoh K, Tajima T, Takeuchi Y, Fujita T, Nakahara K, Yamashita T, Fukumoto S. 2002. Increased circulatory level of biologically active full-length FGF-23 in patients with hypophosphatemic rickets/osteomalacia. *J Clin Endocrinol Metab.* Nov;87(11):4957-60.

Yokote 2002 Abstracts from the 24th Annual Meeting of the American Society for Bone and Mineral Research (ASBMR 24th Annual Meeting in Phoenix, Arizona, USA)

Zehnder D, Bland R, Williams MC, McNinch RW, Howie AJ, Stewart PM, Hewison M. (2001). Extrarenal expression of 25-hydroxyvitamin d(3)-1 alpha-hydroxylase. *J Clin Endocrinol Metab.* Feb;86(2):888-94.

Zhang JD, Cousens LS, Barr PJ, Sprang SR. (1991). Three-dimensional structure of human basic fibroblast growth factor, a structural homolog of interleukin 1 beta. *Proc Natl Acad Sci* Apr 15;88(8):3446-50.

